Hashemite Kingdom of Jordan

Hashemite University

Jordan Journal of Earth and Environmental Sciences

JJEES

An International Peer-Reviewed Scientific Journal

Financed by the Scientific Research Support Fund

http://jjees.hu.edu.jo/

Volume (6) Special Publication (3) ISSN 1995-6681 June 2014 / Shaban 1435

The Jordan Journal of Earth and Environmental Sciences (JJEES)

JJEES is an international peer-reviewed research journal, issued by the Deanship of Academic Research and Graduate Studies, the Hashemite University, in corporation with, the Jordanian Scientific Research Support Fund, the Ministry of Higher Education and Scientific Research.

SUBMISSION ADDRESS:

Professor **Eid A. Al-Tarazi**
Deanship of Academic Research and Higher Studies
Hashemite University, P.O. Box 150458, Postal Code 13115, Zarqa, Jordan.
Phone: +962-5-3903333 ext.4229
E-Mail: jjees@hu.edu.jo

Hashemite Kingdom of Jordan

Hashemite University

Jordan Journal of Earth and Environmental Sciences

JJEES

An International Peer-Reviewed Scientific Journal

Financed by the Scientific Research Support Fund

Special Publication 3

http:// jjees.hu.edu.jo/

ISSN 1995-6681

JJEES
Jordan Journal of Earth and Environmental Sciences

Editorial Preface

It gives me a great pleasure to publish the third special issue of the Jordan Journal of Earth and Environmental Sciences. This special issue includes research papers presented at the international conference that was held under the patronage of Her Royal Highness Princess Sumaya Bint Al-Hassan between 3-5/4/2014 in Amman/ Jordan. The conference, which was supported by many governmental, academic and international institutions, was held under the title: "Building International Networks for Enhancement of Research in Jordan."

The research papers that were accepted for publication in this special issue are of paramount importance and significance to Jordan since they address issues related to Economic Geology and the development of Mineral Ores, such as Zeolites, Uranium Ores as well as Mud and Concrete Processing in Jordan. The papers that were selected for publication in this special issue passed a process of review and evaluation according to the policies duly followed by our Journal.

I would like to extend my sincere thanks and regards to my colleagues in the Journal's Editorial Board for their efforts without which this special issue could have never seen light. I would also like to extend my thanks to the Language Editor of the Journal, Dr. Qusai Al-Thebyan, and to Mr. Obada Smadi, the Publishing Layout Editor at the Hashemite University for their efforts.

Editor-in-Chief,
Prof. Dr. Eid Abdel Rahman Al-Tarazi
Jordan Journal of Earth and Environmental Sciences
Faculty of Natural Resources and Environment
The Hashemite University,
Zarqa, Jordan

JJEES
Jordan Journal of Earth and Environmental Sciences

Building International Networks for Enhancement of Research in Jordan
Int. Conference / Humboldt Kolleg
April 3 - 5, 2014

Conference Preface

The conference "Building Int. Networks for Enhancement of Research in Jordan" was held in Amman between April 3 - 5th, 2014 at Princess Sumaya University for Technology (PSUT) and the German Jordanian University (GJU). Generous support by the Alexander von Humboldt Foundation (AvH), Science Research Support Fund (SRSF), King Abdullah II Fund for Development among others played important role in the success of the Conf.

The Conf. was one of the most successful activities the Jordanian Club of Humboldt Fellows (JCHF) ever organized since it was established in 1997. More than 300 people attended including 100 Int. participants from 25 countries. Ph.D. students, representatives of Associations, AvH, DAAD, AGYA (Arab German Young Association), Federal Foreign Office, German Embassy in Amman, German Archaeological Protestant Institute in the Holy Land, the AvH - MED (Mediterranean) Network participated.

Eighty papers and 75 posters were presented. Parallel sessions were organized. Several workshops took place: Cultural, Physics, Chemistry, Biological and Pharmaceutical Sciences and Archaeology. Humboldtian Prof. Luay Rashan organized the Pharmaceutical Workshop. A price for the best poster was chosen by a Committee chaired by Dr Nelli Wanderka from Berlin.

A 2-days pre-Conference training workshop, organized at the Univ. of Jordan (JU) in Amman, "Opportunities & Problems of scientific Research in MENA Region" for Jordanian and MENA graduate students was run by three German top scientists and an active Humboldtian Prof. Bothina Hamad. Those young scientists presented their improved works at the Conf.

A workshop for Junior Scientists was also organized, where Dr Thomas Hesse made a presentation about the AvH Foundation and its programs. DAAD Director in Amman gave a presentation about DAAD programs.

The AvH- MED (Mediterranean) Network chairman Prof. Claudio Borri chaired the workshop which discussed major issues of common interest. Strengthening cooperation, joint research and to exchanges were discussed.

Archaeology German team (2 professors and 9 PhD. Students from several German universities) stayed 16 days in Jordan. The chairman of the team, Hans-Peter Kuhnen from Mainz University, chaired a workshop that had presentations from the visiting scientists and the Jordanian counterparts in cooperation with the German Archaeological Protestant Institute in Amman.

Participants were able to visit some Jordanian universities. Prof. Mohammad El Khateeb arranged the visit to JUST in Irbid. A meeting with members of staff took place. Prof. Ziad Al-Saad and Prof. Hani Hiagneh arranged the visit to Yarmouk Univ. and its Archaeology Museum.

Humboldtians Prof. Bothina Hamad and Prof. Hani Khoury arranged the visit to JU. Humboldtian Prof. Dr Sultan Abu Orabi, Secretary General of the Association of Arab universities, participated at the activities aimed at increasing cooperation with German Universities.

Visits were facilitated to the Royal Geographic Center, Jerash, Um Qeis, Madaba, Baptism site, Dead Sea, Petra, Wadi Rum, Aqaba, Iraq El Amir and Roman Theater in Amman.

A busy program and successful outcome with Ambassador/ Foreign Office in Germany Dr Heinrich Kreft, Deputy Sec. General of the AvH Dr Thomas Hesse gave distinguished talks.

HRH Princess Sumaya bint el Hassan opened the Conf. and gave excellent talk praising Scientific and cultural cooperation, Humboldt Foundation, JCHF and its role. Ambassador of Germany to Jordan, HE Mr. Ralph Tarraf expressed appreciation of what JCHF is doing to strengthen the German-Jordanian relations. Chairman of the Conf. HE Prof. Khaled Toukan gave an excellent talk at the Conf. Evaluation of the Conf. took place, with HE Ralph Tarraf, Dr Kreft and Dr Thomas Hesse took part. Director of DAAD office in Jordan Mr. Andreas Wutz was very supportive.

Marwan S. Mousa
Director of the Conference/Kolleg
Humboldt Ambassador Scientist
President of the Jordanian Club of Humboldt Fellows
President of the Jordanian Physics Society
Prof. of Materials
Dept. of Physics
Mu'tah University
Al-Karak, Jordan
Tel: 00962-79-5659761
Fax: 00 962-3-2375540

JJEES
Jordan Journal of Earth and Environmental Sciences

Building International Networks for Enhancement of Research in Jordan
Int. Conference / Humboldt Kolleg
April 3 - 5, 2014

Conference Organizing Committee:

- **Prof. Dr. Khaled Toukan Chairman of JAEC**
(Chairman of the Conference)
- **Prof. Dr. Natheer Abu-Obeid President of GJU**
(Co-Chairman of the Conference)
- **Prof. Dr. Marwan S. Mousa**
(Physics Dept., Mu'tah Univ) (Director of the Conference)
- **Dr. Nelli Wanderka**
(Helmholtz Zentrum Berlin for Materials and Energy, Berlin, Germany)

Scientific Committee:

HE Prof. Dr. Khaled Toukan	chairman@jaec.gov.jo; Dr.khaled.toukan@jaec.gov.jo
Prof. Dr. Natheer Abu Obeid	natheer.abuobeid@gju.edu.jo
Prof. Dr. Marwan S. Mousa	marwansmousa@yahoo.com, mmousa@mutah.edu.jo
Dr. Ramia Al Bakain	ramia.bakain@yahoo.com, r.bakain@ju.edu.jo
Prof. Dr. Hani Khoury	khouryhn@ju.edu.jo
Prof. Dr. Nizar Abu Jaber	nizar.abujaber@gju.edu.jo
Prof. Dr. Majed Abu Zreig	majed.abuzreig@gju.edu.jo
Prof. Dr. Muwaffaq Alomoush	ma@aabu.edu.jo
Prof. Dr. Talal Abu Rjai	deanphar@ju.edu.jo aburjai@ju.edu.jo
Prof. Dr. Eid Al Tarazi	eid@hu.edu.jo, ealtarazi@yahoo.com
Prof. Dr. Ahmad Malabeh	am@hu.edu.jo; malabite.ahmad@yahoo.com
Prof. Dr. Mohammed Al-Khateeb	kateeb@just.edu.jo
Prof. Dr. Lauy Rashan	luayrashan@yahoo.com
Prof. Dr. Yousef Hiary	hiary@ju.edu.jo
Prof. Dr. Mohammed Al-Omari	alakmoh@just.edu.jo
Prof. Dr. Bothina Hammad	b.hamad@ju.edu.jo
Dr. Awni Khasawneh	kawni@yahoo.com
Dr. Khaldoun Tarawneh	khaldoun@psut.edu.jo
Dr. Galeb Saraireh	g_saraireh@aou.edu.jo
Dr. Khaled Al- Nawayseh	Khalid.na@arabpotash.com
Dr. Hmoud Dmour	hmoud79@mutah.edu.jo
Prof. Dr. Kamil Al-Shiekh	kamilaliamen@yahoo.com
Dr. Abdullah AL-Zaghameem	aoz_q2q@yahoo.com
Dr. Ahmad Telfah	telfah.ahmed@gmail.com
Prof. Dr. Abdelrahim Hunaiti	hunaiti2001@yahoo.com
Prof. Dr. Nihad Yusuf	nihadyusuf@yu.edu.jo
Prof. Dr. Ibrahim Abu Al-Jarayseh	ijaraysh@yu.edu.jo
Prof. Dr. Saed Dababneh	dababneh@bau.edu.jo
Prof. Dr. Eqab Rabei	eqabrabei@gmail.com
Prof. Dr. Mousa Abu Orabi	mousa@just.edu.jo
Prof. Dr. Mohammed Khasawneh	mkha@just.edu.jo
Prof. Dr. Ziad Al Saad	alsaad@gmail.com
Prof. Dr. Hani Hayajneh	hani@yu.edu.jo
Prof. Dr. Ahmad Mousa	mousa@rocketmail.com

المجلة الأردنية لعلوم الأرض والبيئة
Jordan Journal of Earth and Environmental Sciences (JJEES)
http://jjees.hu.edu.jo

Hashemite University

Deanship of Scientific Research and Graduate Studies

TRANSFER OF COPYRIGHT AGREEMENT

Journal publishers and authors share a common interest in the protection of copyright: authors principally because they want their creative works to be protected from plagiarism and other unlawful uses, publishers because they need to protect their work and investment in the production, marketing and distribution of the published version of the article. In order to do so effectively, publishers request a formal written transfer of copyright from the author(s) for each article published. Publishers and authors are also concerned that the integrity of the official record of publication of an article (once refereed and published) be maintained, and in order to protect that reference value and validation process, we ask that authors recognize that distribution (including through the Internet/WWW or other on-line means) of the authoritative version of the article as published is best administered by the Publisher.

To avoid any delay in the publication of your article, please read the terms of this agreement, sign in the space provided and return the complete form to us at the address below as quickly as possible.

Article entitled:----------

Corresponding author: ----------

To be published in the journal: Jordan Journal of Earth & Environmental Sciences (JJEES)

I hereby assign to the Hashemite University the copyright in the manuscript identified above and any supplemental tables, illustrations or other information submitted therewith (the "article") in all forms and media (whether now known or hereafter developed), throughout the world, in all languages, for the full term of copyright and all extensions and renewals thereof, effective when and if the article is accepted for publication. This transfer includes the right to adapt the presentation of the article for use in conjunction with computer systems and programs, including reproduction or publication in machine-readable form and incorporation in electronic retrieval systems.
Authors retain or are hereby granted (without the need to obtain further permission) rights to use the article for traditional scholarship communications, for teaching, and for distribution within their institution.

☐ **I am the sole author of the manuscript**

☐ **I am signing on behalf of all co-authors of the manuscript**

☐ **The article is a 'work made for hire' and I am signing as an authorized representative of the employing company/institution**

Please mark one or more of the above boxes (as appropriate) and then sign and date the document in black ink.

Signed:_____ **Name printed:** _____

Title and Company (if employer representative) : _____

Date: _____

Data Protection: By submitting this form you are consenting that the personal information provided herein may be used by the Hashemite University and its affiliated institutions worldwide to contact you concerning the publishing of your article.

Please return the completed and signed original of this form by mail or fax, or a scanned copy of the signed original by e-mail, retaining a copy for your files, to:

Hashemite University
Deanship of Scientific Research and Graduate Studies
Zarqa 13115 Jordan
Fax: +962 5 3903338
Email: jjees@hu.edu.jo

Subscription

Jordan Journal of Earth & Environmental Sciences (ISSN 1995-6681)
An International Peer- Reviewed Research Journal
Published by the deanship of Research and Graduate Studies- The Hashemite University

Name:	الاســـــــــــم:
Specialty:.....	التخصـــــــــص:
Address:.....	العنـــــــــوان:
P.O. Box:.....	صنـــدوق البريـــــد:
City & Postal Code:	المدينة: الرمز البريدي:
Country:.....	الـــــــــــدولة:
Phone:.....	رقـــم الهاتـــــف:
Fax No:.....	رقـــم الفاكـــــس:
E-mail:.....	البريـــد الإلكترونـــي:
Method of payment:	طريقـــــة الدفـــع:
Amount Enclosed:.....	المبلـــــغ المرفـــق:
Signature:.....	التوقيـــــــــع:

Cheques should be paid to Deanship of Research and Graduate Studies- The Hashemite University

I would like to subscribe to the Journal:

For

- ☐ One year
- ☐ Two years
- ☐ Three years

One year Subscription Rates		
	Inside Jordan	Outside Jordan
Individuals	10JD	70$
Students	5JD	35$
Institutions	20JD	90$

Correspondence

Subscriptions and sales:

Prof. Dr. Eid Al-Tarazi
The Hashemite University
P.O. Box 330127- Zarqa 13115 - Jordan
Tel. +962-(0) 795651567 (mobile)
+962-5-3903333 - 4229 (office)
Fax: +962 5 3903338
Email: jjees@hu.edu.jo

JJEES
Jordan Journal of Earth and Environmental Sciences

PAGES	PAPERS
1 - 10	Importance of clay minerals in Jordan Case study: Volkonskoite as a sink for hazardous elements of a high pH plume *Hani N. Khoury*
11 - 22	Geochemistry of surficial uranium deposits from central Jordan *Hani N. Khoury*
23 - 28	High Calcium Ash Incorporated Into Clay, Sand and Cement Mortars Used For Encapsulating of Heavy Metals *Tayel El-Hasan, Bassam Z. Mahasneh, Nafeth Abdel Hadi and Monther Abdelhadi*
29 - 34	Geology and Mineralogy of Zeolitic Tuff in Tulul Unuqar Rustum Ash Shmaliyya, NE JORDAN *Khalil M. Ibrahim*
35 - 40	Characterization of Pozzolana from Tafila area and its potential use as soil amendment for plant growth *Reyad Ali Al Dwairi*

JJEES

Jordan Journal of Earth and Environmental Sciences

Volume 6, (Special Publication, Number 3), June, 2014
ISSN 1995-6681
Pages 1- 10

Importance of Clay Minerals in Jordan Case Study: Volkonskoite as a Sink for Hazardous Elements of a High pH Plume

Hani N. Khoury*

Department of Geology, Faculty of Science, The University of Jordan, Amman, Jordan

Abstract

Among the most potential clay deposits in Jordan are kaolinite, bentonite, and palygoskite, volkonskoite, illite, and black mud. A novel geopolymerization process has been recently developed by activating local raw kaolinite to produce green building materials. The clay mineral volkonskoite, a unique green earthy smectite, is widely distributed in central Jordan and is associated with yellow uranium vanadate minerals. Volkonskoite is hosted by altered marble and quaternary thick travertine and recent calcrete deposits. The green clay occurs as thin layers, encrustations and fillings in voids and cavities. The Cr_2O_3 content of the ignited smectites in the new localities ranges between 18.88% and 28.28%. The following are the structural formulae (oxygen = 11) calculated from the microprobe spectral results with the highest and lowest Cr^{+3} content: $Ca_{0.22}Na_{0.03}(Cr_{0.8}Al_{0.89}Mg_{0.3})(Si_{3.92}Al_{0.08})O_{10}(OH)_2$ and $Ca_{0.22}Na_{0.12}(Cr_{1.35}Al_{0.4}Mg_{0.25})(Si_{3.68}Al_{0.32})O_{10}(OH)_2$. The green clay has uninterrupted continuous flaky texture that confirms their chemical origin.

Most of the travertine caps the varicolored marble zones that were discharged of hyperalkaline ground waters in the past. The varicolored marble (combusted bituminous marl) from central Jordan was altered by the circulating hyperalkaline waters that dissolved Cr^{3+} with other redox sensitive elements, and that was immobilized in Cr-rich smectite – volkonskoite solid solution series. Such waters are similar to the present day active hyperalkaline seepages (pH ~ 12.7) in Maqarin area, north Jordan. The authigenic volkonskoite was formed at a pH similar to the alkali disturbed zone expected at radioactive waste repositories. The Jordanian sites provide the best currently known localities to examine the processes associated with the long-term behavior of radwaste repository sites.

Keywords: clay minerals, central Jordan, chromium rich smectites, hazardous elements, high pH water.

1. Introduction

Jordan is a country rich in clays of different origins. Clays of industrial importance are found in different stratigraphic units from Paleozoic to Cenozoic. The most potential deposits are kaolinite, bentonite, and palygoskite. Other deposits, such as volkonskoite, illite, and black mud, are also widely distributed in Jordan. Details of the occurrence, nature, character, and economic importance of the different clay deposits are given by Khoury (2002 & 2006). Recently, zeolite –A has been synthesized from Jordanian kaolinite (Al-Thawabeia, et al. 2015). Kaolinitic clay, from Jordan, proved to be dioxin-free for in clays feed additives (Alawi *et al.*, 2013; 2014).

A novel geopolymerization process has been recently devised on developing building products (geopolymers) through the geopolymerization of Jordanian kaolinite. The products could be used as low cost construction materials for green housing. They are characterized by high strength, high heat resistance, low production cost, low energy consumption, and low CO_2 emissions. The results confirmed that natural Jordanian kaolinite satisfies the criteria to be used as a precursor for the production of high quality inexpensive, stable materials (Khoury *et al.*, 2011a, 2011b; Rahier *et al.*, 2010, 2011; Slaty *et al*., 2013; 2015).

Volkonskoite is an important Cr-rich smectite; it was discovered in 1831 by Kammerer in the Okhansak district of perm province of Russia. It was named after Prince A. Volkonskoite, Minister of the Imperial Court (Khoury *et al.*, 1984; Mackenzie, 1988; Eugene *et al.*, 1988).

Volkonskoite is a dioctahedral member of the smectite group that contains chromium as the dominant cation in the octahedral layers. The following is a general chemical formula for volkonskoite (with a molecular weight of 475.69gm.): $Ca_{0.3}\ (Cr^{+3}, Mg, Fe^{+3})_2\ (Si, Al)_4\ O_{10}\ (OH)_2 \cdot 4H_2O$. Volkonskoite has a bright to dark green or emerald green color. In transmitted light, it is emerald green with dull luster. Cr^{3+} is an effective chromophore. In that only small amount, Cr^{3+} gives intensive color to its host mineral (it is used as natural permanent pigment). For this reason, many smectites were called volkonskoite in literature even though their Cr^{3+} content was minor. The term volkonskoite was applied to Cr-bearing smectites with chromium content ranging from 1 % to about 30 % Cr_2O_3 (Foord *et al*., 1987). Other smectites, with Cr_2O_3 less than 15%, are properly termed chromium montmorillonite, chromium nontronite or are mixture of various chromium-bearing minerals (Foord *et al.*, 1987).

* Corresponding author. e-mail: khouryhn@ju.edu.jo

Volkonskoite is found in Kama river area and Perm basin, as epigenitic minerals commonly filling voids left by the decomposition of plant remains and partly or completely replace organic matter. Cr-bearing smectites have also been formed by the decomposition of ultramafic and mafic rocks in Ural Mountains, Brazil, Bulgaria, Italy, Germany, Norway, Yugoslavia and Nevada. The chromium smectites and chlorites at the Colorado plateau are found in uranium-vanadium deposits and are of epigenitic origin (Foord *et al.*, 1987).

Volkonskoite is widely distributed in central Jordan which could be considered a new type locality for this mineral (Khoury and Abu Jayyab, 1995; Khoury, 2006). Volkonskoite was reported in Daba area for the first time by Khoury *et al*. (1984). More sites have been recently discovered in central Jordan (Khan Ez-Zabib, Tulul Al-Hammam, Siwaqa, and Jabal Al Khurayim area). The structural formulae from these localities are given in Table 1. A new locality has been recently discovered by the author of the present study in Suweileh area, near Amman (Khoury and Zoubi, 2014). The first identified volkonskoite type in central Jordan was characterized to be high chromium, high magnesium and iron free with the following structural formula [1.06M + ($Cr_{2.2}$ $Mg_{2.52}$) ($Si_{7.39}$ $Al_{0.61}$) O_{20} $(OH)_4$]. The chromium content (16%) was higher than that of any volkonskoite yet described from outside the USSR (23.50%) apart from that from Lyalevo, and much higher than that of the samples from the same formation in Palestine (Khoury *et al*., 1984). Khoury and Abu Jayyab (1995) showed a variation in the Cr content in the octahedral sheets of smectites from different sites from Jordan. The green smectites have different affinities to interlayer cations. They attributed that to compositional variations and/or differences in the layer charge distribution.

Recently, as a result of quarrying and exploration activities of marble, travertine, and surficial uranium deposits in central Jordan, green clays have been found as encrustations and they are associated with yellow uranium minerals (Khoury *et al.*, 2014). The clays together with uranium minerals are hosted by the Pleistocene-Recent travertine and calcrete deposits and the altered part of the underlying varicolored marble. The Daba (Khan Az-Zabib) and Siwaqa areas, cover 1320 km^2, and are situated between E36° 00' to 36° 15' and N31° 15' to 31° 45' (Fig. 1). Many tracks leading from the Desert are easily reached from the Amman-Aqaba desert highway, making all parts of the two areas accessible by four wheel-drive vehicles in normal weather. The mean annual precipitation in winter is 110 mm. The mean summer temperature is 23° C with a maximum temperature 44° C and high evaporation rate. The newly discovered clay localities in central Jordan have not been studied before. The following work aims at characterizing the green clayey material from the quarries and trenches mineralogically and chemically, comparing it with that of other localities and at tracing their origin. The importance of the present study lies in introducing the new locality as a natural analogue of engineered barriers in radwaste repository sites.

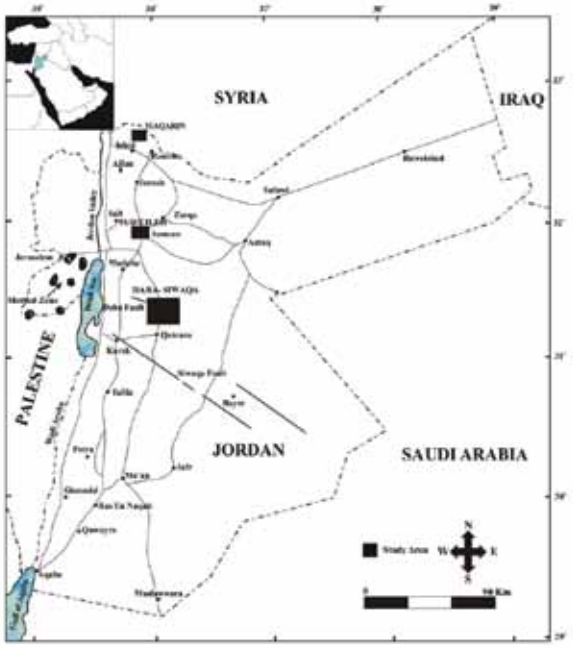

Figure 1: Location map of the study area.

Table 1: Chemical formulae of the studied volkonskoite in Jordan

Structural Formulae	Location	Reference
-$Ca_{0.2}$ ($Cr_{1.1}Mg_{0.4}Al_{0.6}$) ($Si_{3.9}Al_{0.1}$) O_{10} $(OH)_2$ -$Ca_{0.3}$ ($Cr_{0.6}Mg_{0.8}Al_{0.7}$) ($Si_{3.9}Al_{0.1}$) O_{10} $(OH)_2$	Uleimat Quarry	Grathoff & Khoury, 2010
-$Ca_{0.30}Na_{0.23}(Al_{0.47}Cr_{0.63}Fe_{0.13}Mg_{0.66}Zn_{0.06})$ ($Si_{3.88}Al_{0.12}$)O_{10} $(OH)_2$	-Suweileh	Khoury, 2006; Khoury & Zoubi, 2014
-$M^{+}_{0.53}$ ($Si_{3.7}Al_{0.3}$)($Cr_{1.10}Mg_{1.26}$)$O_{10}(OH)_2$	-Zmaileh	
-$Ca_{0.51}Na_{0.03}K_{0.02}(Si_{3.64}Al_{0.036})(Al_{0.08}Ti_{0.02}Fe_{0.08}Cr^{3+}_{0.75}Mg_{1.24})$ $O_{10}(OH)_2$	-Khan Az Zabib	
-$Ca_{0.35}Na_{0.02}(Si_{3.71}Al_{0.29})(Al_{0.29}Ti_{0.01}Fe^{3+}_{0.03}Cr_{1.17}Mg_{0.53})O_{10}(OH)_2$	-Tlul. Al Hammam	
-$Ca_{0.44}Na_{0.03}K_{0.02}(Si_{3.40}Al_{0.6})(Al_{0.44}Ti_{0.04}Fe^{3+}_{0.30}Cr_{0.34}Mg_{0.61})$ $(OH)_2$	-Siwaqa Station	
-$(Ca_{0.22}Na_{0.03})(Si_{3.69}Al_{0.31})(Al_{0.44}Ti_{0.04}Fe^{3+}_{0.23}Cr_{0.53}Mg_{1.07})O_{10}(OH)_2$	-Jabal Khreim	

2. Geology of central Jordan

The geology of central Jordan is illustrated in Fig. 2 and described in details by Khoury *et al*. (2014). The exposed rocks of the studied area (Daba-Siwaqa) are sedimentary and range in age from Upper Cretaceous (Turonian) to Tertiary (Eocene). Pleistocene – Recent travertine, caliche and regolith cover most of the area. The studied area is characterized by unusual colored marble overlain in some areas by travertine and calcrete. The central Jordan varicolored marble is equivalent to the active metamorphic rocks of Maqarin area, north Jordan. The mineralogy is comparable to that of north Jordan (Maqarin) where present day hyperalkaline seepages circulate through the varicolored marble and bituminous marl. The groundwater discharges today in Maqarin is characterized by high hydroxide alkalinity (pH = 12.7), saturation with calcium sulphate and high concentrations of trace elements (Khoury *et al*., 1992; Khoury, 2012). The alkaline meteoric waters circulate through the metamorphic zone and precipitate soft travertine and extract redox sensitive elements from the originally combusted bituminous rocks. All the travertine in

the area are recent and are precipitating as a result of kinetic reaction of the hydroxide waters with atmospheric CO_2 (Khoury and Nassir, 1982 a, b; Khoury *et al*., 1984; Khoury, 1989; Khoury *et al*., 1992).

The studied area (Daba-Siwaqa) was situated in a shallow marine, stable shelf environment of the Tethys Sea during the Late Cretaceous to Early Eocene (~90 - ~50 Ma ago). Transgression took place during Cenomanian times, and marine sedimentation took place until the Late Eocene, despite the fluctuations in sea level. Uplifting caused gentle folding and faulting that was mostly related to the continued tectonic movement along the Jordan Rift which is located ~60 km to the west of the Daba-Siwaqa area (Bender, 1968; Powell, 1989; Powell and Moh'd, 2011).

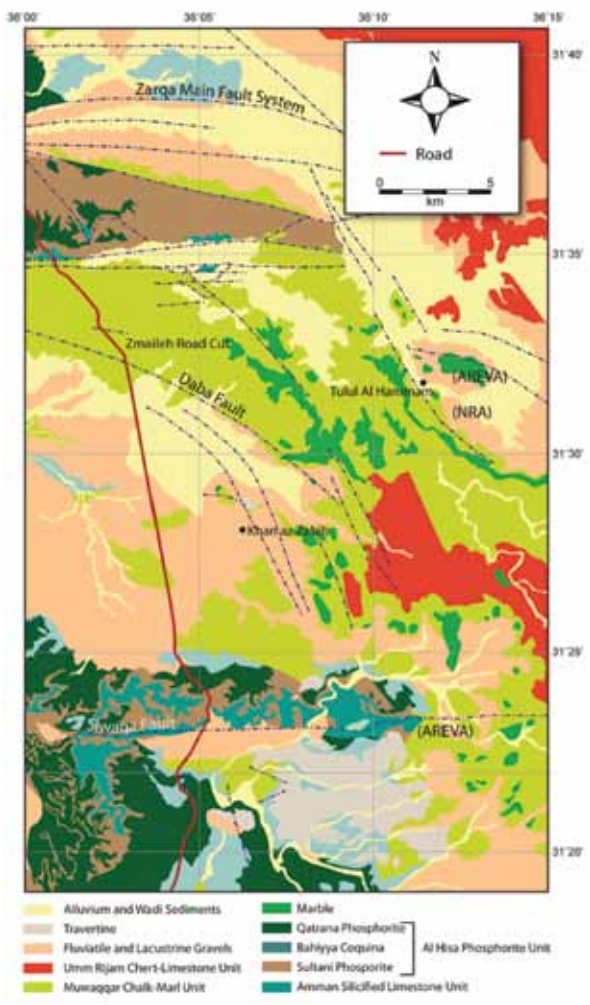

Figure 2: Geologic map of central Jordan (modified after Jasser, 1986; Barjous, 1986; Khoury et al., 2014)

The dominating fault trends are NW-SE and E-W (Fig. 2). The main faults in the area are the Zerqa Main, Daba and Siwaqa fault systems. The fault set is an E-W group of faults and linear features. The folds in central Jordan are of three types: gentle folding associated with regional compression; folding occurring adjacent to faults and directly associated with drag during faulting; and folding in interference structures caused by the interaction of E-W and NW-SE faulting influences (Bender, 1968).

The bituminous marl in central Jordan is biomicrite with average clay content of 10%. Calcite, francolite, quartz, goethite and dolomite are the essential constituents. Framboidal pyrite is found filling the forams cavities. Sensitive reducing elements as U, V, Zn, Cu, Ni, and Fe are present as sulfides and selenides. U-oxides are mostly adsorbed on the clay minerals and organic matter of the bituminous marl and are soluble under reducing environment. The bituminous marl is overlain by the varicolored marble that is composed of prograde and retrograde metamorphic mineral assemblages ((Khoury and Nassir, 1982 a, b; Techer *et al*., 2006; Fourcade *et al*., 2007; Eli *et al*., 2007). The origin of the extreme polymetallic enrichment (Cd, Cr, Mo, Ni, U, V, Zn) of the Late Cretaceous–Early Tertiary rocks, central Jordan was attributed to the bituminous marl (Fleurance *et al*., 2012). Combustion of bituminous marl led to decarbonation and formation of prograde metamorphic minerals (recarbonated calcite, spurrite, larnite, etc.) dominated by isotopically depleted carbonates (Khoury, 2006; Khoury *et al*., 2014). The isotopic evidence supported the high temperature event where the combustion of the organic matter and decarbonation led to the isotopic depletion of $\delta^{13}C$ and $\delta^{18}O$. The increase of the temperature of combustion is positively correlated to the enrichment in light stable isotopes (Clark *et al*., 1993; Khoury, 2006; Khoury *et al*., 2014). Heating sedimentary apatite up to 800° C indicated a change of color into green, where maximum isotopic depletion took place (Nassir and Khoury, 1982).

Travertines and caliche are mainly composed of calcite. Quartz, opaline phases, and sulphates (gypsum and ettringite) are minor constituents of these rocks. These phases are associated with yellow uranium encrustations and green Cr-rich smectite (volkonskoite) that was reported for the first time in central Jordan by Khoury *et al*. (1984).

The source of Cr, U and V is the bituminous marl. The combustion of the organic matter and the formation of varicolored marble, followed by the action of circulating highly alkaline water, accelerated the leaching of the redox sensitive trace elements. Such an alkaline oxidizing environment (pH~12.7) is currently active in Maqarin area, north Jordan.

The alkaline lakes during Pleistocene Recent time in central Jordan were responsible for the precipitation of travertine as a result of kinetic reaction with atmospheric CO_2. Deflation, local subsidence and the prevalence of dry climate in a later stage led to the concentration of trace elements and the precipitation of calcrete that hosted the Cr-rich clay and uranium deposits (Khoury *et al.*, 2013).

3. Field and laboratory work

Field work has concentrated on sampling the green clays associated with varicolored marble, travertine and calcrete. The green clay is associated with the altered marble. The travertine, several meters in thickness is characterized by the presence of green smectite, coprecipitated with calcite. The travertine has a variety of textures including horizontal laminations of porous and massive cryptocrystalline calcite, calcite replacement of opaline phases and green smectite. The excavated trenches indicated the presence of green clay filling the cavities, replacing plant molds, and along bedding planes in travertine and calcrete. Fig. 3 illustrates the green clay with altered varicolored marble (Fig. 3a), filling cavities and replacing plant molds (Fig. 3b), along bedding planes in travertine Fig. 3c) and as encrustationd in calcrete (Fig.3d). Most of the travertines are observed capping the metamorphic (cement) zones and contains brecciated blocks of marble.

Fifteen samples of green smectite rich travertine and marl were collected from the recently opened quarries and trenches; seven (Q-samples) from the quarries and seven from the nearby trenches (T-samples). Table 2 gives a list of the

studied samples. The T-samples were collected from a trench excavated by Areva Co. (N 31° 23' 361", E 36° 11' 361"). The Q-samples were collected from a quarry (N 31° 22' 062", E 36° 11' 280"). Fig. 4 illustrates the location of the sampling sites from central Jordan. The samples were characterized using petrological, mineralogical, and chemical methods. The clay size fraction was separated by using Atterberg techniques. Oriented glass slides (dry and glycolated) were prepared. Part of the analytical work (XRD, XRF, SEM) was carried out in the laboratories of the Federal Institute for Geosciences and Natural Resources, Hannover, Germany, and the Department of Geology, Greifswald University, Germany. Infrared spectra were obtained for the whole rock samples using KBr technique (Merlin spectrometer and software). A Philips diffractometer PW 3710 (40 kV, 30 mA) with CuKa radiation, equipped with a fixed divergence slit and a secondary graphite monochromator was used.

Figure 3: photographs of green clay a) with altered varicolored marble b) filling cavities and replacing plant molds c) along bedding planes in travertine d) as encrustations in calcrete.

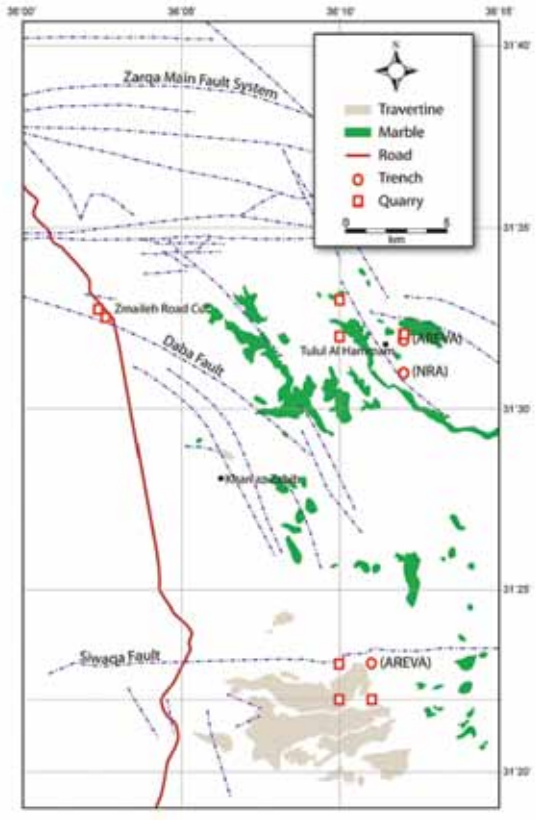

Figure 4: Sampling sites

Table 2: Description of the studied samples.

Sample No.	Description
Q-1	Porous travertine with green clay
Q-2	Porous travertine with green clay
Q-3	Porous travertine with green clay
Q-4	Porous travertine with green clay
Q-5	Porous travertine with green clay
Q-6	Porous travertine with green clay
Q-7 old	Porous travertine with green clay
T2-1	Yellowish gypsum rich calcrete with green clay
T2-3	Yellowish gypsum rich calcrete with green clay
T3-4	Yellowish gypsum rich calcretewith green clay
T3-5	Yellowish gypsum rich calcrete with green clay
T2-6	Dolomite rich calcrete with green clay
T4-1	Red calcrete with green clay
T5-1	Yellowish calcrete with green clay
T5-2	Green yellow calcrete

Q = Quarry T = Trench

Whole rock 'random powder' samples were scanned with a step size of 0.02 - 2 theta and counting time of 0.5 s per step over a measuring range of 2–65 2 theta. Powdered samples were analyzed using a PANalytical Axios and a PW2400 spectrometer. Samples were prepared by mixing with a flux material and melting into glass beads. The beads were analyzed by wavelength dispersive X-ray fluorescence spectrometry (WD-XRF). To determine loss on ignition (LOI), 1,000 mg of sample material was heated to 1,030 ^{o} C for 10 min. After mixing the residue with 5.0 g lithium metaborate and 25 mg lithium bromide, it was fused at 1,200 ^{o} C for 20 min. The calibrations were validated by analysis of reference materials. ''Monitor'' samples and 130 Certified Reference Materials (CRM) were used for the correction procedures.

Polished thin sections were prepared for all the collected samples for both petrographic, Scanning Electron Microscopy, Energy-Dispersive X-Ray spectroscopy (SEM/EDS), and microprobe analyses. This part of the laboratory work was accomplished at the Department of Earth Sciences, University of Ottawa. All green clay rich samples were chemically spot analyzed using scanning electron microscope attached with Oxford INCA large area SDD detector (quantitative analysis of elements for Be to U). The SEM/EDS analyses were done on fine clay crystals. A JEOL 6610LV SEM was used for studying and analyzing the clay phases. A JEOL 8230 Super Probe for quantitative chemical analyses and images of the green clays was used. The electron microprobe is fitted with five WDS spectrometers and a high count-rate Silicon Drift Detector (SDD) EDS spectrometer.

4. Results

The petrographic results indicated that calcite and carbonate-fluorapatite are the essential constituents of the altered varicolored marble. Travertine is mainly composed of micro to cryptocrystalline calcite. Calcite moulds and replacement of vegetation are typical for travertines (Fig. 5a). Smectite, possibly volkonskoite represents the green secondary clay mineral. Mineralized plant molds, replaced by Cr-smectite and calcite are common (Fig. 5b, c). Opaline silica in travertine is common and indicates a later stage of direct precipitation in weakness zones (Fig. 5d). Ettringite, gypsum, fluorite, opal-CT, and secondary apatite are common. The calcrete is mainly composed of calcite and gypsum. Other carbonates (vaterite and aragonite) in addition to secondary calcite were identified from the XRD patterns. Secondary

green Cr-rich smectite and yellow uranium minerals are common in voids and weakness zones of both travertine and calcrete.

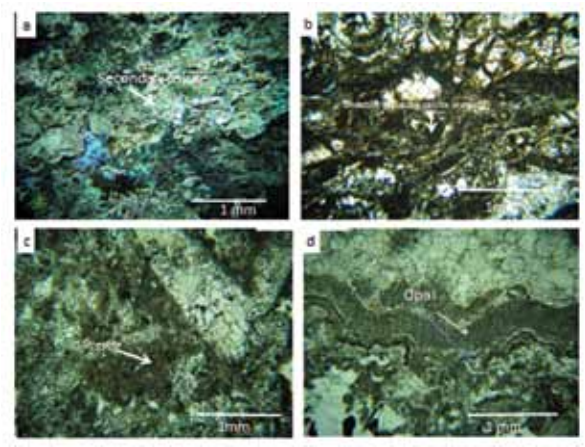

Figure 5: Photomicrographs of a) secondary calcite and replacement of vegetation moulds is typical for travertine (XPL) b, c) mineralized plant molds, replaced by Cr-smectite and calcite are common (PPL) d) opaline silica replacing calcite (PPL)

The secondary green clay from the encrustations, veins of altered marble, travertine, and calcrete was identified from the oriented XRD patterns. The XRD results confirmed the presence of smectite as the essential clay mineral. The XRD basal reflections were constant in all the studied samples. Tyuyamunite, strelkinite, halite and fluorite are associated with the encrustations in the calcrete trench samples. Fig. 6 illustrates a representative XRD pattern of oriented sample of the separated clay fraction. All patterns were identical. The first basal reflection (001) of the dry preparations appears at 12.9 Å and expands to 16.6 Å upon glycolation. The smectite is well ordered and all the basal reflections up to (004) were recorded. The results of the IR spectra of the whole rock samples also confirmed the presence of smectite. Fig. 7 is a representative pattern, illustrating the IR spectra of the minerals in the whole rock samples. This figure illustrates the presence of smectite in addition to calcite and apatite.

The scanning electron micrographs (SEM) photomicrographs indicated that Cr-rich smectites / volkonskoite and the opaline phases are present within the travertine filling voids and cavities and are considered as secondary phases. Opaline phases, however, occur within the some casts of vegetation roots (Fig. 8a). The SEM image indicated that smectite has a cellular and continuous uninterrupted texture (Fig. 8b). The uninterrupted continuous flaky growth of the smectite indicates a chemical origin. The opaline phases associated with the green clay are of late authigenic origin (Fig. 8c). The opaline phases form hexagonal nano-tubes (Fig. 8d).

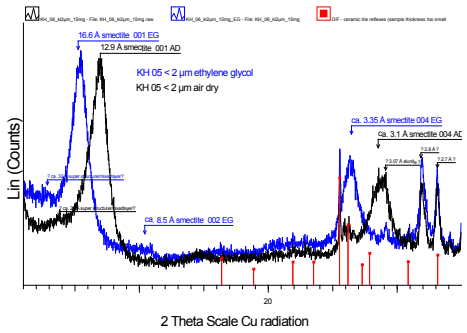

Figure 6: Representative XRD pattern of the studied samples

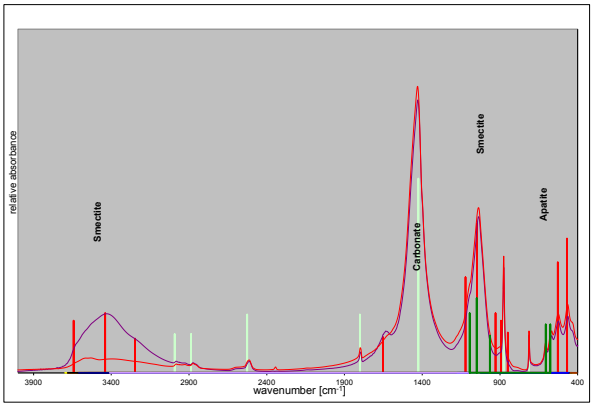

Figure 7: Representative infrared spectra (IR) of the studied samples.

Tables 3 and 4 represent the chemical composition of the major oxides and trace elements of clay hosted travertines and calcrete samples. The CaO and LOI values in Table 3 are related to calcite, apatite and gypsum. The P_2O_5 and F values are related to apatite. SiO_2, Cr_2O_3 and MgO are related to the presence of smectite. The CaO and LOI relationship is plotted in Fig. 9a. The SiO_2 and Al_2O_3 relationship is plotted in Fig. 9b. The MgO and Al_2O_3+Cr_2O_3 relationship is plotted in Fig. 9c. The relatively low positive correlation in these figures is related to the presence of other different phases as calcite, apatite and gypsum. Table 4 shows that the samples are enriched in trace elements as Cr, U, V, Sr, Zn, Zr and Ni up to 7.46 wt. %, 419ppm, 0.74 wt.%, 1042 ppm, 1603 ppm, 117ppm, and 1095ppm, respectively. Cr together with the other elements is considered as redox sensitive elements and is possibly absorbed by smectite. Cr values are related to the presence of Cr-rich smectite as indicated from the EDX/ EDS, XRF (clay fraction) and electron microprobe results. The chemical composition agrees with the XRD results of the whole rock samples.

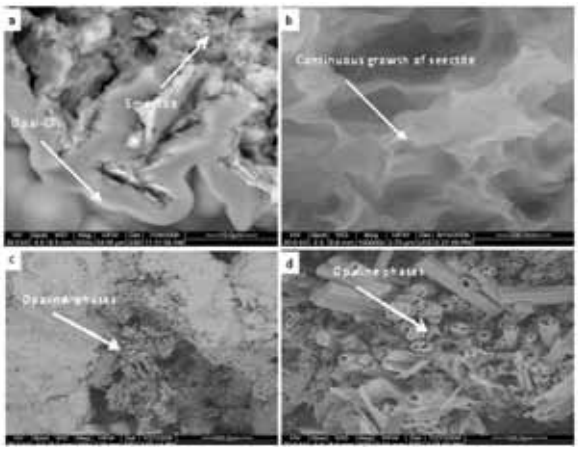

Figure 8: Scanning electron micrographs a) opal-CT with volkonskoite b) continuous growth of volkonskoite c) later authigenic opaline phases d) opaline silica tubes (Khoury, 2012)

Table 3: XRF results of the whole rock samples (Khoury, 2012)

Sample N	SiO2	TiO2	Al2O3	Fe2O3	Cr2O3	MgO	CaO	Na2O	K2O	P2O5	SO3	F	LOI	Total
Q-1	10.17	0.121	2.8	1.023	3.3	0.81	42.721	0.282	0.042	0.731	0	0	35.7	94.4
Q-2	15.37	0.143	4.19	1.397	3.49	1.378	35.894	0.513	0.103	1.192	0	0.24	31.73	92.151
Q-3	11.71	0.11	3.33	0.987	2.3	1.093	41.512	0.429	0.044	0.986	0	0.14	35.19	95.531
Q-4	16.58	0.16	4.38	1.123	2.26	1.55	36.187	0.242	0.035	0.875	0	0.01	33.91	95.057
Q-5	17.63	0.082	3.22	0.611	3.59	2.603	36.464	0.195	0.03	8.063	0	1.16	24.42	94.48
Q-6	11.78	0.085	2.69	0.609	1.84	1.895	42.82	0.156	0.034	8.63	0	1.08	27.1	96.88
Q-7	27.39	0.179	4.03	0.592	10.89	2.232	21.026	1.028	0.23	1.231	0	0.1	27.36	85.398
T-4	4.99	0.05	0.83	0.26	0.77	0.458	50.491	0.042	-0.004	0.914	0	0.3	40.19	98.527
T5-2	4.95	0.066	1.5	0.542	0.68	0.668	31.978	0.207	0.044	0.771	13.44	0.22	23.32	77.717
T2-3	11.36	0.048	1.7	0.368	3.79	2.161	28.37	0.402	0.073	1.093	2.6	0	23.45	71.635
T3-4	5.13	0.041	1.56	0.305	3.88	0.637	31.884	0.368	0.035	1.106	20.5	0.19	25.03	86.788
T3-5	19.93	0.129	3.3	0.893	4.22	3.882	27.564	0.665	0.155	4.84	6.02	0.55	22	89.946
T5-1	20.03	0.163	6.09	1.381	2.9	5.761	24.985	1.087	0.088	4.196	1.24	0.81	25.47	91.333
T2-6	18.11	0.044	2.06	0.278	9.21	2.924	26.348	0.588	0.085	0.488	4.15	0	27.66	82.741
T2-1	36.04	0.414	7.58	2.676	0.09	2.131	19.562	0.943	0.471	1.793	0	0.3	20.97	92.891

Table 4: XRF results of trace elements in the whole rock samples (ppm)

Sample	Cr	Ni	Sr	U	V	Zn	Zr
Q-1	17635.6	124	439.8	8.7	124.3	538.1	37.3
Q-2	23888.1	316.8	418.8	12.8	164.7	687.9	50.7
Q-3	15796.8	211.7	484.4	9.8	135.7	482.6	47.3
Q-4	15936.9	242.3	819	8.8	142.3	245.7	78.8
Q-5	24640.9	277.8	600.5	37.8	193.2	417.8	65.5
Q-6	12660	161.6	733.9	37.1	124.5	452.5	79.7
Q-7	74621	189.6	600.8	33.1	1117	265	75.2
T2-1	594.3	93.2	575.3	33.5	429.3	346.5	117.6
T2-6	63171.4	107.3	726.8	419.4	7137.3	207.9	43.9
T2-3	26059.5	151.8	466.3	41.1	5235.6	3761.3	45.6
T3-4	26600.4	93.5	747.9	76.9	7444.4	287.2	46.2
T3-5	28913.7	300.9	596.9	41.2	4217.6	1228.7	79.5
T-4	530.7	43.9	405.6	6.4	61.9	399.9	27.8
T5-1	19966.7	1095.2	1042.9	32.9	9520.4	1603.7	114
T5-2	4723.1	204.6	381	85.8	2023.5	222.5	46.8
Maximun	74621	1905	1042	419	9520	3761	117
Minimum	530	44	381	6.4	61.9	207.9	27.8
average	23715	240	602	59.02	2538	743	4649

Table 5 gives the chemical composition of the major oxides of the separated clay (QU1 samples) and silt (QU2 samples) size fractions of few selected samples. The table indicates the presence of a lot of impurities in the clay fraction as phosphates (Q1-1, Qu1-2, Qu1-3), carbonates (Qu1-4, Qu1-5), and opaline amorphous silica (Qu1-4 and Qu1-5). The silt size fraction is dominated by carbonates as indicated from the CaO content and the high LOI values. Most of the XRD patterns of the clay fraction indicate the presence of smectite, with few crystalline phases as apatite and calcite. It was difficult to calculate the structural formulae of smectites with all these clay size impurities. The poor correlation between the major oxides is related to the presence of impurities. Table 6 gives the XRF results of the trace elements of the separated clay (QU1 samples) and silt (QU2 samples) size fractions of the same samples.

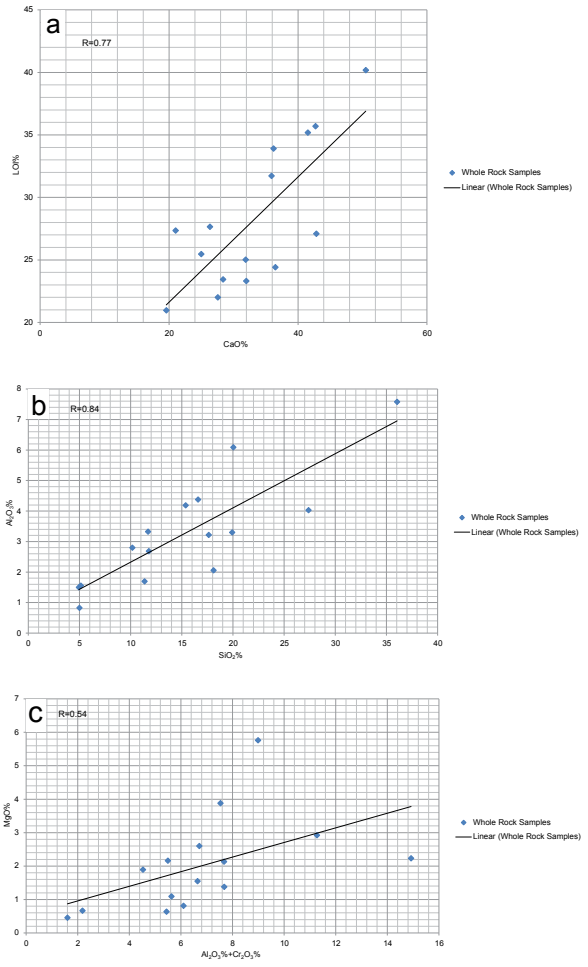

Figure 9: Plot of the relationship between a) CaO and LOI b) SiO_2 and Al_2O_3 c) MgO and Al_2O_3+Cr_2O_3.

The comparison of the average values of the redox sensitive elements As, Cr, Cu, Ni, U, V, Zn and Zr in both fractions, indicates a higher concentration is in the clay size fraction. The only exception is the higher values of Sr in the silt size fraction, that is related to the presence of calcite.

The SEM/EDS results revealed the presence of almost pure crystallites of smectite (Fig. 10a, b, c, d) and are composed of oxides of SiO_2, Al_2O_3, Cr_2O_3 and MgO. These oxides are the essential components of the smectite. These crystallites were analyzed by the electron microprobe (Fig. 11). The results are given in Table 7. The following structural formulae were calculated and indicated the substitution of Cr and Mg for Al in the octahedral layer: $Ca0.22Na0.03$ $(Cr_{0.80}Al_{0.89}Mg_{0.30})$ $(Si_{3.92}Al_{0.08})$ O10 (OH)2; $Ca_{0.22}Na_{0.12}$ $(Cr_{1.35}Al_{0.40}Mg_{0.25})$ $(Si_{3.68}Al_{0.32})$ O10 (OH)2. These formulae added more information about the known volkonskoite from other localities in Jordan and support the idea of possible solid solution between dioctahedral smectites (montmorillonite, Cr-smectite and volkonskoite).

Table 5: XRF results in wt% of the major oxides (%) in the (QU1) and silt (QU2) size fractions.

Sample	SiO2%	TiO2%	Al2O3%	Fe2O3%	MnO2%	MgO%	CaO%	Na2O%	K2O%	P2O5%	SO3%	Cl%	F%	LOI%	Total
QU1-1	28.87	0.57	5.55	0.83	<0.001	2.17	10.955	11.39	1.019	7.073	0.24	4.652	0.5	18.56	92.37
QU1-2	34.6	0.562	6.7	0.87	<0.001	2.19	9.302	7.83	0.612	5.928	0.17	2.054	0.4	18.11	89.33
QU1-3	44.36	0.649	12.49	5.23	0.04	2.06	9.811	0.24	0.557	6.004	<0.01	0.036	0.19	17.65	99.32
QU1-4	68.12	0.406	9.45	7.14	0.054	1.41	0.634	2.36	0.437	0.483	<0.01	0.068	<0.05	9.16	99.76
QU1-5	30.18	0.512	8.27	0.58	<0.001	2.47	22.743	0.15	0.073	14.687	0.06	0.035	1.23	16.41	97.41
QU1-6	79.11	0.229	0.79	0.13	0.031	3.73	0.322	0.58	0.077	0.041	<0.01	0.017	0.09	9.17	94.31
QU1-7	45.08	0.4	13.42	2.96	0.029	6.11	3.873	0.86	0.143	0.838	0.06	0.003	0.05	19.96	93.78
QU2-1	10.13	0.351	1.7	0.36	<0.001	0.72	44.026	0.05	0.036	2.372	0.28	0.093	0.36	35.76	96.24
QU2-2	10.81	0.304	1.65	0.23	<0.001	0.57	42.498	0.08	0.024	2.42	0.36	0.049	0.42	35.5	94.91
QU2-3	27.74	0.542	2.48	1.7	0.025	0.79	34.694	0.38	0.371	9.056	0.28	0.04	1.14	20.67	99.91
QU2-4	75.56	0.46	6.36	6.37	0.225	1.01	1.164	0.03	0.305	0.29	<0.01	0.016	<0.05	7.67	99.67
QU2-5	26.06	0.118	0.31	0.06	<0.001	0.86	38.256	<0.01	0.021	0.187	0.1	0.035	0.25	32.27	98.57
QU2-6	36.47	0.042	<0.05	<0.01	0.002	0.34	33.932	<0.01	<0.005	0.138	0.05	0.029	0.1	28.32	99.44
QU2-7	4.76	0.252	1.07	0.49	0.004	0.76	50.29	<0.01	0.013	0.978	0.35	0.012	0.36	39.55	98.91

QU1 = Clay size fraction; QU2 = Silt size fraction

AV clay	47.18	0.47	8.09	2.53	0.04	2.8	8.23	3.34	0.41	5.0	0.13	0.98	0.41	15.57	95.18
AV silt	27.36	0.29	2.26	1.53	0.064	0.72	30.62	0.135	0.013	2.20	0.23	0.039	0.43	28.56	98.23

Table 6: XRF results of trace elements (ppm) of the clay (QU1) and silt (QU2) size fractions.

Sample	As	Cr	Cu	Ni	Sr	U	V	Zn	Zr
	ppm	ppm	ppm	ppm	ppm	ppm	ppm	ppm	ppm
QU1-1	38	57062	148	259	347	68	981	171	75
QU1-2	65	73532	184	363	349	49	1225	457	75
QU1-3	27	1929	137	250	302	38	659	1085	95
QU1-4	24	226	45	65	22	3	299	276	50
QU1-5	4	12182	181	759	672	79	797	6357	65
QU1-6	13	35670	113	226	8	25	115	2540	4
QU1-7	118	33542	468	673	80	96	1475	5727	65
QU2-1	42	23314	70	81	482	28	459	207	41
QU2-2	54	31977	77	86	536	20	528	196	44
QU2-3	8	145	67	52	578	30	147	233	238
QU2-4	19	127	32	68	77	4	275	325	67
QU2-5	9	6111	38	46	120	42	82	992	17
QU2-6	6	2894	20	12	119	12	26	197	<3
QU2-7	36	2590	68	105	167	48	336	521	37

QU1 = Clay size fraction; QU2 = Silt size fraction

AV clay	41.28	30591	182	370	254	51	793	2373	61
AV silt	24.85	9594	35.14	64.28	297	26.28	264	381	74

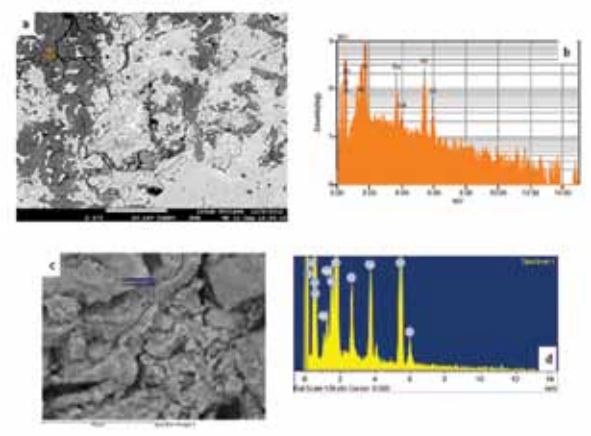

Figure 10: SEM/EDS photomicrographs and spectra of the green clay showing Al, Mg, Cr and Mg as the major components a & b) polished thin section b & d) uncoated sample.

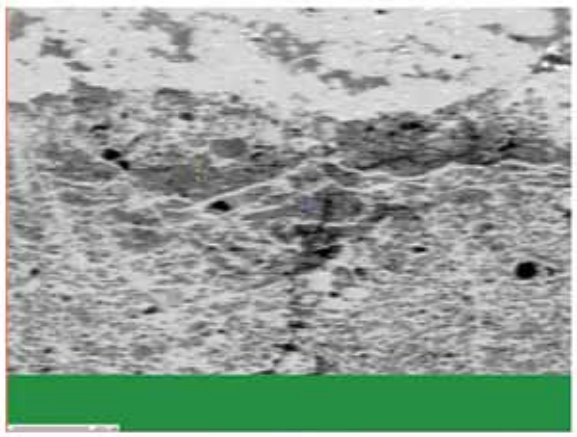

Figure 11: Some selected spots for the electron microprobe analysis.

Table 7: Electron microprobe analyses in wt% of green clay used for the calculation of structural formulae.

Oxides%	18 tq-1 1	19 tq-1 2	20 tq-1 3	21 tq-1 4	22 tq-1 5	24 tq-1 6	25 tq-1 7	26 tq-1 8
SiO2	45.551	51.516	39.264	51.744	45.698	49.117	40.504	53.621
Al2O3	7.627	8.66	6.544	11.982	9.885	10.395	13.063	12.372
TiO2	0.809	0.872	0.084	0.062	0.041	0	0.027	0.091
FeO	0.102	0.095	0.04	0.178	0.134	0.05	0.079	0.133
Cr2O3	22.295	22.953	18.21	17.34	16.393	25.439	21.067	16.764
MgO	1.975	1.923	1.746	3.411	2.959	2.22	2.299	3.934
CaO	2.471	2.492	2.259	2.197	1.932	2.559	2.633	1.816
K2O	0.039	0.06	0.038	0.075	0.071	0.026	0.013	0.039
MnO	0.017	0.028	0.022	0.018	0.02	0.027	0.007	0.015
ZnO	0	0.036	0.062	0.048	0.01	0	0.071	0.033
Cl	0.959	0.481	0.555	0.486	0.52	0.144	1.092	0.161
F	0.037	0.056	0.487	0.46	0.241	0.062	0.06	0.128
SO3	0.105	0.103	0.105	0.137	0.021	0.12	0.137	0.069
P2O5	0.018	0.052	0.039	0	0.046	0.02	0.104	0
Calc Total	82.26	89.58	70.13	88.25	78.16	90.44	81.68	89.46

5. Discussion

The XRD basal reflections of the studied Cr-rich smectite/volkonskoite were constant, although the chemical composition and the structural formulae show variation in the Cr content in the octahedral sheets. Specimens from different sites have different affinities to interlayer cations (Table 1; current study). This is attributed to compositional variations and/or differences in the layer charge distribution. The negative charge in the tetrahedral and octahedral sheets is not equally distributed. The differential substitution would result in the variation of the total negative charge within the layers, and accordingly would lead to the variation in the adsorption capacities of the interlayer cations.

Cr-rich smectites/volkonskoite associated with the travertines, calcrete and altered marble in central Jordan were precipitated from ascending high alkaline solution, following the combustion of the original bituminous marls and limestones. The free continuous crystal growth suggests an epigenetic origin and was probably precipitated after calcite and opal. The water chemistry was ideal for the precipitation of the green clay after the removal of CaO and silica from solution (Figs. 5 & 8). The travertine and calcrete were precipitated from highly alkaline groundwater containing calcium hydroxide (pH=12.5) through the uptake of atmospheric CO_2 and subsequent precipitation of calcite (Khoury, 2012; Khoury *et al*., 2014). Such waters were similar to cement pore water and equivalent to the present day hyperalkaline seepages at Maqarin, north Jordan (Khoury *et al*., 1992).

The mineralogy of the varicolored marble in central Jordan (Daba-Siwaqa area) is comparable to that of cement clinker and to hydrate cement products (Khoury and Nassir, 1982a, b; Khoury *et al*., 2014). These rocks are long term natural analogues of Portland cement for sealing of nuclear waste. Premature failure could present serious hazards or release of radionuclides into the environment. Many repository designs, especially those for low- and intermediate-level waste, involve the use of very large amounts of cementitious materials. Bentonite (70% smectite) is one of the most safety-critical components of the engineered barrier system for the disposal concepts developed for many types of radioactive waste (radwaste). The choice of bentonite results from its favourable properties – such as plasticity, swelling capacity, colloid filtration, low hydraulic conductivity, high retardation of key radionuclides and its stability in relevant geological environments (Alexander and McKinley, 1999). However, bentonite (smectites) are unstable at high pH. The interaction of cement with groundwater results in a hyperalkaline leachate which contains any radionuclides dissolved from the waste. The interaction of such leachate with surrounding rock and the mobility of radionuclides in this complex system must be considered in repository safety assessment. The very slow kinetics of many of the reactions involved, however, greatly limit the applicability of conventional laboratory studies. The varicolored marble, travertines and calcrete of Daba-Siwaqa sites of central Jordan can serve as natural analogues of a cementitious repository. Quaternary travertines capping the metamorphic (cement) zones are the fossilized products of ancient hyperalkaline groundwater discharges (pH ~ 12.7) (Khoury, 2012; Khoury *et al*., 2014). The travertine and calcrete indicate a long-term analogue of carbonation and remobilization of silica in cementitious barriers for radioactive waste repositories.

Relatively high levels of Cr, Ni, Cu, Zn, U, V, and Zr, are associated with the clay size fraction with the exception of Sr that is associated calcite (Table 6). The presence of Cr-rich smectites - volkonskoite with relatively high levels of U and other redox elements may suggest the use of central Jordan outcrops as analogues with the repository disturbed zone. Smectites are expected to be a sink of alteration products in the late stage evolution of a high pH plume.

6. Summary and Conclusions

The present work demonstrated the value of the altered marble, travertine and calcrete in central Jordan as analogues of cementitious repositories. The sites indicate a long-term analogue of carbonation and remobilization of hazardous elements in cementitious barriers for radioactive waste repositories. The sites offer a good chance to investigate the interaction of the high-pH water enriched with leached hazardous trace elements (Zn, Cr, U, Cu, Ni, V, etc.) with rocks. Heavy metals if removed into groundwater may be hazardous. Co-precipitation of these elements in mineral phases is of great importance to control the concentration of these elements in groundwater. For example, the unusual Cr-smectite - volkonskoite precipitated from the mobile alkaline water may act as sinks for such trace elements.

Mineralogical investigations of natural analogues of cement systems, which underwent reaction with CO_2 over time periods measurable in thousands of years, could give us

an idea about the uptake history of atmospheric CO_2. Central Jordan areas however, represent unique sites to study the durability of Portland cement and concrete, especially for long term assessment of radioactive waste storage. The interface of marble (natural cement zone) overlain by travertine offers large size sampling site which is similar to a sedimentary disposal site. Further investigations of the area and detailed work on the mineral phases in the marble (cement) zone and travertine may aid in understanding the processes likely to occur in the repository near site disturbed zone.

Acknowledgments

The author would like to thank the Deanship of Scientific Research at the University of Jordan for their financial support during my sabbatical year at the Department of Earth Sciences, University of Ottawa, Canada. Thanks are extended to Prof. Ian Clark and Late Prof. Andre Lalonde for supporting part of the analytical work in the different laboratories.

The other part of the analytical work was done at the laboratories of the Federal Institute for Geosciences and Natural Resources, Hanover, and the Department of Geology, Greifswald University, Germany. Special thanks are due to Dr. R. Dohrmann and Dr. J. Grathoff, for their help and cooperation.

References

[1] Alawi, M., Najjar, A., and Khoury, H., 2013. Analytical Method Development for the Screening and Determination of Dioxins in Clay Matrices. www. clean-journal.com. Clean – Soil, Air, Water, 41, 1-7.

[2] Alawi, M., Najjar, A., and Khoury, H. 2014. Levels of Polychlorinated Dibenzodioxins/Dibenzofurans in Jordanian Clay, Clean – Soil, Air, Water, 41, 1-7. DOI: 10.1002/ clen.201400240.

[3] Al-Thawabeia, R., Khoury, H., and Hodali, H. 2015. Synthesis of zeolite 4A via acid–base activation of metakaolinite and its use for water hardness treatment. Desalination and Water Treatment. DOI: 10.1080/19443994.2014.941413. (In Publication)

[4] Alexander, R., and McKinley, M. 1999. The chemical basis of near-field containment in the Swiss high-level radioactive waste disposal concept. pp 47-69 in Chemical Containment of Wastes in the Geosphere (eds. R.Metcalfe and C.A.Rochelle), Geol.Soc.Spec.Publ. No. 157, Geol Soc, London, UK.

[5] Barjous, M., 1986. The geology of Siwaqa, Bull. 4, NRA, Amman – Jordan.

[6] Bender, F., 1968. Geologie von Jordanien. Beiträge zur Regionalen Geologie der Erde, Band 7 Gebrüder Bornträger; Berlin.

[7] Clark, I., Firtz, P. Seidlitz, H., Khoury, H., Trimborn, P., Milodowski, T., and Pearce, J., 1993. Recarbonation of metamorphosed marls, Jordan. App. Geochem. 8: 473 - 481.

[8] Elie, M., Techer, I., Trotignon, L., Khoury, H., Salameh, E., Vandamme,D., Boulvais, P. and Fourcade, S., 2007. Cementationof kerogen-rich marls by alkaline fluids released during weathering of thermally metamorphosed marly sediments. Part II: Organic matter evolution, magnetic susceptibility and metals (Ti, Cr, Fe) at the Khushaym Matruck natural analogue (central Jordan). Applied Geochemistry, 22, 1311 - 1328.

[9] Eugene, E., Foord, Starkey, H., Joseph, T., Taggart, E., and Shawe, D., 1988. Reassessment of the volkonskoite-chromian smectite nomenclature problem; reply, Clays and Clay Minerals, 36: 541.

[10] Fleurance, S., Cuney, M., Malartre, M., and Reyx, J., 2012. Origin of the extreme polymetallic enrichment (Cd, Cr, Mo, Ni, U, V, Zn) of the Late Cretaceous–Early Tertiary Belqa Group, central Jordan, Palaeogeography, Palaeoclimatology, Palaeoecology, http://dx.doi.org/10.1016/j.palaeo.2012.10.020.

[11] Foord, E. E., Starkey, H. C., Taggart, J. E., Jr., and Shawe, D.R., 1987. Reassessment of the volkonskoite-chromian smectite nomenclature problem: Clays & Clay Minerals, 35, 139-149.

[12] Fourcade, S., Trotignon, L., Boulvais, P., Techer, I., Elie, M., Vandamme, D., Salameh, E., and Khoury, H., 2007. Cementation of kerogen-rich marls by alkaline fluids released during weathering of thermally metamorphosed marly sediments. Part I: Isotopic (C,O) study of the Khushaym Matruk natural analogue (central Jordan). Applied Geochemistry, 22, 1293 - 1310.

[13] Grathoff, G., and Khoury, H.N., 2010. A long-term natural analogue for radioactive waste repositories? Mineralogy and Chemistry of a Volkonskoite (Cr-rich smectite) in Travertine deposits from Central Jordan.SEA- CSSG- CMS. (Abstract), Trilateral Meeting on clays, Madrid.

[14] Jasser, D., 1986. The geology of Khan Ez Zabib, Bull. 3, NRA, Amman – Jordan.

[15] Khoury, H.N., 2002. Clays and clay minerals in Jordan, Amman: Special Publication, University of Jordan.

[16] Khoury, H., 2006. Industrial rocks and minerals in Jordan (second edition). Publications of the University of Jordan, Amman.

[17] Khoury, H. N. 2012. Long-Term Analogue of Carbonation in Travertine from Uleimat Quarries, Central Jordan. Environmental and Earth Science. 65:1909-1916. 4.

[18] Khoury, H., and Nassir S., 1982a. A discussion on the origin of Daba – Siwaqa marble, Dirasat, 9 : 55-56.

[19] Khoury, H. N. and Nassir S.,1982b. High temperature mineralization in Maqarin area, Jordan. N. Jb. Miner. Abh. 144, 187-213.

[20] Khoury, H. N. and Abu-Jayyab 1995. A short note on the mineral volkonskoite. Dirasat, No 1, 189-198.

[21] Khoury, H., and Al-Zoubi, A. 2014 Origin and characteristics of Cr-smectite from Suweileh area, Jordan. Applied Clay Science, 90, 43–52.

[22] Khoury, H. N., Salameh, E. M. and Clark I. D. 2014. Mineralogy and origin of surficial uranium deposits hosted in travertine and calcrete from central Jordan. Applied Geochemistry, 43, 49–65

[23] Khoury, H., Mackenzie, R., Russell, J., and Tait, J., 1984. An iron free volkonskoite. Clay Minerals, 19: 43-57.

[24] Khoury, H. N., Salameh,E., Clark, I., Fritz,P., Bajjali,W., Milodowski, A., Cave, M., and Alexander, R., 1992. A natural analogue of high pH cements pore waters from the Maqarin area of northern Jordan 1: Introduction to the site. Jour. Geoch. Expl. 46, 117-132.

[25] Khoury, H., Al Dabsheh, I., Slaty, F., Abu Salha, Y., Rahier, H., Esaifan, M.,and Wastiels, J., 2011a. The Effect of Addition of Pozzolanic Tuff on Geopolymers.The American Ceramic Society Advanced Ceramics and Composites (ICACC), Developments in Strategic Materials and Computational Design II: Ceramic Engineering and Science Proceedings, Volume 32, Issue 10, pages 53-69. A. Gyekenyesi, W. Kriven, J. Wang, M. Singh (Editors).Wiley. ISBN: 978-1-1180-5995-1.

[26] Khoury, H., Abu Salha, Y., Al Dabsheh, I., Slaty,Alshaar, M., F., Rahier, H., Esaifan, M., and Wastiels, J., 2011b. Geopolymer Products from Jordan for Sustainability of the Environment. Advances in Materials Science for Environmental and Nuclear Technology II. The American Ceramic Society: Ceramic Transactions, 227, 289-300, S. Sundaram, T. Ohji, K. Fox, E. Hoffman (Editors). Wiley, ISBN: 978-1-1180-6000-1

[27] Rahier, H., Slatyi F., Aldabsheh, I., Alshaaer, M., Khoury, H., Esaifan M., and Wastiels J. 2010. Use of local raw materials for construction purposes Advances in Science and Technology Vol. 69 pp 152-155. Trans Tech Publications, Switzerland. www.scientific.net/AST.69.152.

[28] Rahier, H., Esaifan, M., Wastiel,s J., Slatyi, F., Aldabsheh, I., Khoury H., 2011. Alkali activation of kaolinite for production of bricks and tiles. Non-traditional cement and concrete IV, pp.162 - 170, eds. Vlastimil Bilek, Zbynek Kersner.

[29] Nassir, S., and Khoury, H., 1982. Mineralogy, petrology, and origin of Daba-Siwaqa marble, Jordan. Dirasat. 9: 107-130.

[30] Powell, J.H., 1989. Stratigraphy and sedimentology of the Phanerozoic rocks in central and southern Jordan. Bull. 11, Geology Directorate, natural resources Authority (Ministry of Energy and Mineral resources) Amman, Part B: Kurnub, Ajlun and Belqa group, 161.

[31] Powell, J. H., Moh'd, B.K., 2011. Evolution of Cretaceous to Eocene alluvial and carbonate platform sequences in central and south Jordan. GeoArabia, 16, 4, 29-82.

[32] Slaty, F., Khoury, H., Wastiels, J H. Rahier ., 2013. Characterization of alkali activated kaolinitic clay. Applied Clay Science, 75–76 (2013) 120–125.

[33] Slaty, F., Khoury, H., Wastiels, J H. Rahier. (2015): Durability of alkali activated cement produced from kaolinitic clay. Applied Clay Science. (In Publication)

[34] Mackenzie, R. C., 1988. Reassessment of the volkonskoite-chromian smectite nomenclature problem; comment. Clays and Clay Minerals 36: 540.

[35] Techer, I., Khoury, H., Salameh, E., Rassineux, F., Claude, C., Clauer, N., Pagel, M., Lancelot, J., Hamelin, B., and Jacquot, E, 2006. Propagation of high-alkaline fluids in an argillaceous formation: Case study of the Khushaym Matruk natural analogue (Central Jordan). Jour. of Geoch. Exploration, 90, 53-67.

JJEES
Jordan Journal of Earth and Environmental Sciences

Volume 6, (Special Publication, Number 3), June, 2014
ISSN 1995-6681
Pages 11- 22

Geochemistry of Surficial Uranium Deposits from Central Jordan

Hani N. Khoury*

Department of Geology, Faculty of Science, The University of Jordan, Amman, Jordan

Abstract

Inhomogeneous unusual surface uranium mineralization hosted by chalk marl/travertine and calcrete/top soil covers large areas in central Jordan. Quarries and trenches with bituminous marl, varicolored marble, travertine and caliche were sampled to understand the geochemistry of the uranium deposits. The samples were characterized mineralogically and chemically using XRD, XRF, SEM, EDX techniques. Relatively high uranium concentrations were found in the calcrete samples where it reaches up to 419 ppm. The secondary uranium mineralization is restricted to the permeable fractured and porous zones. The combustion of the bituminous marl led to the formation of the varicoloured marble in central Jordan. This was followed by the action of circulating highly alkaline water that accelerated the leaching of the redox sensitive trace elements as U and V. Such an alkaline oxidizing environment (pH~12.7) is currently active in Maqarin area, north Jordan. The paleo-circulating water in the combusted rocks of central Jordan oxidized the dissolved V^{4+} to V^{5+} and fixed the uranyl-ion as uranyl vanadate. Strelkinite and/or tyuyamunite precipitation and the solid solution, between the two end members, were dependent on the Ca/Na ratio in solution. Carnotite is restricted to the veins associated with the varicoloured marble. The uranyl-vanadate minerals were precipitated from highly alkaline solutions during the dry periods after the precipitation of the thick travertine deposits.

Keywords: Surficial uranium minerals, central Jordan, U-V minerals, travertine, calcrete.

1. Introduction

Uranium deposits are found in all types of rocks as a result of magmatic, metamorphic and sedimentary processes (Dahlkamp, 1993). Genetic classification of uranium deposits has indicated the exceptional diversity of processes involved in their formation (Cuney, 2009).

Surficial uranium deposits are defined by the International Atomic Energy Agency as young (Tertiary to Recent) near-surface uranium concentrations in sediments or soils (IAEA, 2009). The largest surficial deposits are the calcrete soils and usually cemented by calcium and magnesium carbonates. Such soils form uranium-rich sediments by evapotranspiration process in fluviatile to playa systems in a semi-arid to arid climate (Mckay and Miezitis, 2001). Calcrete related uranium deposits occur in valley-fill and in Playa Lake sediments in Western Australia, and at the top of the alluvial sediments in central Namib Desert of Namibia. Uranium is entirely deposited as UO_2 minerals carnotite $K_2(UO_2)_2(VO_4)_2 \cdot 3H_2O$ and tyuyamunite $Ca(UO_2)_2(VO_4)_2 \cdot 5\text{-}8H_2O$ (Cuney, 2009). Tyuyamunite is closely related to carnotite as indicated by the chemical formula, which is the same except that calcium substitutes for the potassium of carnotite. Strelkinite $Na_2(UO_2)_2(V_2O_8).6H_2O$ is the sodium analogue of carnotite and tyuyamunite.

In central Jordan, unusual surface uranium deposits cover large areas and are mainly associated with the varicolored marble, Pleistocene-Recent travertine and calcrete. Yellow uranium encrustations are also associated with the varicolored marble (pyrometamorphic rocks) and the underlying bituminous marl (oil shale) and phosphorites (Khoury et al., 2014). The uranium bearing rocks are widely distributed in two areas: Daba (Khan Az-Zabib) and Siwaqa (Fig. 1). The northern boundaries of the first and second areas are located 25 km and 60 km south of Amman with the first area situated between E36° 00' to 36° 15' and N31° 15' to 31° 30' and the second area between E35° 00' to 36° 15' and N31° 15' to 31° 30'.

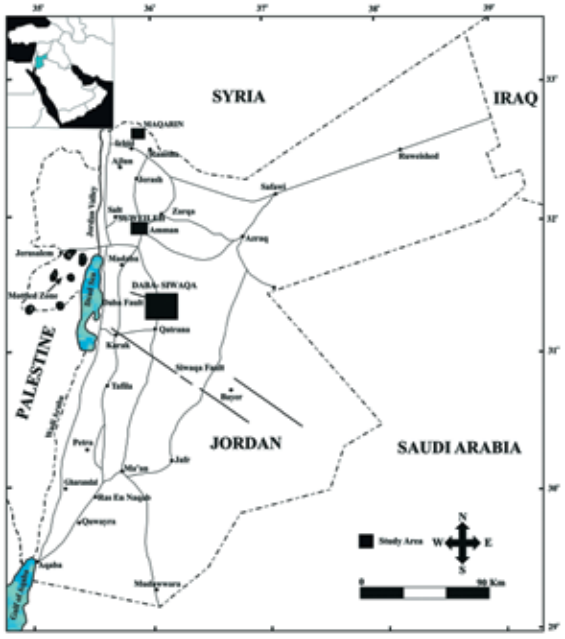

Figure 1: Location map of Daba-Siwaqa area, central Jordan.

* Corresponding author. e-mail: khouryhn@ju.edu.jo

Daba covers 662 sq. km and Siwaqa covers about 660 sq. km. Many tracks leading from the Desert are easily reached from the Amman-Aqaba desert highway, making all parts of the two areas accessible by four wheel-drive vehicles in normal weather. The mean annual precipitation in winter is 110 mm. The mean summer temperature is 23°C with a maximum temperature 44°C and high evaporation rate.

Yellow uranium crystals from the calcrete of central Jordan were analyzed by Healy and Young, (1998) and they found that U-minerals are inhomogeneous and the U and V content ranges are 37- 41%, and 7 – 11% respectively. They concluded a mixed mineralogy of 50% tyuyamunite, 40% tyuyamunite, 5% carnotite with the following mineral solid solution series:

- $Na_{0.929}Ca_{0.379}K_{0.119}Sr_{0.057}Mg_{0.038})(UO_2)_2(V_{1.914}Si_{0.062}Al_{0.019}Fe_{0.006})O_8.nH_2O.$
- $(Na,Ca,K,Sr,Mg)(UO_2)_2(V,Si,Al,Fe)_{2.001}O_8.nH_2O$

The mineralogy of surficial uranium deposits in central Jordan and uranium source rocks, transport conditions, and deposition processes were explained in detail by Khoury et al., 2014. The geochemistry of uranium and vanadium of the mineral phases was not investigated in detail. The following work aims at understanding the geochemistry of the surficial uranium minerals of central Jordan.

2. Geology

2.1. Previous Work

Previous work on the varicolored marble from central Jordan has indicated that a multiple phase metamorphism has occurred as a result of spontaneous combustion of the bituminous rocks. The bituminous marl (the non-metamorphic protoliths) varies in composition from argillaceous to siliceous marl. The event is related to the epirogenic movements that took place in late Miocene to Pliocene along the Jordan Rift Valley. The Miocene tectonism and/or a meteorite impact were most probably the triggering factor which initiated the metamorphic event in central Jordan. Recently a large meteoritic impact structure has been discovered in Jabal Waqf as Suwwan, some 30 km east of the marble (cement) area (Salameh, et al., 2006, 2008).

The event was not simultaneous and was not one event (Khoury and Nassir, 1982 a, b; Khoury et al., 1984; Khoury, 1989; Khoury et al., 1992). The product minerals reflect the chemical composition of the original bituminous marl. The mineralogy of the marble is comparable to that of cement clinker (high temperature assemblage) and to hydrate cement products (low temperature assemblage). The high temperature mineral assemblage includes among others: diopside, wollastonite, monticellite, gehlenite-akermanite, spurrite, and merwinite, garnet, anorthite, pervoskite, magnesioferrite, fluorapatite and recrystallized calcite. The low temperature assemblage includes among others: calcium silicate hydrates (tobermorite, jennite, afwillite, apophyllite), sulfates (ettringite, hashemite, barite, thaumasite, gypsum), stable and metastable carbonates (calcite, vaterite, aragonite, kutnahorite), oxides and hydroxides (goethite, portlandite, hydrocalumite), and many calcium silicate hydrates (Khoury and Nassir, 1982a, b). The mineralogy of similar areas in Israel was recently reviewed by Gellerhe et al., 2012. They concluded that isochemical reactions took place as a result of the combustion of the organic matter. They compared between the different metamorphic rocks and their bituminous marl equivalents using the three component system Al_2O_3-SiO_2-CaO and isocon plots. The average mass loss of 30% of the protolith volume was the result of oxidation and decarbonation processes. The oxidation of the organic matter during combustion has led to an average mass loss of 30% and some volume loss as a result of dehydration and decarbonation processes. The stable isotopes ($\delta^{18}O$ and $\delta^{13}C$) were depleted from the carbonates (recrystalline calcite, spurrite and larnite). The isotopic depletion in $\delta^{18}O$ and $\delta^{13}C$ from equilibrium values supports the thermal event (Clark et. al., 1993; Khoury, 2012). A similar type of travertine forming from highly alkaline waters has been observed in Oman (Clark et al., 1992; 1993). A mud-volcanic hypothesis was suggested by Sokol et al., (2007; 2008; 2010), Sharygin et al., (2008); Vapnik et al., (2007) for the origin of the marble of the mottled zone. The active metamorphism in Maqarin area, north Jordan however, supports the combustion model (Khoury and Nassir, 1982b).

2.2. Geology of the studied area

The studied area was mapped in details by the Natural Resources Authority (NRA) (Barjous, 1986; Jasser, 1986). The geology, stratigraphy and sedimentology of central Jordan were described in details (Powell, 1989, Powell and Moh'd, 2011). The exposed rocks are sedimentary and range in age from Upper Cretaceous (Turonian) to Tertiary (Eocene). Outcrops in central Jordan illustrate the presence of three main rock types: Bituminous marl; varicolored marble (pyrometamorphic rocks); travertine and calcrete. The Bituminous Marl Unit overlies the Phosphorite Unit and underlies the varicolord marble and all are of Maestrichtian – Lower Paleocene age. Recent work of Alqudah et al., 2014 and 2015 has indicated that the bituminous marl of central Jordan contain abundant calcareous nannofossil taxa of Eocene age along with varying abundances of Maestrichtian and Paleocene taxa that suggests major reworking. Travertine and calcrete deposits are of Pleistocene – Recent age. They found up to 60 m thick succession of Early Eocene bituminous marl.

Figure 2: An outcrop in central Jordan illustrating travertine, caliche, bituminous marl and marble.

Figure 2 illustrates the different lithological units' that crop out in central Jordan. The thickest outcrop (up to 30 m) is found on the downthrown side of Siwaqa fault. Gentle folding and faulting that trend NW-SE and E-W are the main structures. In Jordan, synsedimentary uranium deposits are formed during sedimentation of bituminous marl (oil shale) and phosphorites in shallow continental shelves. Jordan was part of the phosphorite belt along the southern margin of the Tethys Ocean (paleolatitude 8–15° N), (Cuney, 2009; Abed, 2012). Uranium concentration values range between 60-379 ppm (parts per million or g/ton) with an average value of 153 ppm. Certain phosphorite horizons in central and south Jordan have higher U values than the average and reach up to 242 ppm (Abed, 2012). The phosphorites of Jordan are carbonate fluor-apatite (francolite) with a structural formula [$Ca_{9.86}Mg_{0.005}Na_{0.14}$] [$PO_{4.93}$ CO_3 1.07 $F_{2.06}$] (Abed and Fakhouri, 1996). Uranium substitutes for Ca in the carbonate fluor-apatite structure and correlates well with Ca in the Jordanian phosphorites (Abed, 2012; Khoury et al., 2014). The travertine and calcrete that host the main uranium deposits overlie the varicolored marble (pyrometamorphic rocks) in all the studied outcrops. Secondary clay smectite fillings (volkonskoite) are mainly responsible for the green color of the travertine and calcrete (Khoury, et al., 2014; Khoury and Zoubi, 2014). Apatite, barite, hashemite, ettringite, tobermorite and opaline phases are also present as secondary minor phases (Khoury, 2012).

2.3. Field and laboratory work

Most of the field work was done during summer of 2011 and 2012. Sampling has concentrated on outcrops from the quarries and trenches excavated by the private sectors and/or the Natural Resources Authority. Samples were collected from the bituminous marl, varicolored marble, intermixed chalk marl/travertine and calcrete/top soil outcrops.

Figure 3: a-f. Secondary yellow uranium encrustation in (a) black marble (b) highly altered marble (c) travertine (d) calcrete (e) Cr - rich plant molds in travertine (f) varicolored marble breccia embedded in travertine.

The bituminous marl is highly fractured and is affected by the alkaline circulating water as indicated by the secondary minerals (mainly secondary carbonates and sulfates) filling the cracks and cavities. Few outcrops of the varicolored

marble are not altered (Fig. 3a). The highly altered marbles by the alkaline circulating water are characterized by low temperature minerals filling fractures as hydrous Ca-silicates and Al-silicates (Fig. 3b). The travertine thickness in the studied areas reaches up to 30 meters. The outcrops are white yellow – brown and are characterized by wavy, vesicular, banded structure and are composed of calcite with mineralized plant remains and other secondary minerals. Secondary U- and V-rich phases are present as yellow encrustations and filling voids, cavities and along bedding planes in travertine (Fig. 3c, d). Few intermixed chalk marl/travertine and calcrete/top soil outcrops show the association of uranium encrustations and green Cr-rich smectite. Plant molds and replacement of vegetation by Cr-rich minerals are typical for central Jordan travertine (Fig. 3e). The calcrete is massive hard to nodular and sometimes friable to white, with voids and fractures. It varies in color between pale brown to creamy to white. The earthy calcrete as observed in the trenches forms a fairly continuous layer that grades upwards into the overlying regolith. The hard porous calcrete is intermixed with gypsum in many trenches. Secondary green Cr-rich smectite and yellow uranium encrustations are common (Fig. 3e). Brecciated varicolored marbles are noticed associated and embedded in travertine cement (Fig. 3f). The chalk marl/calcrete and/or travertine/ top soil are underlain by baked bituminous limestone and or varicolored marble.

Thirty five bituminous samples of the varicolored marble, travertine and calcrete were collected and are described in Table 1. Fifteen samples were collected from quarries and trenches of Siwaqa area (Q and T samples) and twenty from Daba quarries (KH samples). Another ten selective samples of yellow encrustations were also collected from two trenches excavated by Areva Co. (N 31° 23’ 361”, E 36° 11’ 361”) and Natural Resoures Authority (NRA) (N 31° 31’ 643”, E 36° 12’ 301”). Figure 3(a-f) illustrates some of the uranium rich outcrops.

All samples were subjected for mineralogical and chemical characterization. Polished thin sections were prepared for all the samples at the Department of Earth Sciences, University of Ottawa, Canada. Part of the analytical work was carried out using X-Ray fluorescence spectrometer (XRF), scanning electron microscope (SEM) and X-Ray diffractometer (XRD)

Table 1: Description of the samples from central Jordan and the XRD results (Khoury, 2012).

Sample No.	Description	XRD Results
KH01	Baked bituminous marl	Calcite*, gypsum, illite/smectite, francolite
T2-1	Bituminous limestone	Calcite*, gypsum, illite/smectite
KH02	Black marble	Calcite*
KH03	Pale green marble (altered)	Calcite*, smectite, francolite
KH04	Gray marble	Calcite*, apatite, smectite
KH05	Yellow marble	Calcite, wollastonite, aragonite
Q-1	Porous travertine with green clay	Calcite*, Cr-smectite
Q-2	Porous travertine with green clay	Calcite*, Cr-smectite
Q-3	Porous travertine with green clay	Calcite*, Cr-smectite
Q-4	Porous travertine with green clay	Calcite*, Cr-smectite
Q-5	Porous travertine with green clay	Calcit*e, Cr-smectite
Q-6	Porous travertine with green clay	Calcite*, Cr- smectite
Q-7 old	Porous travertine with green clay	Calcite*, Cr-smectite
KH06	Travertine with green clay	Calcite*, Cr-smectite, francolite
KH07	Travertine with green clay	Calcite*, Cr-smectite, francolite
KH08	Travertine with green	Calcite*, francolite
KH09	White travertine	Calcite*
KH10	Travertine	Calcite*, Cr- smectite, francolite
KH18	Green soft travertine	Calcite*, quartz, smectite
KH19	Green travertine	Calcite*, quartz, smectite
KH20	Green travertine	Calcite*, quartz, opal-CT
KH21	Green travertine	Calcite*, quartz, opal-CT
KH22	Green travertine	Calcite*, gypsum, opal-CT, Cr-smectite
KH23	Green travertine	Calcite*, opal-CT, Cr-smectite, gypsum
T2-3	Yellowish gypsum rich calcrete with green clay	Calcite, gypsum, Cr-smectite
T3-4	Yellowish gypsum rich calcrete with green clay	Calcite*, gypsum,ettringite, Cr-smectite
T3-5	Yellowish gypsum rich calcrete with green clay	Calcite*, gypsum, Cr-mectite
T2-6	Dolomite rich caliche with green clay	Calcite*, gypsum, Cr-smectite
T4-1	Red calcrete with green clay	Calcite*, Cr-smectite
T5-1	Yellowish calcrete with green clay	Calcite*, gypsum, ettringite, Cr-smectite
T5-2	Green yellow calcrete	Calcite*, gypsum, Cr-smectite

(*): major component

in the laboratories of the Federal Institute for Geosciences and Natural Resources, Hanover (BGR), the Geology Department, Greifswald University, Germany and Mango Center, University of Jordan. Most of the work (XRD, SEM, EDX, and Microprobe) was accomplished at the Department of Earth Sciences, University of Ottawa. A JEOL 8230 Super Probe for quantitative chemical analyses and images of minerals was used. The electron microprobe is fitted with five WDS spectrometers and a high count-rate silicon drift detector (SDD) EDS spectrometer. A JEOL 6610LV SEM was also used for studying and analyzing the uranium phases. All uranium rich samples were investigated for single crystal EDS analysis where hundreds of spot EDS analyses were accomplished. The XRD is a Philips double goniometer X'Pert system with CuK*α radiation*. The whole rock 'random powder' samples were scanned with a step size of 0.02° 2 theta and counting time of 0.5 s per step over a measuring range of 2 to 65° 2 theta. Powdered samples were chemically analyzed using a PANalytical Axios and a PW2400 spectrometer available in BGR. Samples were prepared by mixing with a flux material and melting into glass beads. The beads were analyzed by wavelength dispersive x-ray fluorescence spectrometry (WD-XRF). The loss on ignition (LOI) was determined by heating 1000 mg of each powdered sample to 1030 °C for 10 min. After mixing the residue with 5.0 g lithium metaborate and 25 mg lithium bromide, it was fused at 1200 °C for 20 min. The calibrations were validated by analysis of Reference Materials. «Monitor» samples and 130 certified reference materials (CRM) are used for the correction procedures.

3. Results

Tables 1, 2 and 3 represent the mineralogical and chemical composition of the different rock varieties. Table 1 describes the samples and their mineral content as indicated from the XRD results. The petrographic results indicated that the bituminous marl is biomicrite with 10% average clay content. Clay minerals are mostly highly expansive mixed layer illite/smectite. In addition to micritic calcite, francolite (fluor-carbonate apatite) and dolomite are the essential constituents of the rocks. Frambiodal pyrite, other sulfides, rare earth minerals and organic matter are found filling the forams cavities and intermixed with the matrix. The photomicrographs of Fig. 4 describe the laminated biomicritic texture, the bioclasts and the rare earth minerals of the bituminous marl. The EDS results of rare earth minerals vary in their crystal chemistry (Fig. 4d). Some crystals are composed of Y_2O_3 (15.2%-24.8%), V_2O_5 (18.8%-20.30%) and Fe_2O_3 (2.5%-16.20%). Some crystals have additional Nd_2O_3 (2.1%-4.6%) and CeO_2 (7.5%-7.8%). Detrital quartz, K-feldspar and mica are also present. Traces of Zn, Cu, Ni, Fe sulfides and selenides, native selenium, sulphates and selenates, and goethite are also present. In the equivalent bituminous rocks in north Jordan (Maqarin) pyrite, other sulfides and selenides as sphalerite, galena, Ni-Se, Ag-Se, AgCuNiFeZnCd-S-Se, FeCuZnNi-S, ZnCuFeNi-S and ZnFeCuNi-Se were reported (Milodowski et al., 1998).

Table 2 illustrates the chemical composition of the major elements that agrees with the XRD results. The XRD results have indicated that calcite is the major mineral in all rock varieties. Gypsum and mixed layer illite-smectite are present in the bituminous marl. Wollastonite, calcite, aragonite, and francolite are among the minerals associated with the marble. Gypsum, ettringite, hashemite, opal CT, quartz, francolite, Cr-smectite, fluorite and halite are among the secondary minerals in the travertine and calcrete.

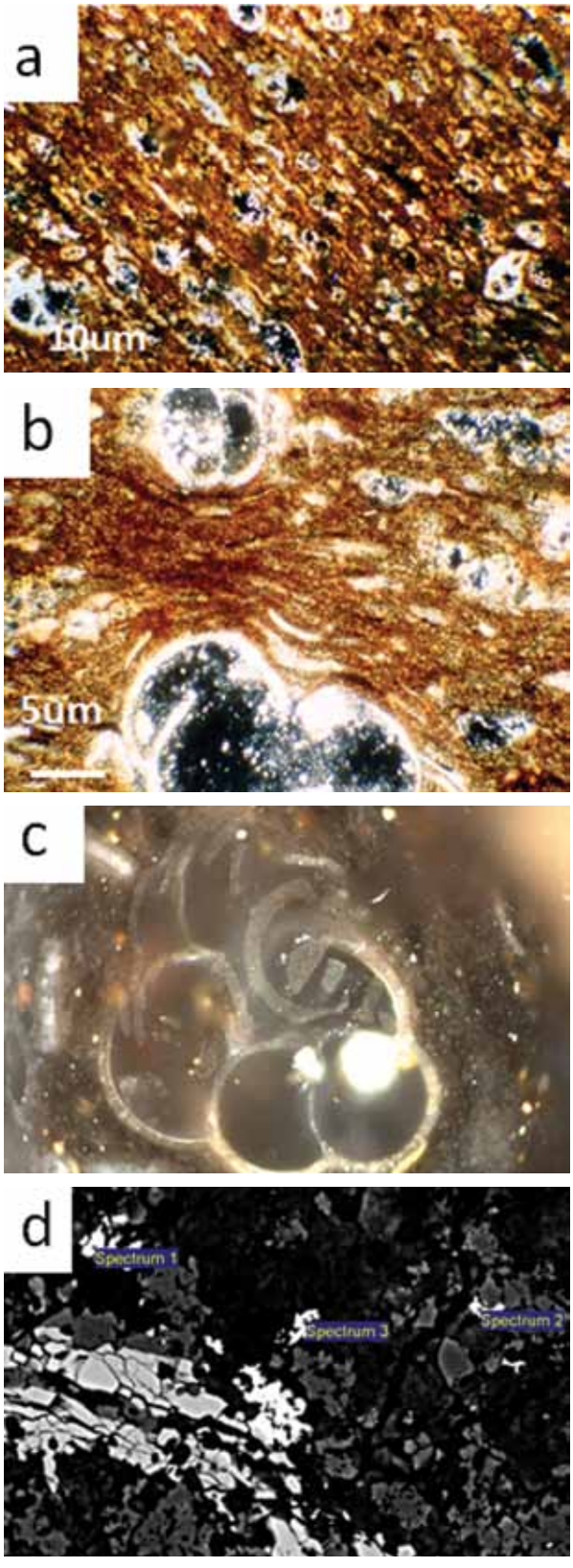

Figure 4: Photomicrographs of bituminous marl (a) silt-size bioclasts embedded in a laminated organic-rich matrix (b) fossil shell fragments filled with organic matter (c) bioclasts (forams) in micritic matrix (d) rare earth minerals in micritic matrix (Khoury et al., 2014)

Table 2: Chemical composition (%) of bituminous marl, marble, travertine and calcrete (Khoury, 2012).

Sample No	SiO2	Al2O3	Fe2O3	MgO	CaO	Na2O	K2O	P2O5	SO3	F	LOI	Total
Bituminous marl												
KH01	18.89	2.45	1.0	0.65	39.35	0.16	0.105	4.731	0.3	0.66	30.15	98.57
T2-1	36.04	7.58	2.67	2.13	19.56	0.943	0.471	1.793	nd	0.29	16.13	87.6
Varicolored marble												
KH02	1.24	0.18	0.15	1.02	53.06	<0.01	<0.005	0.538	0.13	0.17	42.6	99.14
KH03	5.88	1.96	0.58	1.38	48.08	0.05	0.006	0.893	0.73	0.22	39.01	98.89
KH04	2.64	0.66	0.44	0.69	51.52	0.05	0.008	1.624	0.43	0.28	40.47	98.89
KH05	25.45	7.27	2.35	1.75	35.48	0.21	0.068	1.622	0.4	0.14	24.02	99.11
Travertine												
Q1	10.17	2.8	1.02	0.81	42.72	0.282	0.042	0.731	nd	nd	34.33	92.9
Q2	15.37	4.19	1.39	1.378	35.89	0.513	0.103	1.192	nd	0.24	29.71	90.0
Q3	11.71	3.33	0.98	1.093	41.51	0.429	0.044	0.986	nd	0.14	33.29	93.5
Q4	16.58	4.38	1.12	1.55	36.18	0.242	0.035	0.875	nd	0.01	30.01	91.0
Q5	17.63	3.22	0.61	2.603	36.46	0.195	0.03	8.063	nd	1.16	22.60	92.6
Q6	11.78	2.69	0.60	1.895	42.82	0.156	0.034	8.63	nd	1.08	25.83	95.5
Q7	27.39	4.03	0.59	2.232	21.02	1.028	0.23	1.231	nd	0.1	19.66	77.5
KH06	12.08	2.07	0.35	1.19	41.01	0.29	0.061	2.946	0.44	0.4	34.61	95.75
KH07	17.0	2.94	0.4	1.45	34.10	0.57	0.08	2.987	0.47	0.4	32.7	93.53
KH08	2.30	0.56	0.39	0.23	52.55	0.07	<0.005	4.645	0.66	0.57	37.46	99.51
KH09	11.88	0.08	0.07	1	47.27	<0.01	<0.005	0.166	0.26	0.12	38.34	99.18
KH10	4.09	1.26	0.49	0.73	50.21	0.06	<0.005	3.33	0.47	0.42	38.18	99.34
KH18	41.26	0.3	0.06	0.68	29.81	0.07	0.009	0.147	0.16	0.18	25.93	98.62
KH19	43.56	0.1	0.01	0.8	28.72	0.06	0.006	0.024	0.16	0.13	24.92	98.49
KH20	41.99	0.11	<0.01	0.54	29.59	0.07	0.034	0.024	0.22	0.08	26.2	98.89
KH21	35.25	0.13	<0.01	0.41	33.67	0.07	0.02	0.256	0.1	0.11	28.99	99.01
KH22	47.14	0.08	0.01	0.57	26.04	0.13	0.006	0.075	0.96	0.1	23.68	98.82
KH23	36.85	0.54	0.17	0.4	31.17	0.03	0.017	0.472	0.94	0.17	28.15	98.93
Calcrete												
T-4	4.99	0.83	0.26	0.458	50.49	0.042	0.004	0.914	nd	0.31	39.49	97.8
T2-2	2.69	0.92	0.298	6.276	44.79	0.033	0.008	0.207	nd	nd	42.34	97.6
T5-2	4.95	1.5	0.542	0.668	31.97	0.207	0.044	0.771	13.44	0.22	9.36	63.7
T2-3	11.36	1.7	0.368	2.161	28.3	0.402	0.073	1.093	2.6	nd	12.44	60.6
T3-4	5.13	1.56	0.305	0.637	31.88	0.368	0.035	1.106	20.52	0.19	12.08	73.8
T3-5	19.93	3.3	0.893	3.882	27.56	0.665	0.155	4.84	6.02	0.55	15.13	82.9
T5-1	20.03	6.09	1.381	5.761	24.98	1.087	0.088	4.196	1.24	0.81	18.74	84.4
T2-6	18.11	2.06	0.278	2.924	26.34	0.588	0.085	0.488	4.15	nd	21.91	76.9

The chemical composition of the studied samples illustrate that CaO is the main oxide (highest value = 51.5%) and is mainly related to the presence of calcite. The highest SiO_2 value (47.14) is related to the opaline phases found in travertine. The highest MgO, Fe_2O_3 and Al_2O_3 values (2.1%, 2. 6% and 7.6% respectively) are found in the bituminous marl and are related to clay minerals. The highest P_2O_5 (8.6%) and F (1.1%) are found also in travertine and are related to the presence of francolite and fluorite. The trace elements composition is given inTable 3. The table illustrates that all samples are enriched in redox sensitive trace elements as U, Cr, V, Zn, and Ni. The highest trace elements content is present in the calcrete samples. The wide range of trace elements composition in the whole rock samples indicates a non-homogeneous distribution because the yellow and green mineralization of the secondary minerals is restricted to voids, fractures and bedding planes. The green travertine with Cr-smectite has the highest Cr content that reaches up to 4.1%. Strontium substitutes for calcium in the carbonates and francolite. Cr, Ni, U, V, Zn and Zr are associated in the different sulphide-selenide mineral phases. The U values in the whole rock samples of the bituminous marl, varicolored marble, travertine and calcrete range between 32-34 ppm, 6-17 ppm, <3-52 ppm and 6-419 ppm respectively. The highest uranium concentration (419 ppm) is found in a surface calcrete sample (T2-6). The V values in the whole rock samples of the bituminous marl, varicolored marble, travertine and calcrete range between 429-558 ppm, 21-196 ppm, 27-1117 and 62-7136 ppm respectively. The highest V concentration (0.74%) is in a surface calcrete sample (T5-1). The high V values are related to its incorporation in phases other than uranium vanadate.

The chemical composition of hundreds of spotted crystals has revealed 10 varieties of uranium phases. The results are summarized in Table 4. The EDS spot analyses of polished thin sections were carried out on crystals associated with

calcrete and aggregates associated with travertine (Fig. 5). Hundreds of spotted selected uranium crystals and aggregates with EDS are illustrated in Fig. 6 (a-j). The results are summarized in Table 4. The table illustrates the variability in the chemistry of the surficial uranium minerals. The U-V minerals are the most common in the Areva and NRA uranium rich trench samples. Fig. 7 illustrates the positive correlation between UO_3 and V_2O_5 that confirm their presence in the same phase. The high V_2O_5 values in some crystals are related to the dominance of V_2O_5 in the structure. The low correlation coefficient between U and V in the whole rock samples (Fig. 8) is related to the presence of V in the structure of other minerals in the travertine and calcrete. The XRD results have indicated that metatyuyamunite $Ca(UO_2)_2V^{5+}2O_8.3(H_2O)$ and strelkinite $Na_2(UO_2)_2V_2O_8.6(H_2O)$ are the main uranium vanadate minerals. All possible solid solution between the two end members is also present (Fig. 9). The XRD results have also indicated the occurrence of a vanadium free carbonate phase urancalcarite $Ca(UO_2)_3(CO_3)(OH)_6 \bullet 3H_2O$. Table 4 indicates also the presence of other minerals as carnotite $K_2(UO_2)_2V_2O_8.3(H_2O)$ and other unidentified varieties (carbonates -silicates) that need further studies. Carnotite is found as a minor constituent associated with the marble and depends on the availability of K as indicated by the presence of secondary K-apophyllite (Fig. 10). Carnotite is found in brown marble as yellow - green encrustations restricted to the secondary veinlets. Table 4 illustrates also the presence of other phases with: U and V - possibly ferganite $U_3 (VO_4)_2. 6H_2O$? ; U and V and low Ca silicate; U and V with high Ca silicate; U, V, and Na carbonate; U and V, Na silicate-carbonate; only U and Ca possibly vorlanite ($CaU^{6+}O_4$). All varieties are associated with altered marble, travertine and calcrete with the exception of the last variety with no vanadium that is restricted to unaltered marble.

Table 3: Trace elements composition (ppm) of bituminous marl, marble, travertine and calcrete.

Sample No	Cr	Ni	Sr	U	V	Zn	Zr
Bituminous marl							
KH01	3552	361	1043	32	558	1860	33
T2-1	594	93	575	34	429	347	118
Range	**594-3552**	**93-361**	**575-1043**	**32-34**	**429-558**	**347-1860**	**33-118**
Varicolored marble							
KH02	174	24	656	7	21	124	10
KH03	2612	92	748	6	135	374	17
KH04	621	245	742	17	46	877	10
KH05	583	198	2177	17	196	135	53
Range	**174-2612**	**24-245**	**656-2177**	**6-17**	**21-196**	**124-877**	**10-53**
Travertine							
Q-1	17636	124	440	9	124	538	37
Q-2	23888	317	419	13	165	688	51
Q-3	15797	212	484	10	136	483	47
Q-4	15937	242	819	9	142	246	79
Q-5	24641	278	601	38	193	418	66
Q-6	12660	162	734	37	125	453	80
Q-7	74621	190	601	33	1117	265	75
KH06	26379	105	619	34	473	253	38
KH07	41156	163	666	31	657	634	40
KH08	272	31	266	25	27	264	22
KH09	49	3	147	16	46	993	9
KH10	70	145	483	17	68	778	32
KH18	5450	34	129	52	96	718	9
KH19	6317	36	97	48	84	600	<3
KH20	4022	13	105	21	51	259	6
KH21	2469	13	130	19	39	218	7
KH22	5035	24	101	16	63	337	5
KH23	3284	92	119	42	59	448	10
Range	**49-74621**	**3-317**	**97-819**	**9-52**	**27-1117**	**218-993**	**<3-80**
Calcrete							
T-4	531	44	406	6	62	400	28
T5-2	4723	205	381	86	2024	223	47
T2-3	26060	152	466	41	5236	3761	46
T3-4	26600	94	748	77	7444	287	46
T3-5	28914	301	597	41	4218	1229	80
T5-1	19967	1095	1095	33	9520	1604	114
T2-6	63171	107	727	419	7137	208	44
T2-1	594	93	575	34	429	347	118
Range	**531-6317**	**44-1095**	**381-1095**	**6-419**	**62-7137**	**208-3761**	**28-118**

  - Volume 6, (Special Publication, Number 3), (ISSN 1995-6681)

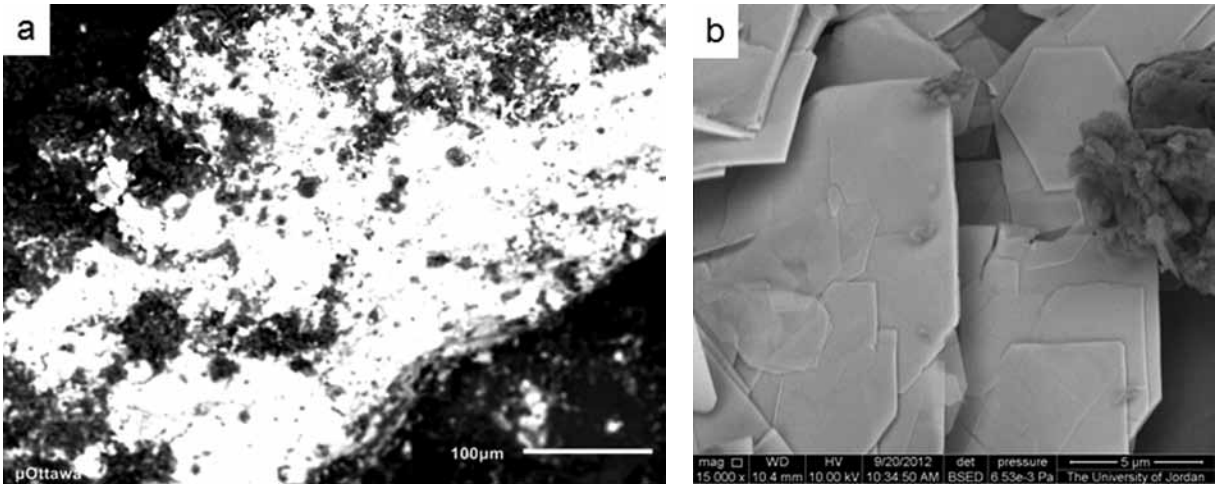

Figure 5: Yellow uranium (metatyuyamunite-strelkinite (a) aggregates associated with travertine (b) orthorhombic crystals associated with calcrete.

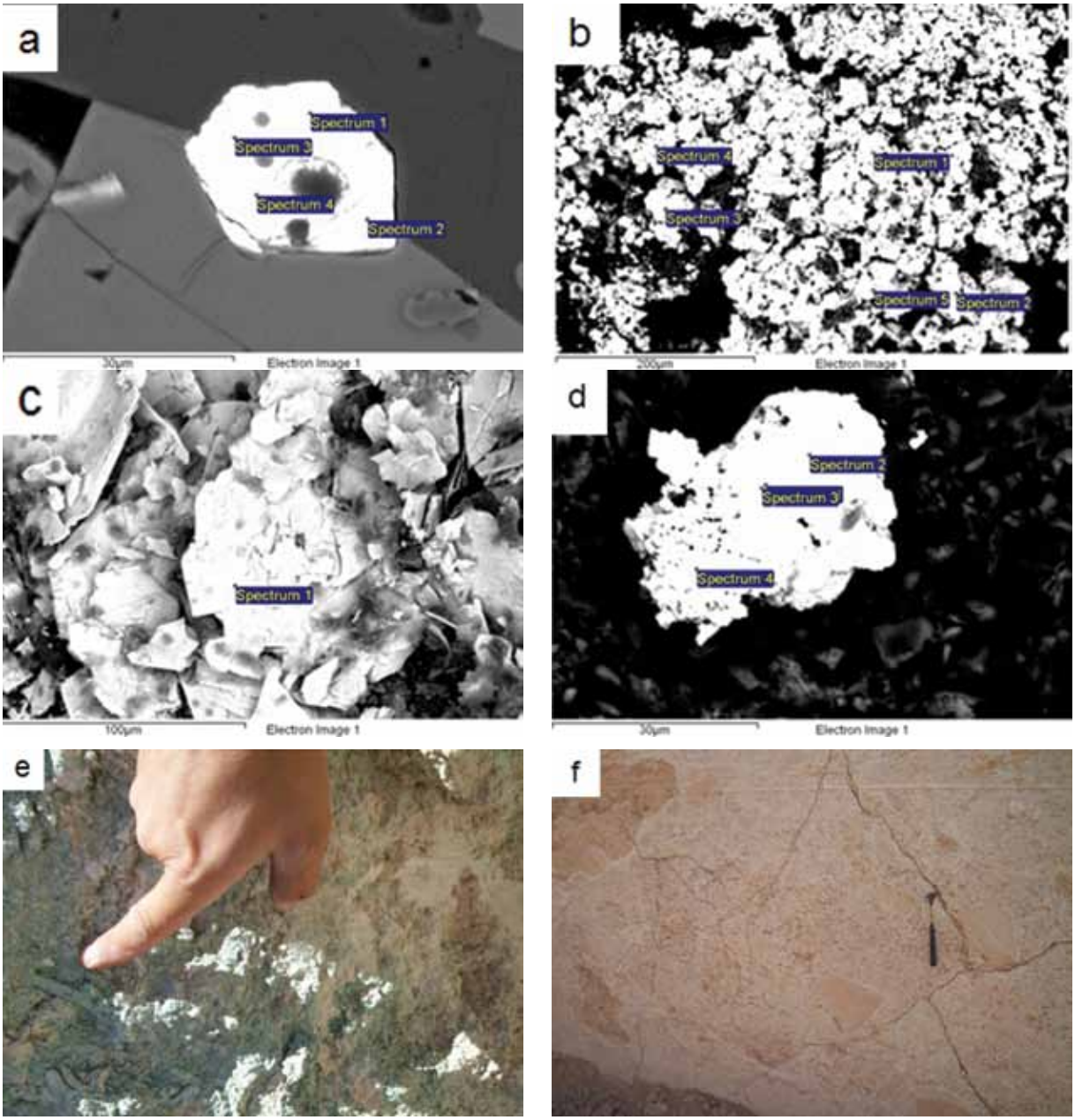

Figure 6: a-f. Secondary yellow uranium encrustation in (a) black marble (b) highly altered marble (c) travertine (d) calcrete (e) Cr - rich plant molds in travertine (f) varicolored marble breccia embedded in travertine.

Table 4: Chemical composition of uranium minerals.

Type of sample	UO_3	V_2O_5	CaO	Na_2O	K_2O	SiO_2	CO_2	U-Minerals
Marble	81.9-83.5		13.1-13.3					V
Marble/travertine	73.1-77.0	21.3-27.1						F
Marble/travertine	65.5-69.9	18.3-20.0	11.7-14.0					Mt
Marble/travertine	56.3-60.2	31.8-36.5	6.5-10.2					Mt
Travertine	68.8-69.2	24.1-24.3		6.0-6.1				S
Marble/ Secondary veins	64.2-71.3	18.6-23.1			3.8-5.9			C
Travertine	57.6-71.5	21.4-27.8	1.7-9.1	3.1-5.5				SS (Mt-S)
Travertine	38.5-41.4	13.1-13.5		2.9-3.3			41.1-43.9	?
Calcrete	62.3-68.5	19.9-21.6	8.8-11.4			1.6-3.0		?
Calcrete	37.4-42.8	15.1-18.2	35.8-38.1			6.2-6.3		?
Calcrete	52.7-55.2	17.2-18.8	6.1-9.2			6.1-10.4	14.5-18.9	?
Calcrete	38.8-58.0	13.1-18.9	2.5-14.8	1.4-5.5		1.1-5.7	6.0-18.2	?

- Mt = Metatyuyamunite $Ca(UO_2)_2V_25+O_8.3(H_2O)$
- S = Strelkinite $Na_2(UO_2)_2V_2O_8.6(H_2O)$
- C = Carnotite $K_2(UO_2)_2V_2O_8.3(H_2O)$ – restricted to K-rich marble
- F = Ferganite $U_3(VO_4)_2 . 6H_2O$?
- V = Vorlanite $(CaU_6+)O_4$
- SS (Mt-S) = Solid solution between metatyuyamunite -strelkinite

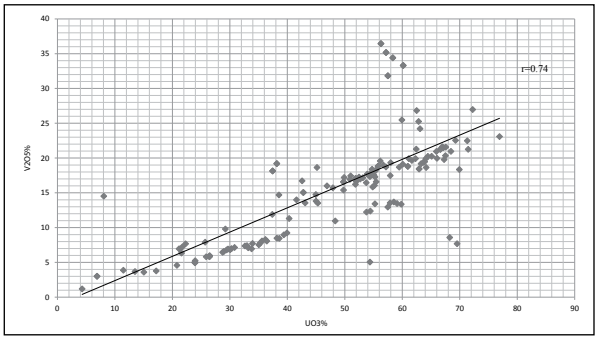

Figure 7: EDS results: UO3 vs V2O5 correlation of the uranium minerals.

4. Discussion

4.1. Source of U and V

The results have indicated the association of uranium and vanadium in the surficial deposits of central Jordan. The main sources of redox sensitive trace elements U, Cr, Ni, V and Zn in central Jordan is the bituminous marl and the underlying phosphorites. Organic matter and sulfides enable the reducing environment. The marine phosphorite beds immediately below the bituminous marl are enriched in U up to 200 ppm (Khoury, 2006; Abed, 2012; El-Hasan, 2008; Khoury et al., 2014). Uranium, as well as Cr, Ni, V and Zn are trace elements that precipitate in suboxic and fully anoxic bottom-water environments and accumulate in marine sediments, such as oil shale (Piper and Calvert 2009).The same conditions resulted in the concentration of trace elements in the form of sulfides and selenides in the bituminous marl (Al Nawafleh, 2007). Organic acids may increase the solubility of U in the bituminous marl, but its mobility may be limited by the formation of slightly soluble precipitates (e.g., phosphates and oxides) and by adsorption on clay minerals and organic matter (Kim, 1993; Read et al., 1993). Sr and U are hosted by calcite and francolite structures as a result of substitution for Ca. The sulfides and selenides were formed during the early diagenetic reducing stage (Khoury and Nassir, 1982 a and b; Milodowski, et al, 1998). The bituminous marl in central Jordan is characterized by unusual high concentrations of U, Cr, Ni, V, Zn, and Zr (Table 3). The average U content is 33 ppm. Uranium and vanadium are mostly associated with francolite structure and are adsorbed onto the organic material and the clay minerals.

The spontaneous combustion of the bituminous marl in central Jordan as indicated by Khoury and Nassir (1982b) is responsible for the formation of the varicolored marble (pyrometamorphic rocks). The chemical composition of the combusted bituminous rocks of central Jordan remained the same with a mass loss of 30% as indicated in the equivalent bituminous rocks of the mottled zone (Gellerhe et al., 2012). Combustion has further enriched the metamorphic rocks with trace elements. The source rock for uranium mineralization in central Jordan is the combusted bituminous marl (varicolored marble). Meteoritic water similar to the active system in Maqarin, north Jordan is responsible for the travertine and calcrete precipitation in central Jordan (Khoury, 2012). The groundwater discharges today in Maqarin, is characterized by high hydroxide alkalinity (pH ~ 12.7), and saturation with calcium sulfate and high concentrations of redox sensitive trace elements and precipitates soft travertine (Khoury et al., 1992). The original protolith (the bituminous rocks) in Maqarin is highly enriched in trace elements and is equivalent from the stratigraphical, lithological, mineralogical and chemical point of view to those in central Jordan and the mottled zone. All the travertine deposits in Maqarin area are recent and are precipitating as a result of the reaction of the hydroxide-sulfate waters with atmospheric CO_2.

The same mechanism has prevailed in an ancient system in central Jordan where travertine and caliche deposits overly the varicolored marble. The travrtine is an evidence for discharges of hyperalkaline groundwater in the past (Khoury, 2012; Khoury et al., 2014). Thick travertine deposits were formed during wet periods in the low topography areas, and calcrete was formed later during dry period. The dry climate has contributed to increase metals concentration such as U, Cr, Ni, V and Zn.

The widely distributed brecciated varicolored marbles embedded in the travertine cement indicates a wet pluvial period. The presence of gypsum, fluorite and halite in the calcrete indicate a dry evaporation period.

4.2. Uranium mineralization

The U content of the rocks is variable and reaches up to 419 ppm in the whole rock trench samples (Table 3). Both U and V are associated together as uranyl vanadate phases in most of the studied yellow crystals as (Table 4). The low correlation coefficient between U and V in the whole rock samples (Fig. 8) is related to the presence of V in the structure of sulphates, phosphates, REE hosted minerals and Cr-smectite. Uranium solubility in solution is predominantly controlled by the oxidation-reduction potential and pH (Murphy and Shock, 1999). Uranium mineralization in the travertine and calcrete is favored by the presence of source rocks of uranium and vanadium, and oxidizing alkaline circulating water. The uranyl ion is an oxycation of uranium in the oxidation state +6, with the chemical formula $[UO_2]^{2+}$. Uranium +6 is considerably more soluble than uranium +4 and is highly mobile as hexavalent uranyle ion (UO_2^{2+}) under oxidizing conditions (Langmuir, 1978; 1997). Under reducing conditions, uranium (+4) complexes with hydroxide or fluoride are the only dissolved species (Gascoyne, 1992). The precipitation of uranium (+4) under reducing conditions is the dominant process leading to naturally enriched zones of uranium in the subsurface (Osmond and Cowart, 1992). The hydroxide $UO_2(OH)_2$ dissolves in strongly alkaline solution to give hydroxy complexes of the uranyl ion. As pH increases the hydroxide species $[(UO_2)_2(OH)_2]^{2+}$ and $[(UO_2)_3(OH)_5]^{+}$ form before the precipitation of $UO_2(OH)_2$ (Hagberg, et el., 2005). The association of vanadium with uranium in the secondary uranium minerals needs an oxidizing environment to oxidize dissolved V^{4+} to V^{5+}. Complexing agents such as vanadium compounds are necessary to fix the uranyl-ion and vanadate to precipitate very low solubility uranium minerals in the form of uranyl vanadates (Battey et al., 1987; Brookins, 1988). Hydroxyl vanadate VO_3OH^{+5} is the dominant complex under alkaline conditions.

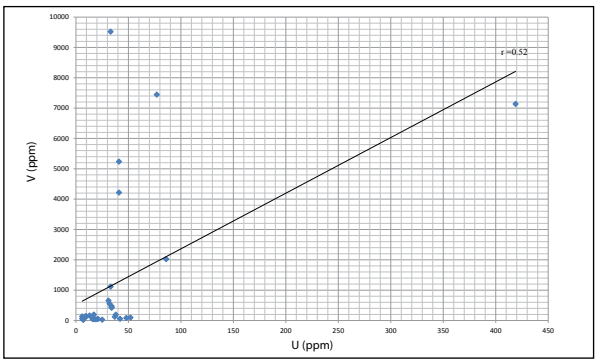

Figure 8: U values (ppm) plot versus V values (ppm) in the whole rock samples (Table 3).

The combustion of the organic rich source rock has accelerated leaching out the redox sensitive trace elements among others in the circulating highly alkaline water. The highly altered varicolored marble with its complex mineralogy shows yellow secondary U-minerals as encrustations and/or filling the veins, weakness zones and voids with other hydrous silicates (Nassir and Khoury, 1982; Khoury and Nassir 1982a and b; Khoury, 2012). Uranium and vanadium with other trace elements were leached out from the varicolored marble and were carried out by the oxidizing alkaline circulating water. Such conditions are indicated by the presence of relatively high levels of Sr, Cr, Ti, Mn, Ni, Zn, V, Zr, Cl, F, Se and REE in the Pleistocene-Recent carbonate sediments (Khoury, et al., 1984). The absence of Cs in the surface uranium phases indicates a low temperature solution (Healy and Young, 1998). U-levels up to 160 ppm were found in opaline phases adjacent to open voids (Hyslop, 1998). The yellow uranium phases are present in patches at the surface and along weakness zones in the travertine and caliche.

The oxidizing environment of the alkaline water in central Jordan is indicated by the presence of abundant Cr^{6+} mineralization (Cr^{6+}-bearing ettringite and hashemite). Uranium +6 is considerably more soluble than uranium +4 and is highly mobile as hexavalent uranyle ion (UO_2^{2+}) under oxidizing conditions (Langmuir, 1978; 1997). Oxidizing alkaline circulating water is a prerequisite to oxidize dissolved V^{4+} to V^{5+}, and to mobilize uranium as uranyl complexes thereby establishing the conditions required for the precipitation of uranium vanadate minerals as strelkinite and tyuyamunite and carnotite (Battey et al., 1987; Dahikamp, 1993). Complexing agents such as vanadium compounds are necessary to fix the uranyl-ion and vanadate to precipitate very low solubility uranium minerals in the form of uranyl vanadates as strelkinite and metatyuyamunite. The solid solution series between strelkinite and metatyuyamunite is dependent on the Ca /Na ratio in solution. Carnotite precipitates are dependent on the availability of K in the circulating water. The composition of other unidentified U-V phases was dependent on the solution chemistry. In the absence of uranyl vanadates complexes in the alkaline conditions, soluble uranyl-carbonate complexes as uranyl carbonates $UO_2(CO_3)_2^{2-}$ are the most probable to dominate (Langmuir, 1978; 1997; Battey, et al., 1987; Brookins, 1988). After the removal of $Ca(OH)_2$ from the alkaline water and the precipitation of calcite, uranium carbonates as urancalcarite could precipitate.

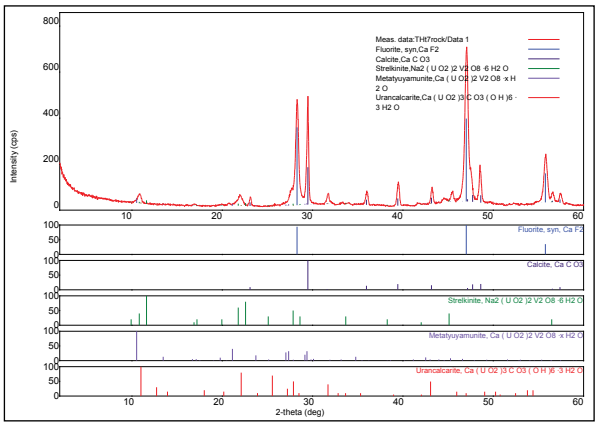

Figure 9: XRD results of a representative sample of uranium yellow encrustations.

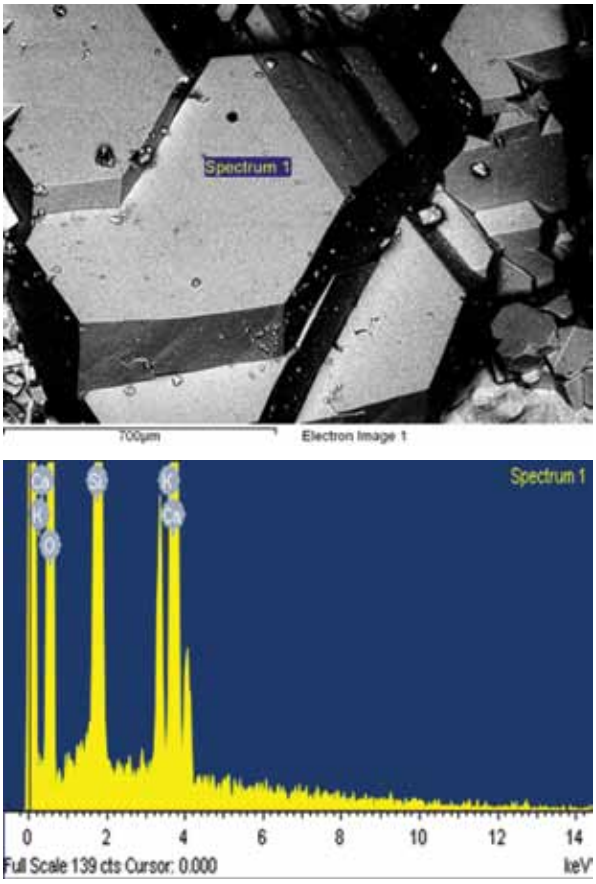

Figure 10: SEM –EDX photomicrograph of secondary K-rich apophyllite associated with brown marble.

5. Conclusion

Unusual surface uranium deposits cover large areas in central Jordan. Uranium distribution is inhomogeneous and follows porous weakness zones of chalk marl/travertine and caliche/top soil deposits. The source of uranium and other redox sensitive metals Cr, Ni, V, Zn, and Zr is the combusted bituminous marl (varicolored marble). The high concentration of these metals is reflected by the chemistry of secondary low temperature minerals hosted by the travertine and caliche. Quaternary travertine and caliche in central Jordan are the fossilized products of ancient hyperalkaline oxidized groundwater discharges that prevailed during wet /dry periods in the Peistocene –Recent time.

The main surficial secondary uranium minerals in central Jordan are strelkinite and metatyuyamunite with all possible solid solution between the two end members. Other unidentified U-V silicates and carbonates possibly were precipitated under the same conditions.

Acknowledgment

The author would like to thank the Deanship of Scientific Research at the University of Jordan for their financial support of supporting my sabbatical year at the Department of Earth Sciences, University of Ottawa. Canada. Thanks are extended to Prof. Ian Clark and Late Prof. Andre Lalonde for supporting the analytical work in the different laboratories.

The work entitled "The geochemistry of surficial uranium deposits from central Jordan" was accomplished during the sabbatical year 2012/2013. Part of the analytical work was done at the laboratories of the Federal Institute for Geosciences and Natural Resources, Hanover, and the Department of Geology, Greifswald University, Germany.

References

[1] Abed, A., 2012. Review of uranium in the Jordanian phosphorites: Distribution, genesis and industry. Jordan Journal of Earth and Environmental Sciences 4, (2) 35-45.

[2] Abed, A.M., Fakhouri, K., 1996. On the chemical variability of phosphatic particles from Jordanian phosphorite deposits. Chemical Geology 131, 1–13.

[3] Alnawafleh, H., 2007. Geological factors controlling the variability of Maastrichtian bituminous rocks in Jordan. Unpublished Ph.D thesis. The University of Nottingham, England. 279P.

[4] Alqudah, M., Hussein, M., Podlaha, O., Boorn, S., Kolonic S., and Mutterlose, J. 2014. Calcareous nannofossil biostratigraphy of Eocene oil shales from central Jordan. GeoArabia, 19, (1), 117-140.

[5] Alqudah, M., Hussein, M., Podlaha, O., Boorn, S., Podlaha, O., and Mutterlose, J. 2015. Biostratigraphy and depositional setting of Maastrichtian Eocene oil shales from Jordan, Marine and Petroleum Geology. (In Publication)

[6] Barjous, M., 1986. The geology of Siwaqa, Bull. 4, NRA, Amman – Jordan.

[7] Battey, G., Miezitis, Y., and Mckay, A., 1987. Australian Uranium Resources, Bureau of Mineral Resources, Resource Report No. 1, Australia Government Publishing Service, Canberra.

[8] Brookins, D., 1988. Eh-PH diagrams for geochemistry. Springer-Verlag Berlin.

[9] Clark, I. D., Fontes, J-Ch., and P. Fritz, 1992. Stable isotope disequilibria in travertine from high pH waters: laboratory investigations and field observations from Oman. Geochimica Cosmochimica Acta, 56: 2041 - 2050.

[10] Clark, I., Firtz, P. Seidlitz, H., Khoury, H., Trimborn, P., Milodowski, T., and Pearce, J., 1993. Recarbonation of metamorphosed marls, Jordan. App. Geochem. 8: 473 - 481.

[11] Cuney, M., 2009. The extreme diversity of uranium deposits. Miner Deposita 44:3–9

[12] Dahikamp, F.J., 1993. Uranium Ore Deposits. Springer-Verlagm, Berlin Heidelberg. p 460.

[13] Gascoyne, M., 1992. Geochemistry of the actinides and their daughters. In Uranium-series Disequilibrium: Applications to Earth, Marine, and Environmental Science (ed. M. Ivanovich and R. S. Harmon), 34-61. Clarendon Press.

[14] El-Hasan, T. (2008): Geochemistry of the redox-sensetive trace elements and its implication on the mode of formation of the Upper Cretaceous oil Shale, Central Jordan. Neues Jahrbuch fuer Geologie und Palaeontologie Abh. 249(3): 333-344.

[15] Gellerhe, Y., Burg A., Halicz, L., Kolodny Y., 2012. System closure and isochemistry during the Mottled Zone event, Israel. Chemical Geology. 334, 102-115.

[16] Hagberg, D., Karlström, G., Roos BO., Gagliardi, L., 2005. "The Coordination of Uranyl in Water: A Combined Quantum Chemical and Molecular Simulation Study". J. Am. Chem. Soc. 127 (41): 14250–14256.

[17] Healy, R., and Young, J., 1998. Mineralogy of U-bearing marls from The Jordanian desert. Unpublished Report for Cameco Corporation, Canada. A report submitted to the Natural Resources Authority, Amman, Jordan.

[18] Hyslop, E., 1998. Uranium distribution and whole rock geochemistry. In phase II report (Nirex S/98/003) edited by C.M. Linklater.

[19] IAEA, 2009. World distribution of uranium deposits (UDEPO) with uranium deposit classification. IAEA- Vienna, TECDOC-1629.

[20] Jaser, D., 1986. The geology of Khan Ez Zabib, Bull. 3, NRA, Amman, Jordan

[21] Khoury, H. N., 1989. Mineralogy and petrology of the opaline phases from Jordan. N. Jb. Miner. Mh., 10, 433-440.

[22] Khoury, H., 2006. Industrial rocks and minerals in Jordan (second edition). Publications of the University of Jordan, Amman.

[23] Khoury, H. N., 2012. Long-Term Analogue of Carbonation in Travertine from Uleimat Quarries, Central Jordan. Environmental and Earth Science. 65:1909-1916.

[24] Khoury, H., and Al-Zoubi, A. 2014. Origin and characteristics of Cr-smectite from Suweileh area, Jordan. Applied Clay Science, 90, 43–52.

[25] Khoury, H., Mackenzie, R., Russell, J., and Tait, J., 1984. An iron-free volkonskoite. Clay Minerals, 19: 43-57.

[26] Khoury, H., and Nassir, S., 1982a. A discussion on the origin of Daba – Siwaqa marble, Dirasat, 9: 55-56.

[27] Khoury, H., and Nassir, S., 1982b. High temperature mineralization in Maqarin area, Jordan. N.Jb.Miner.Abh., 144, 187-213.

[28] Khoury, H., and Milodowski, A., 1992. High temperature metamorphism and low temperature retrograde alteration of spontaneously combusted marls.The Maqarin cement analogue. Water Rock Interaction, Kharaka & Maest (Eds), Roterdam. 1515-1518.

[29] Khoury, H., Pearce, J., and Hyslop, E., 1992. In Phase I. Nagra Technical Report,NTB 9-10,Nagra,Wettingen,Switzerland.

[30] Khoury, H. N., Salameh, E. M. and Clark I. D. 2014. Mineralogy and origin of surficial uranium deposits hosted in travertine and calcrete from central Jordan. Applied Geochemistry, 43, 49–65.

[31] Khoury H. N., Salameh, E., Clark, F., Fritz, R, Bajjali, W., Miolodwski, A., Cave, M., and Alexander, W., 1992. A natural analogue of high pH waters from the Maqarin area of northern Jordan 1: Introduction to the site. J. Geochem. Explor. 46, 117-132.

[32] Kim, J. I., 1993. The chemical behaviour of transuranium elements and barrier functions in natural aquifer systems. Mater. Res. Soc. Symp. Proc., 294, 3-21.

[33] Langmuir, D., 1978. Uranium solution-mineral equilibria at low temperatures with applications to sedimentary ore deposits. Geochim. Cosmochim. Acta 42, 547-569.

[34] Langmuir D., 1997. Aqueous environmental chemistry. Prentice Hall.

[35] Mckay, A., and Miezitis, Y., 2001. Australia's uranium resources, geology and development of deposits, AGSO — Geoscience Australia Resource Report 1.

[36] Milodowski, A., Hyslop, E., Pearce, J., Wetton, P., Kemp, S., Longworth, G., Hodginson, E., and Hughes, C., 1998. Mineralogy and Geochemistry in Phase III SKB Technical Report.TR-98-04. PP401.

[37] Murphy, W. M., and Shock E. L., 1999. Environmental Aqueous Geochemistry of Actinides. In Uranium: mineralogy, geochemistry and the environment, Mineralogical Society of America.38 (ed. P. C. Burns and R. Finch), 221-254.

[38] Nassir, S., and Khoury, H., 1982. Mineralogy, petrology, and origin of Daba-Siwaqa marble, Jordan. Dirasat.9: 107-130.

[39] Osmond J. K. and Cowart J. B., 1992. Ground water. In Uranium-series Disequilibrium: Applications to Earth, Marine, and Environmental Science (ed. M. Ivanovich and R. S. Harmon), (Gascoyne, 1992). 290-333. Clarendon Press.

[40] Powell, J.H., 1989. Stratigraphy and sedimentology of the Phanerozoic rocks in central and southern Jordan. Bull. 11, Geology Directorate, natural resources Authority (Ministry of Energy and Mineral resources) Amman, Part B: Kurnub, Ajlun and Belqa group, 161.

[41] Powell, J. H., Moh'd, B.K., 2011. Evolution of Cretaceous to Eocene alluvial and carbonate platform sequences in central and south Jordan. GeoArabia, 16, 4, 29-82.

[42] Read, D., Bennett, D.G., Hooker, P.J., Ivanovich, M., Longworth, G., Milodowski, A.E., Noy, D.J., 1993.The migration of uranium into peat-rich soils at Broubster, Caithness, Scotland. J. Contam. Hydrol., 13, 291-308.

[43] Piper, D.Z. and Calvert, S.E., 2009. A marine biogeochemical perspective on black shale deposition. Earth Science Reviews, 95, 63–96.

[44] Salameh, E., Khoury, H., and Schneider, W., 2006. Jebel Wagf as Suwwan, Jordan: a possible impact crater – a first approach. Z. dt. Geowiss. 157/3, p. 319-325.

[45] Salameh, E., Khoury, H., Reimold, W., and Schneider, W., 2008. The first large meteorite impact structure discovered in the Middle East: Jebel Waqf as Suwwan, Jordan. Meteoritics and Planetary Science. 43, Nr 10, 1681-1690.

[46] Sharygin, V.V., Sokol, E.V., Vapnik, Ye., 2008. Minerals of the pseudobinary perovskite-brownmillerite series from combustion metamorphic larnite rocks of the Hatrurim Formation (Israel). Russian Geology and Geophysics. 49, 709-726.

[47] Sokol, E.V., Novikov, I.S., Vapnik, Ye., Sharygin, V.V., 2007. Gas fire from mud volcanoes as a trigger for the appearance of high-temperature pyrometamorphic rocks of the Hatrurim Formation (Dead Sea area). Doklady Earth Sciences. 413A, 474-480.

[48] Sokol, E.V., Novikov, I.S., Zateeva, S.N., Sharygin, V.V., Vapnik, Ye., 2008, Pyrometamorphic rocks of the spurrite-merwinite facies as indicators of hydrocarbons discharge zones (the Hatrurim Formation, Israel). Doklady Earth Sciences. 420, 608- 614.

[49] Sokol, E., Novikov, I., Zateeva, S., Vapnik, Ye., Shagam, R., Kozmenko, O., 2010. Combustion metamorphism in the Nabi Musa dome: new implications for a mud volcanic origin of the Mottled Zone, Dead Sea area. Basin Research. 22, 414-438.

[50] Vapnik, Ye., Sharygin, V.V., Sokol, E.V., Shagam, R., 2007. Paralavas in a combustion metamorphic complex: Hatrurim Basin, Israel. Geological Society of America, Reviews in Engineering Geology. 18, 133-154.

JJEES
Jordan Journal of Earth and Environmental Sciences
Volume 6, (Special Publication, Number 3), June, 2014
ISSN 1995-6681
Pages 23- 28

High Calcium Ash Incorporated Into Clay, Sand and Cement Mortars Used For Encapsulating of Heavy Metals

Tayel El-Hasan[1*], Bassam Z. Mahasneh[2], Nafeth Abdel Hadi[3] and Monther Abdelhadi[4]

[1]Department of Chemistry, Faculty of Science, Mu'tah University, 61710, Al-Karak – Jordan
[2]Department of Civil Engineering, Faculty of Engineering, Mutah University, Jordan
[3]Department of Civil Engineering, Faculty of Engineering Technology, Al-Balqa Applied University, Jordan
[4]Department of Civil Engineering; Al-Ahliyya Amman University; Amman – Jordan

Abstract

Many heavy and toxic metals are found in variable concentrations contained in the High Calcium Ash (HCA) produced by direct combustion of the bituminous limestone. Huge quantities of ash will be produced when bituminous limestone is utilized as energy source for electricity production or retorting process to produce crude oil in Jordan. One of the main serious environmental impact of this ash is the leachability of heavy metals and its potential contamination of the surface and groundwater reservoirs in the catchment area of Wadi Al-Mujieb.

Encapsulation of Lead, Zinc, and Manganese ions were investigated by mixing of HCA with sand, cement and clay (kaolin) mortars. HCA was added with different percentages (e.g. 0%, 3.5% and 10%) to variable ratios of sand-cement-clay mixtures. Beside heavy metal encapsulation analysis; the unconfined compressive strength, water consumption and permeability were carried out for the produced mortars. The results shows that an effective heavy metal encapsulation were achieved with 10% HCA added to 25% clay, 50% sand and 25% cement mixture. Pb and Mn was encapsulated, very low Zn was detected and leached from the mortars. On the other hand, the maximum unconfined compressive strength (16.83 MPa) was reached when 10% HCA was added to the mixture of 25% clay, 25% sand and 50% cement. The permeability was decreasing with increasing HCA, because of the pozzolanic composition of HCA similar to Ordinary Portland Cement (OPC).

Keywords: High Calcium Ash, Heavy Metals, Encapsulation, Compressive Strength, Leaching, Permeability.

1. Introduction

Huge amounts estimated as billions of tons of bituminous limestone are considered as promising reserves to solve the increasing energy demands in Jordan in the foresight future. Extraction of crude oil by retorting and generation of electricity by direct combustion of organic rich bituminous limestone will produce bulk quantities of high alkali ash which is rich in calcium oxide and various heavy metals Abdel Hadi et al. (2008).

Organic-rich rocks such as black shale are potentially hosted economic metal accumulations, and many have been discovered all over the world (Pasava, 1991 a). Moreover, Many studies indicated that black shales are very important host for Platinum Group of Elements (PGE) Pasava et al. (1993). Pasava (1990), reported a higher trace elements concentrations in the Barrandian Upper Proterozoic (Bohemian Massif) accompanied with high organic carbon. This metal enrichment was attributed to the role of organic matter that acts as geochemical reduction barrier for metal precipitation and accumulation. El-Hasan (2008), indicates that XRF analysis for trace elements in shale samples collected from El-Lajjoun, shows moderate contents of trace element enrichments compared to the average shale, where enrichment series is Cd > Mo > U > Cr > Zn > Ni > Cu > V. It seems that the poly-elemental ores sources in black shales became a significance resource for Ni, Mo and precious metals Pasava (1991 a).

The source of these metals is most probably volcanogenic-hydrothermal exhalations. Rimmer, (2004) has used the paleoredox indicators to elucidate the paleo-environmental nature of Devonian black shales at central Appalachian basin. Particularly C-S-Fe analysis and the enrichment of Mo, Pb, Zn, V, Cu, Cr, and Co. Algeo and Maynard (2004) found that trace elements commonly exhibit considerable enrichment in laminated, organic-rich facies, especially those deposited under euxinic conditions. Moreover, previous study showed that Jordanian organic-rich Oil shale contains high amounts of trace and toxic elements such as Mo, V, Cr, Zn and other (El-Hasan, 2008). Han et al. (2014), Found that the concentrations of biogenic elements, implying a genetic relationship between Mo and Ni enrichment and organic matter.

The combustion process of Oil shale is expected to produce huge ash tailing that is considered as hazardous pollution source to the environment due to its friable nature and its enrichment of toxic elements. Among those elements chromium is the most hazardous. Especially Cr(IV) which are highly mobile and could reach water resources easily. El-Hasan et al. (2011), used the synchrotron based XANES analytical procedure and found a potential environmental risk in the form of high oxidation state toxic elements particularly

* Corresponding author. e-mail: tayel.elhasan@gmail.com

the Cr (IV), which was highly increased due to the aerobic combustion process.

Al-Haraheshah et al. (2010) found that surface water at the area of oil shale utilization are facing medium to high potential to pollution risk. The leachability tests showed that there will be substantial amounts of amany pollutants such as Pb, Cr possibly leached out to surface water from oil shale utilizations plant. Abdel Hadi et al. (2008), has tested the change in engineering properties of the limy ash produced from the direct combustion of El-Lajjun oil shale mixed with brown clayey soil from various locations of Jordan. The results revealed a very high increase in the unconfined compressive strength and California Bearing Ratio values.

This work aims to carryout a comprehensive investigation regarding the metallogenesis and leachability of heavy metals and other chemical elements by infiltration of water through dumped ash. The geochemical mobility of these metals accompanied with their toxicity to human and animal paid the attention toward finding suitable technologies or designs aims to maximize the remediation or solidification for these metals. Therefore, in this work two percentages (3.5% and 10%) of HCA is added to the sand-cement-clay mixture. In order to determine the best mix ratio of (Sand-Cement-Clay and HCA) that would show higher compressive strength and at the same time encapsulates higher concentrations of heavy metals within its structure.

2. Materials and Methodology

Unconfined compressive test after 1 and 4 weeks, heavy metals leaching test and the permeability test were carried out for different mixtures.

2.1. Materials

2.1.1 High Calcium Ash (HCA)

Calcium ash was brought from EL-Lajjun area. Ash is the solid waste product of surface combustion of the EL-Lajjun bituminous limestone. The ash has a plasticity index less than 10 limit of 25 according to ASTM D4318 and thus; classified as a non plastic material, with specific gravity equal to 2.39. The chemical composition and the concentrations of major oxides and trace elements of the three representative bituminous limestone samples are given in Table (1). Moreover, the physical properties of the ash samples from El-Lajjun are given in Table (2).

The ashing process was done on the labs of Natural Resources Authority . More than 5 kilogram of gravel size oil shale were burned directly on an aerobic conditions, then smaller amount of samples were completely burned using muffle furnace at different temperature up to 925 ºC. The chemical composition of major oxides of the ash samples compared with standard Ordinary Portland Cement (OPC) are given in Table (3).

Table 1: Chemical composition of the bituminous limestone samples from El-Lajjun

	Sample 1	Sample 2	Sample 3	Average
SiO_2 %	12.2	12.6	13.6	12.8
Al_2O_3 %	2.5	2.7	2.9	2.7
Fe_2O_3 %	1.3	1.8	1.5	1.5
CaO %	25.7	26.9	28.4	27.0
MgO %	0.46	0.45	0.47	0.46
MnO %	0.005	0.005	0.003	0.004
TiO_2 %	0.13	0.14	0.14	0.14
K_2O %	0.5	0.47	0.44	0.47
P_2O_5 %	2.40	2.96	2.42	2.59
Li ppm	5	6	6	6
B ppm	22	22	26	23
V ppm	133	174	154	154
Cr ppm	474	467	534	492
Co ppm	46	48	56	50
Ni ppm	268	241	285	265
Cu ppm	110	124	118	117
Zn ppm	472	507	539	506
As ppm	91	117	87	98
Sr ppm	796	900	817	838
Y ppm	22	20	23	22
Nb ppm	16	20	19	18
Mo ppm	122	160	155	146
Ag ppm	3	4	4	4
Sn ppm	90	100	113	101
La ppm	8	5	5	6
Ce ppm	44	52	57	51
Pb ppm	34	38	41	38
W ppm	23	28	33	28
Zr ppm	661	722	415	599

*Analysis was accomplished by using the coupled plasma technique (ICP).
* Loss on ignition is 51.98 %.

Table 2: Physical characteristics of El-Lajjun bituminous limestone

Physical property	**Sample (1)**	**Sample (2)**	**Sample (3)**	**Average**
Bulk density g/cm^3	1.96	1.94	1.95	1.95
Specific gravity	2.39	2.38	2.41	2.39
Moisture content %	0.9	0.75	1.05	0.9

Table 3: Chemical composition of ash sample compared with standard Ordinary Portland Cement (OPC). The analysis was done using XRF technique.

Oxide Wt. %	Ash Sample	OPC
SiO_2	25.30	23
Al_20_3	2.35	4
Fe_2O_3	1.37	2
CaO	45.21	64
MgO	1.63	2
P_2O_5	5.47	---
Na_2O	0.85	---
TiO_2	0.14	---
MnO	0.02	---

2.1.2 Natural clay

As a source for natural clay, a bulk disturbed brown soil sample was obtained from the vicinity of Al Karak - Mutah area which is located about 130 km south of Amman. Its chemical composition is determined by ICP and listed in Table (4). The sample was tested to determine natural moisture content, grain size distribution, and its classification according to the Unified Soil Classification System (USCS) (Evett & Cheng, 2007) in addition to Atterberg limits. The sample parameters are given in Table (5).

Table 4: Chemical composition of the brown soil determined by using ICP technique.

Oxide	**Wt %**
SiO_2	67.1
Al_2O_3	12.4
Fe_2O_3	7.1
CaO	1.9
MgO	0.8
MnO	0.16
TiO_2	1.7
K_2O	0.8
P_2O_5	0.11
L.O.I	7.5

Table 5: Physical and mechanical properties of brown soil.

Parameter	
Liquid limit (LL)	46.3
Plastic limit (PL)	23.5
Shrinkage limit(SL)	11.7
Plasticity index	22.8
Passing #200%	93.65
Clay fraction %	56.6
Specific gravity	2.64
Unconfined compressive strength Kg/cm^2	6.5
Maximum dry density g/cm^3	1. 88
California Bearing Ratio	4.2

2.1.2.1 Characterization of brown soil

The XRD analysis revealed that quartz and smectites (montmoorillonite) are the major components of the brown soil. The chemical analysis for major oxides was determined using the ICP. The major chemical constituents are given Table (4). Which indicates that SiO_2 is the major constituent, while Al_2O_3 and Fe_2O_3 are present in considerable amounts as compared with the very low CaO content. P_2O_5 is presented in relatively low concentration and the organic matter content is measured as (3%).

The physical and mechanical properties are determined and listed in Table (5). Atterberg limits have revealed that the soil is medium to high plastic clay. The maximum dry unit weight is 1.81 g/cm^3 and the optimum water content is 16% at standard Proctor effort (ASTM D 698).

The soil is classified into A-7-6 according to the American Association of Highway and Testing Organization (AASHTO), and classified as silty clay according to the Unified Soil Classification System (USCS) as shwon in Fig. (1).

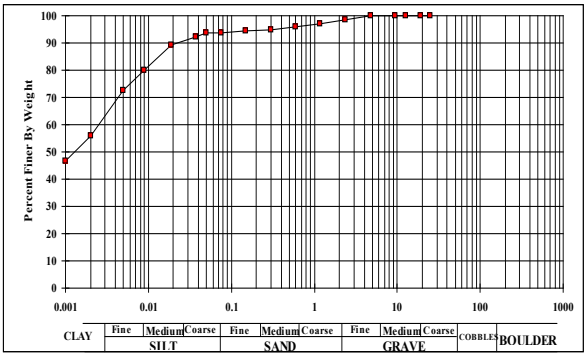

Figure 1: USCS plotting of particle size distribution of the brown soil used in the study

2.1.2.2 Unconfined Compressive Strength of the brown soil

The sample for the test was obtained with optimum moisture content and prepared using a Harvard miniature compaction device and measured the height and diameter of sample. The average of unconfined compression strength of clay equal (353.36 kN/m^2 = 3.60 Kg/cm^2) OR (347.16 kN/m^2 = 3.54 Kg/cm^2).

2.1.3 Sand

Sand was brought from Sweileh area western Amman. Flesh color and has a specific gravity equal to (2.66).

2.1.4 Cement

Ordinary Portland Cement (OPC), type-1 manufactured by Jordan Cement Factories Company was used.

2.2. Analytical methods

The study procedure of heavy metal encapsulation was done for Zn, Mn and Pb only. The conditions during the analytical procedure were done at room temperature. The permeability test was carried out for Sand-Clay mixture with 0, 3.5 and 10% of HCA, because the hydration reaction of the cement continued more than 28 days. The samples of this study were inserted into tight plastic bags during the study period (1 and 4 weeks) for curing purpose. Unfortunately, there is no standard basics to explain or predict the behavior of the mixture when adding the calcium ash so far due to the lack of similar results.

Chemical composition of the HCA samples was investigated using X-Ray Fluorescence machine (XRF-Pioneer F4), manufactured by Broker at the labs of Natural Resources Authority (NRA), Amman. The machine has an attached 72-position sample changer. The pellets were made by fusing 0.8 g of sample powder and 7.2 g of $L_2B_4O_7$ in Au/Pt crucible using a flexor machine (Leco 2000) for 4 minutes at 1200 ºC. The melt was poured in a mold and left to cool to form glass disc. The machine was calibrated with international standards, the analytical error was within ± 5%.

For the unconfined compressive strength test, the samples were obtained from mixtures of sand, clay and cement in percentages given in Table (6). Then HCA was added to mixture with (0.0%, 3.5% and 10%), herethen they will be called HCA0, HCA1 and HCA2 respectively. Three trials were done of each test. Water was added to make the sample saturated and the sample was compacted and prepared using Harvard miniature compaction device. The height and diameter were measured of each sample. The curing of samples is to put the sample in package, this sample contain the moisture content to time of test after one and four week. Because the compressive strength of samples were expected to be high we used the CBR machine.

Table 6: Percentage of mixed sand, clay and cement in the sample

Sample #	Sand (%)	Clay(%)	Cement (%)
1	25	50	25
2	25	25	50
3	50	25	25

3. Results and Discussion

3.1 Mixtures

3.1.1 Compressive strength of Mixture for HCA0

The procedure unconfined compressive strength test was done for mixture without HCA. The result are shown in Fig. (2).

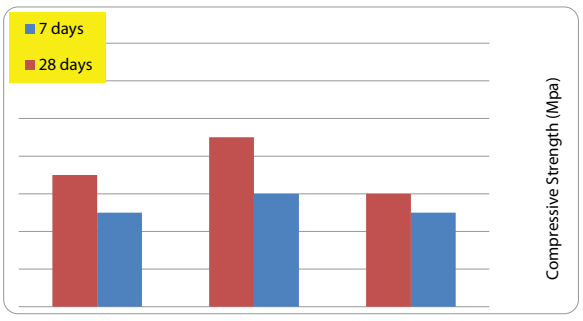

Figure 2: Compressive strength of samples of HCA0

3.1.2 Compressive strength of Mixture for HCA1

The procedure of the test unconfined compressive strength test was repeated but with adding 3.5% of HCA to the mixture, results are illustrated in Fig. (3).

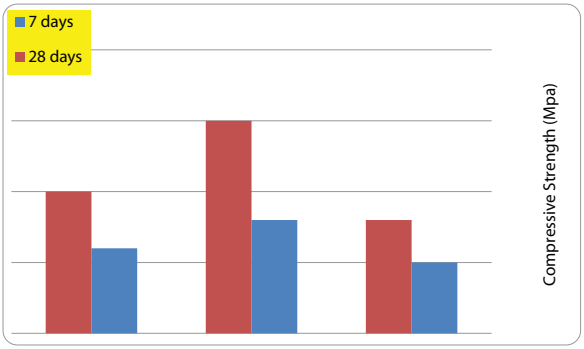

Figure 3: Compressive strength of samples of HCA1

3.1.3 Compressive strength of Mixture for HCA2

The same procedure of the unconfined compressive strength test was repeated with addition of 10% of HCA to the mixture, the results are shown in Fig. (4).

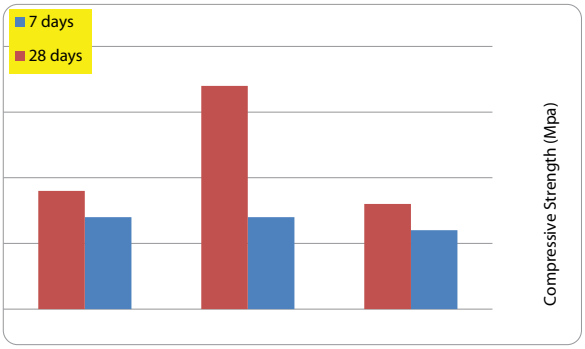

Figure 4: Compressive strength of samples of HCA2

3.1.4 Water Consumption

Table (7) shows that among the best mortars that contain all components (i.e. samples No. 1, 2, and 3), Sample No. 2 was the lowest consuming water mortars. The highest Cement percentages (50%) and equal Clay (25%) and Sand (25%) is the reason for that. However, this sample shows the highest compressive strength as shown in Figs. (2, 3 & 4). In general the effect of HCA percentage on the water consumption was clear and it found to be of proportional trend.

Table 7: Amount of water consumed by the three mixtures.

Sample #	Water (ml) in mixture with 10% high calcium ash (HCA2)	Water (ml) in mixture with 3.5% high calcium ash (HCA1)	Water (ml) in mixture without high calcium ash (HCA0)
1	29	24.9	24.94
2	29.1	28.3	26.5
3	25.2	18.5	20.35

3.1.5 Permeability of Mixture HCA0, HCA1 and HCA2

The permeability test was done for samples (HCA0, HCA1 and HCA2). Permeability coefficient (K) was decreased with increasing HCA content as revealed in Table (8). The highest K value was recorded for the HCA0 sample. Therefore, the lowest value of K was recorded in Sample No. 2 of HCA2,

which was equal to 2.7x 10-6 cm/sec. This might be attributed to the mixing ratio of mixture components that affects the water consumption.

Table 8: Result of permeability test for all mixture samples.

Sample No.	h_1 (cm)	h_2 (cm)	K (cm/sec)		
			HCA0	HCA1	HCA2
1	143	133	$1.29*10^{-5}$	$7.74*10^{-6}$	$3.5*10^{-6}$
2	143	133	$3.1*10^{-5}$	$4.74*10^{-6}$	$2.7*10^{-6}$
3	143	133	$2.8*10^{-5}$	$5.17*10^{-6}$	$4.35*10^{-6}$

3.2 Heavy Metal Encapsulation

The samples submerged in the water put into the permeability mold for 24 hours before tested. Table (9) shows the results of the analyzed water. It shows that sample No. 3 has the lowest leached Zn % of mortars of HCA2, while Pb and Mn were not detected in all samples.

The sample of high ratios of cement (50% of mixture) reflects increasing compressive strength with increasing both the percentage of ash and curing period as shown in Figs. (2, 3 & 4). High calcium ash played the role as a cementing binder of binding for sand so it increased the mixture compressive strength. The sample with mixed ratio (25 % sand, 25 % clay, 50 % cement) has the maximum compressive strength of (16.83 Mpa) of HCA1, there is no big difference if compared with samples of HCA2 mortars. While the sample with mixed ratio (50% sand, 25% clay, 25 % cement) of HCA2 has highest ability to encapsulation the metal ions. Where Mn and Pb were not detected and has the lowest Zn content released to the solution. However, the mixture sample that proved the test result with high compressive strength of (16.83 Mpa) and proper encapsulation of heavy metals from solution was with mixed ratio (25% sand, 25 % clay, and 50% cement) of HCA1. Shawabkeh and Mahasneh (2004), had studied the encapsulation of Lead ions in Sand-Cement-Clay mixture, and assured the ability of such mixture with mass percentages of 25% sand, 50% cement and 25% clay to encapsulate metal ions from solution. This mass ratio showed the maximum adsorption capacity toward lead with high compressive strength.

El-Hasan et al. (2011) found that oil shale ash produced from aerobic combustion is composed mainly from Calcite and Quartz beside clay, gypsum and apatite as gangue minerals. Such assemblage is considered as composite of OPC and clay. Moreover, the HCA has a pozzolanic composition similar to OPC, which reacts with the alkali portion of the mixture to produce self-cementaceous compounds. Eventually, an increase in HCA would increase the compressive strength, which is similar to the increase of OPC to the mixture. This might be attributed to the fact that HCA act as the role of OPC, therefore it enhances the compressive strength of mixture. And therefore, sample No. 2 of HCA2 is showing the higher compressive strength because of its higher cement content and this would explain the reverse relationship between the HCA and permeability.

Moreover, there is no relationship between permeability and water consumption. Which can be explained as HCA increased it needs more water for mixing, this was obvious from the proportional relation between HCA and water consumption as shown in Table (7).

Table 9: Result of permeability test for all mixture samples.

Sample No.	Zn (ppm)	Mn (ppm)	Pb (ppm)
1	0.68	Nd	Nd
2	0.53	Nd	Nd
3	0.38	Nd	Nd

4. Conclusions

Before starting this study we were expecting a negative results on compressive strength and water consumption after adding the high calcium ash to the mixture. But the research outputs revealed positive results. The encapsulation of heavy metals are acceptable too. The HCA1 and HCA2 with percentages 3.5% and 10% are the best to achieve higher compressive strength. Moreover, the HCA2 (10%) are the better in attain the higher metal encapsulation. Further studies needed to investigate the fate of toxic elements such as Cr, V and As.

Acknowledgemnet

The authors are grateful to the Natural Resources Authority (NRA) for providing the Oil Shale samples and helping in the ashing and chemical analysis procedures. As well we are thankful to Lafarge Cement Factory for providing the OPC.

References

[1] Abdel Hadi, N; Khoury, H. and Suliman, M (2008): Utilization of bituminous limestone ash from EL-LAJJUN area for engineering applications. Acta Geotechnica (2008) 3:139–151.

[2] Algeo, J.A.; and Maynard J.B. (2004): Trace element behavior and redox facies incore shales of upper Pennsylvanian Kansas-type cyclothem. Chemical Geology 206(3-4): 289-318.

[3] Al-Harahsheh, A.; Al-Adamat, R.; Al-Farajat, M. (2010): Potential impacts on surface water quality from the utilization of oil shale at Lajjoun Area/Southern Jordan using geographic information systems and leachability tests. Energy Sources A. 32: 1763–1776.

[4] ASTM D4318, Standard Test Method for Unconfined Compressive Strength of Cohesive Soil.

[5] ASTM D 698, Standard Test Methods for Laboratory Determination of Water (Moisture) Content of Soil and Rock by Mass

[6] Evett, J. and Cheng, L. (2007), Soils and Foundations (7 ed.), Prentice Hall.

[7] Han, S. Hu, K.; Cao, J., Pan, J., Liu, Y., Bian, L., and Shi, C., (2014): Mineralogy of Early Cambrian Ni-Mo Polymetallic Black Shale at the Sancha Deposit, South China: Implications for Ore Genesis. Resource Geology. 65(1):1-12.

[8] El-Hasan, T.; Szczerba, W.; Radtke, M.; Riesemeier, H.; Buzanich, G.; and Kersten, M. (2011): Cr(VI)/Cr(III) and As(V)/As(III) Ratio Assessments in ordanian Spent Oil Shale Produced by Aerobic Combustion and Anaerobic Pyrolysis. Environmental Science & Technology. 45(22): 9799-9805.

[9] El-Hasan, T. (2008): Geochemistry of the redox-sensetive trace elements and its implication on the mode of formation of the Upper Cretaceous oil Shale, Central Jordan. Neues Jahrbuch fuer Geologie und Palaeontologie Abh. 249(3): 333-344.

[10] Pasava, J. (1990): Anomalous Balck Shales-a new type of mineralization in the Barrandian Upper Proterozoic, Bohemian Massif, Czechoslovakia (in Czech with English abztract). Ph.D. Thesis, 1-145, Geological Survey, Prague.

[11] Pasava, J. (1991a): Comparison between the distribution of PGE in Black Shales from the Bohemian Massif (CSFR) and other black shale occurrences. Mineral. Deposita. 26: 66-103.

[12] Pasava, J. (1991b): Metal-rich black shales from the Barrandian Proterozoic (Bohemian Massif, Czechoslovakia). In: Pagel

& Leroy (eds.): Source, Transport and Deposition of Metals. Balkeme, Rotterdam. 577-580.

[13] Pašava J., Sulovský P., Kovalová M. (1993) Geochemistry and mineralogy of metal-rich black shales from the Bohemian Massif with a description of possible new molybdenum selenide and telluride. Canadian Mineralogist, 31, 745-754.

[14] Rimmer, S.M. (2004): Geochemical paleoredox indicators in Devonian-Mississipian Black shales, Central Appalachian Basin (USA). Chemical Geology. 206(3-4):373-391.

[15] Shawabkeh, R.A. & Mahasneh, B. Z. (2004): Encapsulation of Lead Ions in Sand-Cement-Clay Mixture. Electronic Journal of Geotechnical Engineering. EJGE; 2004; Vol. 9.

JJEES
Jordan Journal of Earth and Environmental Sciences
Volume 6, (Special Publication, Number 3), June, 2014
ISSN 1995-6681
Pages 29- 34

Geology and Mineralogy of Zeolitic Tuff in Tulul Unuqar Rustum Ash Shmaliyya, NE JORDAN

Khalil M. Ibrahim*

Department of Earth & Environmental Sciences, Hashemite University, Zarqa, Jordan

Abstract

Detailed geological mapping and drilling campaign in Tulul Unuqar Rustum Ash Shamaliyya (URS) volcanic center have been carried out to evaluate the geology and mineralogy of zeolitic tuff. The most abundant rock type in the volcano is scoriaceous tuff and zeolitic tuff. The zeolites occur as cement to palagonite clasts and as filling inside the vesicles, making about 30% of the rock. Phillipsite is the most abundant zeolites mineral with spherulitic radiating aggregates or stout-prismatic crystals. The second zeolites mineral is chabazite which occurs as rhombohedra with simple penetrating twinning. Chemical analysis of the phillipsite indicates that they are K-rich type with similar Na/K and Ca/K ratios and has small variation in the Si/Al ratio. The zeolitic tuff samples have a wide range of SiO_2 content indicating wide range of alteration and formation of authigenic minerals. The model of zeolites formation in the URS volcano is believed to be an open hydrological system model, where soluble elements released from the fresh basaltic glass by the hydrolysis reaction due to the raised higher pH and saline conditions, re-deposited in the of form zeolites, smectite and calcite.

Keywords: phillipsite, chabzite, zeolitic tuff, NE Jordan.

1. Introduction

Harrat Ash Shaam Basaltic Group (HAS) exposed in northeast Jordan is considered the largest volcanic field in the Arabian Plate (Ibrahim, 1993, Ibrahim et al., 2003, Shaw et al., 2003) (Fig. 1). The basaltic activity of the HAS was manifested in form of intermittent pulses of eruption started from about 26 Ma and continued to about 0.1 Ma ago (Illani et al., 2001). As a result, volcanic tuff deposits were extensively formed from isolated volcanic centers, which are confined to three volcanic fields as shown in Fig. 1 (Ibrahim et al., 2006). Locally, the black variety of the volcanic tuff is commercially exploited as pozzolanic tuff in cement industry. The estimated annual production of the black pozzolana from the HAS Basaltic Group is about 500,000 ton. Zeolites were discovered and reported in several volcanic centers associated with the volcanic tuff (Dwairi, 1987, Ibrahim, 1996; Al Dwairi et al., 2009; Khoury et al., 2015). A new occurrence of zeolites was reported in Tulul Unuqar Rustum Ash Shamaliyya (URS) area during an intensive geological exploration program to delineate the commercial pozzolanic tuff deposits. The URS is a cinder cone of Tlul Esh Shahba volcanic field (Fig. 1, Field 2), which is about 55 km east of As Safawi town along the Amman – Baghdad highway. It is situated about 20 km to the south of the highway. The study area is bordered by the coordinates 394900 – 395900 E and 180700 -181700 N; Palestine Grid. The main objective of this paper is to contribute to the geology, mineralogy and geochemistry of the zeolitic tuff in the URS area.

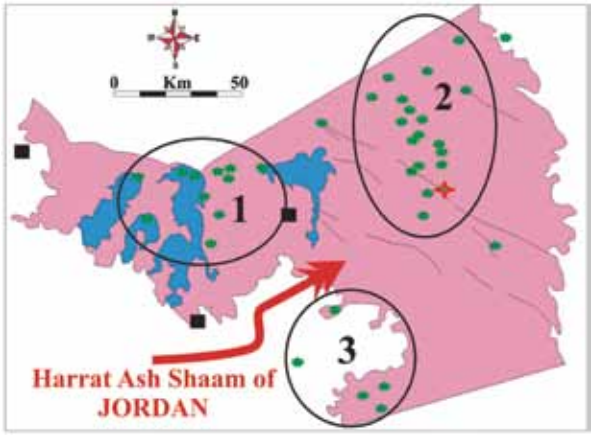

Figure 1: Location map of Harrat Ash Shaam Basaltic field and location of Tulul Unuqar Rustum Ash Shmaliyya (URS) volcanic center. (1): Asfar volcanic field, (2): Tlul Esh Shahba volcanic field, (3) Qatafi volcanic field.

2. Geological Setting

The HAS was classified by Ibrahim (1993) into five volcanic groups. As illustrated in Table 1, the URS volcanic center comprises rocks belong to the Asfar and to Rimah groups. The former is defined simply to include the basaltic rocks, which pre-date or associated with the Rimah Group (Ibrahim et al., 2006). The latter is subdivided into two formations of which the Aritayn Formation contains authigenic zeolites (Ibrahim, 1996). The second is Hassan Formation. The Aritayn Formation is developed from composite cinder

* Corresponding author. e-mail: Ibrahim_kh@yahoo.com

strato-volcanoes. The formation consists of stratified, sorted, poorly cemented air-fall tuff and agglomerate, which are rarely intercalated with short lived lava flows from a central vent. Lithologicaly, it is made up of fine-grained ash, angular and spherical lapilli as well as volcanic bombs and blocks of different size and shapes cemented either by carbonate or zeolites and carbonate. However, non-cemented volcanic ash and lapilli is sometimes found forming tephra deposits.

Table 1: Late phases of Harrat Ash Shaam basaltic field (Ibrahim et al., 2006)

Eruption Phase	Age (Ma)
Bishriyya Group	1.80 – 0.15
RIMAH Group	2.19- 0.60
Late NW-SE dykes	3.09-1.64
ASFAR Group	4.52 -1.00

3. Methods of Investigations

Field work was conducted to execute detailed geological mapping and exploration drilling. A detailed geological map at a scale of 1: 5000 was prepared for the area (Fig. 2). Four exploration boreholes 15 to 25 m deep were drilled. Continuous core drilling was used to obtain representative samples. The cores were subjected to detailed and systematic description of their lithology, texture and color (Fig. 3). 20 representative samples were selected from the zeolitic tuff for further studies and analyses. Mineralogical and petrographical characterization of the core samples was carried out using the polarizing microscope. Normal thin sections were prepared for the representative samples. The samples were characterized using petrological, mineralogical, and chemical methods.

The analytical work included the minerals identification using X-ray diffraction analysis (XRD) and chemical analysis using X-ray fluorescence techniques (XRF). A Shimatzu X-ray diffractometer with CoKα radiation was carried out in the Royal Scientific Society according to (SOP) No. 131M03-010 test method. Whole rock 'random powder' samples were scanned with a step size of 0.02° 2 theta and counting time of 0.5 s per step over a measuring range of 2 to 65° 2q. Powdered samples were analyzed using a XRF machine (PANanlytical-Axios and a PW2400 spectrometer). Samples are prepared by mixing with a flux material and melting into glass beads. After mixing the residue with 5.0 g lithium metaborate and 25 mg lithium bromide, it is fused at 1200 °C for 20 min. The calibrations are validated by analysis of Reference Materials. Blank samples and several certified reference materials (CRM) were used for the correction procedures. The beads were analyzed by wavelength dispersive x-ray fluorescence spectrometry (WD-XRF). To determine loss on ignition (LOI) 1000 mg of sample material are heated to 1030 °C for 10 min. To investigate crystal forms and the paragenetic relationships of the zeolites and non-zeolites, scanning electron microscope (SEM) and Energy-Dispersive X-ray (EDX) study of selected samples has been carried out using a PANanlytica based in Mango Center, University of Jordan.

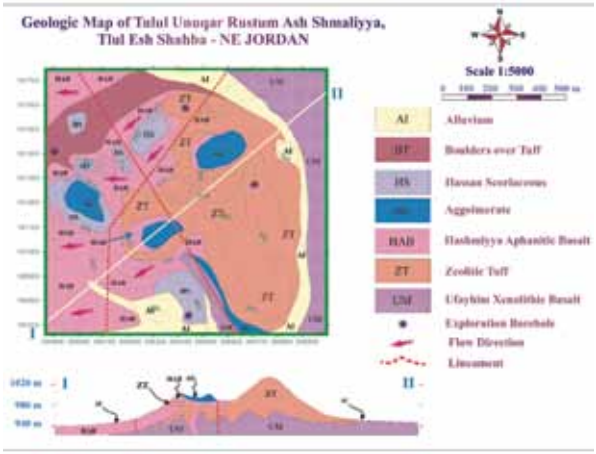

Figure 2: Geological map of Tulul Unuqar Rustum Ash Shmaliyya volcanic center

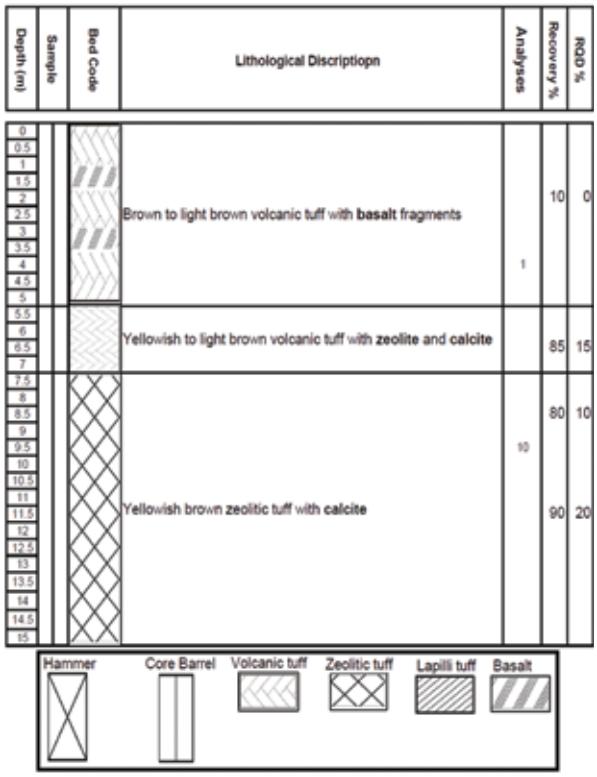

Figure 3: Lithological description of selected borehole drilled in the study area.

4. Results

4.1. Geology and Volcanology

The URS is a conical crescent shape volcano (Fig. 4a & 4b) that is about 750 m wide and 950 m long. It consists of three summits surrounding a depression, facing the southwest (Fig. 4a). The topographic relief in the volcanic cone is about 70 m, varying from altitude about 940 m in the low laying ground surrounding the cone to altitude 1030 m at the north eastern summit of the volcano (Fig 4a & 4b).

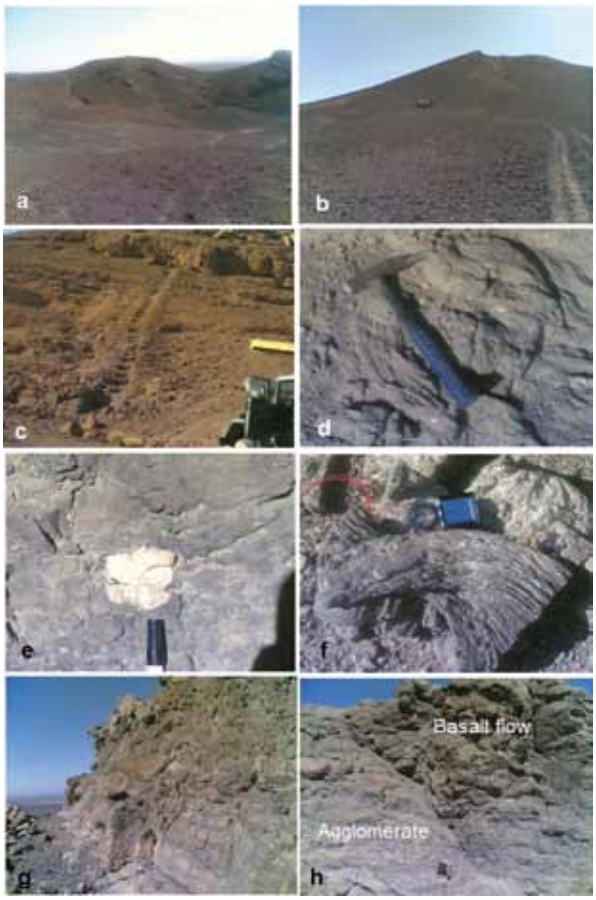

Figure 4: Lithology and morphology of URS volcanic center. (a): Morphology of volcanic center; (b): Zeolitic tuff unit (c): Hassan scoriaceous unit; (d): Sandstone inclusions in Ufayhim basalt unit; (e) Sandstone inclusions in Ufayhim basalt unit; (f): Volcanic bombs; (g): Agglomerates unit; (h): Basaltic flow over agglomerate.

Detailed geological mapping of the URS (Fig. 2) indicate presence of several lithological rock units outcropping in the URS area. The Ufayhim Xenolithic Basalt is the oldest unit. It displays closely spaced horizontal jointing, which appears as thin laminations. It contains huge amounts of lherzolite and dunite xenoliths sometimes forming up to 50-60%. They also host large pyroxene xenocrysts. The xenoliths and xenocrysts vary in size from few millimeters up to 15 cm, and are rounded. The xenoliths have brown reaction rims, comprising mainly granular, orange, olive brown olivine and lesser amounts of dark green tabular pyroxene.

The zeolitic tuff of the Aritayn Formation (Fig. 4c) and the Hassan scoriaceous tuff (Fig. 4d) are very similar in lithology. The difference is that the clasts in the former unit are cemented by zeolites and calcite. The zeolitic tuff consists of stratified, sorted, air-fall volcaniclastic (tuff, labillistone, volcanic breccia and agglomerate). The unit contains ash, lapilli, volcanic bombs and basaltic blocks of different size and shapes that are all cemented by zeolites and carbonate. The volcaniclastic layers are arranged in shower bedding maintaining an even thickness and exhibit graded laminations with particle size from 1 mm to 50 mm. zeolitization of the volcanic tuff is not consistent. Localities with high degree of zeolitization are characterized by presence of yellowish light brown color, soft and friable highly altered lapilli clasts. They are cemented by a thick coating of zeolites and calcite (Fig. 5). The exposed thickness of the zeolitic tuff in the URS is from 10 m to 30 m whereas the scoriaceous tuff is from 2 m to 15 m (Fig. 3). The scoriaceous tuff is characterized by presence of highly vesicular lappili and cinder clasts (grain size >4 mm) called scoria. The unit comprises bedded, friable, reddish brown to violet in color, poorly sorted, coarse-grained scoria (generally 0.5-20 cm long, and with average of 6 cm) making about 85% of the rock, along with volcanic bombs and blocks with various shapes and up to 50 cm-sized (Fig. 4f). Mantle xenoliths and lower crust lithic fragments are abundant in the zeolitic tuff and scoriaceous tuff units (Fig. 4e). They also host large pyroxene xenocrysts.

Figure 5: Hand specimen of the zeolitic tuff

The Hashimyya basalt is the second basaltic phase in the URS area. It covers most of the western and northern parts of the volcano, and makes about 25% of the URS area. It is less than 15m thick and comprises thin flow units, mostly between 2 m and 3 m thick, sometimes inter-bedded within the volcanic tuff units. The basalt is melanocratic, bluish-gray to medium-dark gray, aphanitic, holocrystalline olivine-phyric basalt with microporphyritic textures.

Agglomerate is a very hard pyroclastic unit with large clasts (Fig. 4g). It occurs as a massive, hard, about 5 -10 m thick unit consists of 2 –4 beds occupies the central part of the URS area. It gives weathering colors of brown, red brown and black. It includes bombs with various shapes (Fig. 4f). The clasts are from 15 cm to 50 cm-sized and with average of 20 cm. The unit is associated with thin basaltic dikes and flows (Fig. 4h).

Field evidence for faulting in the basalts of the mapped area is usually equivocal. Therefore, the structure interpretation is based mainly on: interpretation of satellite images, the alignment of volcanic centers and vents along with the abrupt variation in elevation of lava surface. In the mapped area, the faulting is influenced by the regional NW- SE tectonics related to Qitar El Abid dike and the associated fault system (Fig. 1), which is a regional structure extends more than 100 km with not less than 500 m wide (Ibrahim et al., 2003, Rabba' and Ibrahim, 2005). It appears as a normal fault with a possible strike-slip movement. The other important fault trend is the dominant N-S fault associated with the central volcanism of the Asfar Group occurring in the HAS in both the Asfar and Tlul Esh Shahba volcanic fields (Fig 1) (Ibrahim et al., 2006). The fault is indicated based on the alignment of the volcanoes

and the associated volcanic vents, although direct evidence for vertical and/or horizontal displacement is lacking.

4.2. Petrographic Study

The studied samples comprise highly-altered volcanic tuff with variable amounts of secondary minerals including zeolites in the form of phillipsite and chabazite; smectite; calcite and gypsum. The volcanic clasts comprise highly vesicular dark brown, yellowish brown to deep red color palagonite. Color variability reflects the degree of alteration (i.e. palagonitization). The vesicles are either encrusted by rim of the secondary minerals or totally filled with the secondary phases. These vesicles are circular, subcircular and sometimes irregular in shape. The palagonite is characterized by its vitreous luster with conchoidal fracture. Micro-phynocrysts of anhedral olivine and iddingsite are common. Plagioclase is found as euhedral to subhedral phenocrysts or small laths in the groundmass with albite twinning.

All samples contain variable amounts of phillipsite crystals. It occurs mainly as colorless, radial, fan shape crystal aggregates or as spherulitic growth. Phillipsite crystals form thin rim encrusting walls of the vesicles or cementing the palagonite clasts. Chabazite appears as colorless sugar-like, rhombohedral crystals with twinning. Smectite appears as colorless, cloudy rim fringing palagonite granules and/or encrusting the vesicle walls with minute fringes in most of the samples.

4.3. Mineralogy

In addition to presence of primary minerals including olivine, pyroxene and plagioclase, the sample host secondary minerals including zeolites. The zeolites occur in form of phillipsite and chabazite. Quantitative determination of these two minerals was aided by XRD. As Show in Table 2, zeolites content is very high in specific areas among the mapped areas. The total zeolites content is up to 60% in the borehole No. 1 and close to 49% in the borehole No. 2. Phillipsite is the most dominant zeolites mineral which makes up to 49% in some samples. The average zeolites content in the zeolitic tuff in the URS is 30%.

Table 2: Qualitative mineralogical composition of the zeolite samples by (XRD).

Sample No.	BH No.	Depth (m)	Phillipsite (wt%)	Chabazite (wt%)	Total Zeolite (wt%)
1	1	3 – 4	21	12	33
10	1	9 – 10	45	15	60
8	2	5 – 6	28	21	49
9	2	24 – 25	49	0	49
11	2	16 - 17	44	3	47
5	3	5 – 6	8	0	8
6	3	6 – 7	6	0	6

4.4. SEM and EDX Results

The SEM study shows that phillipsite occurs either as spherulitic radiating aggregates or stout-prismatic crystals elongated along the a-axis (Fig 6a, 6b & 6c). Phillipsite forms pseudo-orthorhombic twinned prismatic crystals evident from the two-sided or four sided dome capping the end of the prism (Fig. 6b). Some of the phillipsite twins imitate a tetragonal prism. The spherulites are about 40µm, and range in length from 30µm to 100µm and in width from 10µm to 5µm. EDX study of phillipsite (Fig. 7) indicates that Si/Al ratio is between 2.45 and 2.65, Na/K ratio is 0.95 and Ca/K ratio is around 0.45 (Table 3). It can be concluded that URS phillipsite is K-rich phillipsite.

Chabazite occurs in colorless rhombohedra with simple penetration twinning (Fig. 6e & 6f). Crystals vary in size from 50 up to 250µm. Smectite occurs as colorless aggregates of tiny flakes (Fig. 6d) or as thin rim fringing palagonite clasts, or encrusting vesicle walls.

Table 3: Energy dispersive X-ray analysis of phillipsite crystals.

		BH1			BH2	
El	Z	(Wt %)	Atomic (%)		(Wt %)	Atomic (%)
O	8	43.29	57.71		40.22	54.49
Na	11	2.94	2.73		2.63	2.48
Al	13	13	10.27		13.42	10.78
Si	14	33.1	25.14		36.98	28.54
K	19	5.25	2.86		4.71	2.61
Ca	20	2.42	1.29		2.04	1.1
Si/Al			2.45			2.65
Na/K			0.95			0.95
Ca/K			0.45			0.42

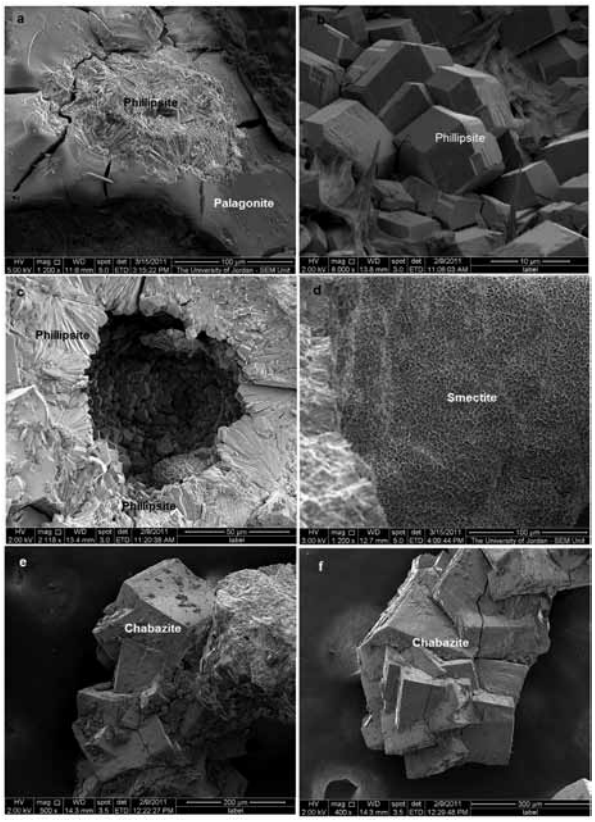

Figure 6: Scanning electron micrograph of the zeolitic tuff (a, b, c): phillipsite, (d): smectite and (e, f): chabazite.

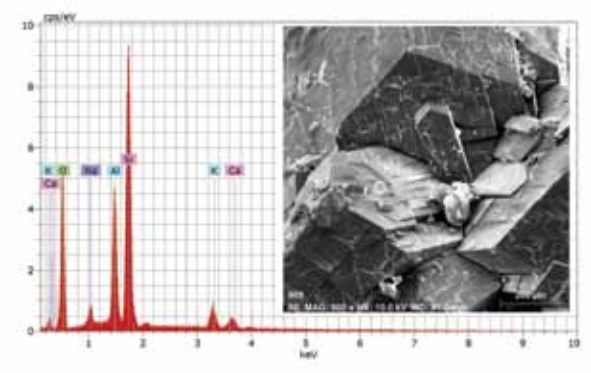

Figure 7: Energy dispersive X-ray analysis of phillipsite crystals.

4.5. Geochemistry

As Illustrated in Table 4, the samples of the zeolitic tuff are characterized by low SiO_2 content with a very wide range of variation. It varies from 21.6% to 40.10% decrease with increasing degree of alteration. The Al_2O_3 wt% in the studied samples is between 7.69% and 12.8%. As shown in Fig 8a and 8b, the Al_2O_3 wt% versus SiO_2 wt% and total alkalis (Na_2O + K_2O wt %) versus SiO_2 wt% display proportional relationships, indicating that they exhibit similar geochemical behavior under the zeolitization process. The studied samples are also typified by high value of LOI, with a very wide range of variation as well, ranging from 10.0 to 30.7 wt%. The inverse relationship between SiO_2 wt% versus LOI content is well illustrated in Fig 8c. This indicates that the samples are highly altered and display several stages of alteration. This is supported by field evidences, including occurrences of abundant zeolites and calcite in the volcanic tuff, occurring as cement in the volcanic clasts. The presence of very high CaO wt% in selected samples up to 24.9% indicates presence of abundant carbonates. Presence of minor amounts of Cl wt% and SO_3 wt% may indicate occurrence of traces of gypsum and halite. The other important constituents of the samples are the Fe_2O_3 and MgO. In detail, the Fe_2O_3 wt% is from 6.26%, to 13.5%, whereas the MgO wt% is from 4.04% to 8.05.

Table 4: Chemical composition of selected zeolitic tuff samples (wt%) by (XRF).

Sample No.	1	5	6	7	8	9	10	17	18
SiO_2	33.40	25.30	21.60	33.90	28.60	29.60	37.60	37.30	40.10
TiO_2	2.09	1.11	1.09	2.15	2.91	1.72	2.09	2.59	2.30
Al_2O_3	10.30	8.07	7.69	11.02	9.23	9.31	12.80	12.80	13.00
Fe_2O_3	11.10	6.26	6.04	11.10	14.80	10.40	11.30	13.50	12.50
MnO	0.13	0.07	0.07	0.13	0.16	0.11	0.13	0.16	0.15
MgO	6.56	4.04	3.31	8.05	7.52	7.84	6.90	6.58	8.47
CaO	8.72	23.20	24.90	6.89	5.11	7.21	8.00	7.21	9.90
Na_2O	1.43	0.13	0.13	1.22	0.88	0.42	1.32	0.85	0.90
K_2O	1.53	0.76	0.43	1.80	2.00	1.82	2.23	1.52	1.91
P_2O_5	0.55	0.15	0.16	0.37	0.71	0.59	0.56	0.67	0.59
SO_3	1.03	0.36	0.16	0.36	0.23	0.14	0.53	0.11	0.11
Cl	0.76	0.04	0.05	0.06	0.92	0.13	0.51	0.03	0.03
LOI	21.80	30.50	34.50	22.70	26.20	30.70	15.80	16.90	10.00

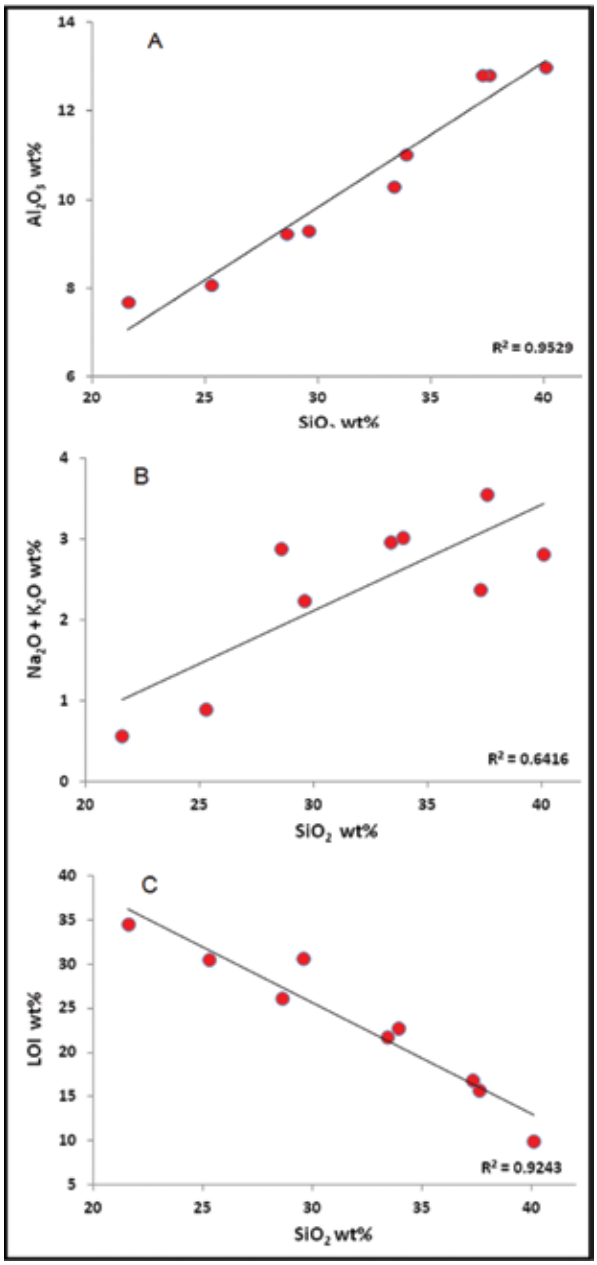

Figure 8: Variation diagram of selected major oxides in the zeolitic tuff, (a): SiO2 vs Al2O3; (b): SiO2 vs (Na2O+K2O) and (c): SiO2 vs LOI.

5. Discussion

The origin of zeolites in Jordan was thoroughly investigated by many authors (Dwairi, 1987; Ibrahim, 1996; Ibrahim & Hall, 1995, 1996; Khoury et al, 2015). The model of zeolites formation in the URS volcano is believed to be the open hydrological system model which was first described by Hay and Iijima (1968a & 1968b) at Koko Crater, Hawaii. This model was already adopted by Ibrahim (1996, Ibrahim and Hall (1995 & 1996) and Khoury et al. (2015).

Following the deposition of the fresh basaltic glass in the volcanic tuff pile, percolating water coming from rainwater interacts with the glass. The interaction of the percolating water with the fresh non-stable basaltic glass in the volcanic tuff increases the pH and salinity of the percolating water with depth. Thus, hydrolysis reaction of the basaltic glass takes place. This leads the volcanic glass to transform to palagonite.

As a result of the transformation of the fresh basaltic glass to palagonite, smectite and different zeolites minerals start to form. Mass movement of the percolating water downwards through the volcanic tuff pile leads to development of vertical zonation of the zeolites minerals (Hay and Iijima, 1968a & 1968b, Ibrahim, 1996). The elements released from the fresh basaltic glass by hydrolysis reaction including Si, Al, Na, K, Ca and Mg have been re-deposited as authigenic minerals (smectite, zeolites and calcite) forming the intergranular cement and the amygdaloidal texture.

The degree of zeolites formation in the open hydrological system depends mainly in many factors including the chemical and mineralogical composition of the parent material (basaltic glass), chemistry of the percolating water, water /rock ratio, the physical properties of the host-rock including its porosity and permeability, hydraulic /topographic gradient and the climatic conditions including rainfall and temperature. Such conditions influence the chemical and structural nature of the zeolites minerals crystallization (Hay, 1986; Barth-Wirsching and Höller, 1989; De la Villa et al., 2001).

6. Conclusions

Exploration program including detailed geological mapping and drilling was executed in Tulul Unuqar Rustum Ash Shamaliyya volcanic centers of the Tlul Esh Shahba volcanic field in northeast Jordan for the purpose of evaluating the geology and mineralogy of zeolitic tuff. The geological mapping indicates that the most abundant rock type is the scoriaceous tuff and zeolitic deposits. The volcanic tuff contains zeolites occurring as cement and as filling inside the palagonite clasts, making about 30% of the rock. Two zeolites minerals were reported, which are phillipsite and chabazite. Chemical analysis of phillipsite indicates that they are K rich type with narrow variation in Si/Al ratio, and similar Na/K and Ca/K ratios. The zeolitic tuff samples have a wide range of SiO_2 content indicating wide range of degree of alteration which leads to formation of authigenic minerals. The model of zeolites formation is believed in the URS volcano is believed to be the open hydrological system model, where soluble elements released from the fresh basaltic glass by the hydrolysis reaction due to the high pH and saline conditions re-deposited in form of zeolites, smectite and calcite.

Acknowledgemnet

The author would like to thank Hamdi Mango Center for Scientific Research at the University of Jordan for their financial support of the project entitled ‘‘Characterization and beneficiation of new-explored Jordanian zeolitic tuff from selected localities in northern, central, and southern Jordan, and investigation their capability for removal of pollutants from water’’. Special thanks extend to Mazen Rial Engineering Office, Amman for providing core samples and boreholes data. Thanks are also extended to the reviewers of this article for their critical comments and suggestions.

References

[1] Al Dwairi, R., Khoury, H., Ibrahim, K., (2009) Mineralogy and Authigenesis of Zeolitic Tuff from Tall-Juhira and Tall Amir, South Jordan, Jordan. J. Earth Environ. Sci. 2 (2), 81–88.

[2] Barth-Wirsching, U., Höller, H., (1989) Experimental studies on zeolite formation conditions. Eur. J. Mineral. 1, 489–506.

[3] De la Villa, R.V., Cuevas, J., Ramírez, S., Leguey, S., (2001) Zeolite formation during the alkaline reaction of bentonite. Eur. J. Mineral. 13, 635–644.

[4] Dwairi, I.M. (1987) A chemical study of the palagonitic tufts of the Aritain area of Jordan, with special reference to nature, origin and industrial potential of the associated zeolite deposits. PbD Thesis, Hull University UK, 408 p

[5] Hay, R.L., (1986) Geologic occurrence of zeolites and some associated minerals. Pure Appl. Chem. 58, 1339–1342.

[6] Hay, R.L., lijima, A., (1968a) Nature and origin of palagonite tuff; of the Honolulu Group on Oahu, Hawaii. Geol. Soc. Am Mere. 116, 331–376.

[7] Hay, R.L., lijima, A., (1968b) Petrology of palagonite tufts of Koko Craters, Oahu, Hawaii. Contrib. Mineral. Petrol. 17, 141–154.

[8] Ibrahim, K.M., 1993. The Geological Framework for the Harrat Ash-Shaam Basaltic Super-group and its Volcanotectonic Evolution. Natural Resources Authority, Geological Mapping Division Report, Amman-Jordan, 61p.

[9] Ibrahim, K.M., (1996) Geology, mineralogy, chemistry, origin and uses of the zeolites associated with Quaternary tuffs of Northeast Jordan. PhD thesis, University of London, UK. 16.

[10] Ibrahim, K.M., Shaw, J., Baker, J., Khoury, H., Rabba’, I., Tarawneh, K., (2006) Pliocene-Pleistocene volcanism in northwestern Arabian plate (Jordan): I. Geology and geochemistry of the Asfar Volcanic Group. Neues Jahrb. Geol. Part-A 242, 145–170.

[11] Ibrahim, K.M., Tarawneh, K., Rabbaa, I., (2003) Phases of activity and geochemistry of basaltic dike systems in northeast Jordan parallel to the Red Sea. J. Asian Earth Sci. 21, 467–472.

[12] lbrahim, K.M, Hall, A. (1995) New occurrences of diagenetic faujasite in the Quaternary tufts of north east Jordan. Eur. J. Mineral. 7:1129 1135

[13] lbrahim, K.M., Hall, A., (1996) The authigenic zeolites of the Aritayn Volcaniclastic Formation, northeast Jordan. Mineralium Deposita 31, 589–596.

[14] Illani, S., Harlavan, Y., Tarawneh, K., Rabba, I., Weinberger, R., Ibrahim, K., Peltz, S. & Steinitz, G. (2001) New K-Ar ages of basalts from the Harrat Ash Shaam volcanic field in Jordan: implications for the span and duration of the upper mantle upwelling beneath the western Arabian plate. - Geology, 29: 171-174.

[15] Khoury H. N., Ibrahim K. M., Al Dwairi R. A., (2015) Wide Spread Zeolitization of the Neogene - Quaternary Volcanic Tuff in Jordan. Journal of African Earth Sciences. (In Publication)

[16] Rabba’, I, Ibrahim, K. M. (2005) Geological map of Tlul Esh Shahba, 355V scale 1:100,000, Natural Resources Authority, Geology Directorate, Amman, Jordan.

[17] Shaw, J., Baker, J., Menzies, M., Thirlwall, M. & Ibrahim, K. M. (2003) Petrogenesis of largest intraplate volcanic field on the Arabian plate (Jordan): a mixed lithosphere-Asthenosphere source activated by lithospheric extension. - J. Petrol., 44: 1657-1679.

JJEES
Jordan Journal of Earth and Environmental Sciences
Volume 6, (Special Publication, Number 3), June, 2014
ISSN 1995-6681
Pages 35- 40

Characterization of Pozzolana from Tafila area and its potential use as soil amendment for plant growth

Reyad Ali Al Dwairi*

Department of Natural Resources and Chemical Engineering, Engineering Faculty, Tafila Technical University, Tafila, Jordan.

Abstract

Volcanic tuff (VT) (Pozzolana) deposits are available in huge quantities in Tafila area. Al Hala Volcano (HV) is one of the biggest deposits for VT located in southern Jordan which was chosen in this study. Characterization of zeolitic tuff (ZT) minerals is the main goal of this study in addition to the agricultural application for possible usage as soil amendment and improvement. Field studies indicate that VT is highly altered to ZT due to percolating alkaline water. ZT is characterized by highly weathered, friable and range in color according to zeolitization process and chemical composition to many different colors. The three main ZT types are reddish (RZT), brownish (BZT) and grayish (GZT). Mineralogical studies indicate that VT is composed mainly of three mineral components: Volcanic glass (palagonit), primary rock forming minerals (idingsite and diobside) and secondary rock forming minerals (zeolites, calcite and clay minerals). The main zeolites minerals in HV are phillipsite and chabazite. The ZT from HV shows acceptable pH with high cation exchange capacity range from (189 meq/gm) for RZT to (136 meq/gm) for GZT. Geochemical studies indicate that ZT from HV has low Na_2O% ranges between 0.34% - 1.44% with a high percentage of important oxides such as Ca, Mg, K, Mn, and Al. The type of Tafila Soil (TS) is silty clay texture which is considered as heavy soil as indicated by size fractionation analysis results.

The ZT from HV is evaluated for agricultural applications by using RZT and GZT as soil amendments for planting tomatoes and pepper vegetables. The mixture with the ratio of 50:50 TS:RZT results shows increasing in terms of growth, yield and roots assemblages for both vegetables.

Keywords: Pozzolana, Al Hala volcano, Volcanic Tuff, Zeolites, Phillipsite, Soil Amendment, Plant growth.

1. Introduction and Backgrund

Pozzolana is the commercial name of the igneous rocks named volcanic tuff (VT). The mineral content of VT varies from geological bed to another bed based on the weathering rate and zeolitization processes which reflect the quantity of secondary minerals associated with volcanic tuff. Zeolites are the most important minerals associated with volcanic tuff, so the name of the volcanic tuff enriched with zeolites is zeolitic volcanic tuff or zeolitic tuff (ZT).

Zeolites are hydrated aluminum silicate framework in which its structure contains channels or pores filled with exchangeable cations and some percentage of water (Mumpton 1978). They characterized by availability, low coast, high ion exchange capacity, excellent adsorption properties and slow release fertilizers. Such important properties make zeolites a good solution as a natural alternative of other used soil fertilizers and amendments. Identification of zeolite as a mineral goes back to 1756, by the Swedish mineralogist, Fredrich Cronstet (Gottardi, 1978). In the world, their commercial production and use started in 1960s, but in Jordan they were discovered for the first time in 1987 by Dwairi in north east area (Arytain Volcano). Jordan has important zeolitic tuff production potentials and reserves that cover large areas that are distributed in three main locations north east, central and south Jordan (Al Dwairi 2007).

The application of natural zeolitic tuff as soil conditioner and fertilizer has known by the Japanese for over a hundred year. Mumpton (1985) discussed the zeolite potential for the use as a source for slow release of fertilizers such as N and K. The zeolitic tuff (soil conditioners) is also used to reduce the agriculture pollution. Al Dwairi and Al-Rawajfeh (2012) listed the recent patents of natural zeolites and their applications in environment, agriculture and Pharmaceutical Industry.

In Jordan zeolites, ZT, and VT have been studied widely for their mineralogy, petrology and their environmental applications. The most important studies were carried out by Dwairi (1987), who was the first to discover zeolites in Jabal Aritain, Ibrahim (1993), who accomplished a lot of mapping, geological and geochemical work, and Khoury, et al (2015) summaries new Neogene – Quaternary zeolitization of the volcanic tuff in Jordan.

Jordanian phillipsitic tuff of Aritain area was suggested for a possible us as a soil amendment (conditioner) in agriculture (Reshiedat, 1991), furthermore Dwairi (1998) used zeolitic phillipsite tuff from Aritain as slow release fertilizer, and he evaluated the exchange and release properties of the natural phillipsite tuff by using NH4–Na system. Ghrir (1998) has evaluated the Jordanian Phillipsitic tuff from Aritain (north east Jordan) and Mukawer (Central Jordan) in agriculture as soil conditioner for planting strawberry under green houses.

Manolov, et al (2005) used Jordanian zeolitic tuff from Aritain (north east Jordan) as raw material for the preparation of

* Corresponding author. e-mail: reyadn@hotmail.com

substrates used for plant growth. The research study concluded that the Jordanian zeolitic tuff has specific properties – high CEC, high content of macro and microelements which makes them one of good alternatives to the traditional potting media.

Al Dwairi (2007) reported new occurrences in the northeast, central, and south of Jordan. The research explored and studied the characterization (mineralogy, petrology and geochemistry) of all possible locations of volcanic tuff in Jordan. Also, in 2009 Al Dwairi et al studied the mineralogy and authigenesis of zeolitic tuff from Tall-Juhira and Tall Amir, in the south of Jordan. New occurrences in northeast, central and south Jordan were later reported by Ghrir (1998), Tarawneh, (2004), Al Dwairi (2007), Al Dwairi et al. (2009) and Al Dwairi and Sharadqah (2014).

The soil of Tafila (TS) area is very poor in terms of minerals necessary for plants growth and also the rainfall percentage is very low, consequently zeolites as a soil conditioner can play a significant role in improving the soil characterization which will be reflected upon agricultural production.

Figure 1: Soil from Al Eis area (Tafila).

Tafila area considered as arid to semiarid regions with a short rainy winter season with an average annual precipitation of 100 mm. The soil of Tafila shown in Fig.(1) is characterized by soft grains, high porosity and low permeability, so this type of soil is called the heavy soil, consequently zeolites as a soil conditioner plays a significant role in improving the physical and chemical characterization of soil which will be reflected upon agricultural sector in Al Tafila.

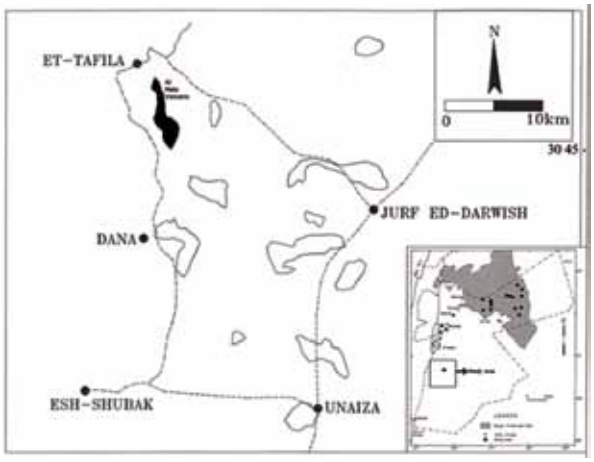

Figure 2: Location map of the southern Jordan basaltic tuff showing the Al Hala Volcano (after Al Dwairi 2007).

To enhance and improve Tafila soil, this research proposes the ZT from HV to be mixed with these soils. There are huge amounts of zeolitic minerals in Al Hala Volcano (HV) (Fig. 2) without investigation or characterization as agricultural fertilizes and amendments. The main problem is the lack of information about these zeolites and their mineral content in HV. In addition to the promising future of using zeolite as agricultural soil conditioner. This encourages the present researcher to extend their production scope to include the soil conditioners and amendments.

2. Methodology

2.1. Materials

The used material in this study is VT obtained from the Great Company of Mining and Agriculture (GC) quarry in HV. Six bulk samples (10 Kg) were collected from the quarry for the characterization analyses and two main bulk Samples (1 Ton) were chosen for the agricultural experiments, Table 1. The grain size fraction (1-0.3mm) was used in the agricultural experiments because of the highest zeolitic content (50-70%) (Al Dwairi 2007). The used soil was collected locally from Al Eis area (TS).

Table 1: Sampling and the used laboratory techniques.

#	Type	Color	Thin section	XRD	SEM	XRF	Agricultural application
1	RZT1	Reddish	X	X	X	X	X
2	BZT2	Brownish	X	X	X	X	-
3	LBZT3	Light Brown	X	X	X	X	-
4	GZT4	Grayish	X	X	X	X	X
5	LGZT5	Light gray	X	X	X	X	-
6	VT6	Black	X	X	X	X	-
7	TS (Control)	Yalow to white	---	---	---	X	X

2.2. Methods

The exploration of zeolites includes many exploration trips, sample collecting, cross section, and mapping. The characterization of the volcanic tuff tuff have been carried out using using different analytical methods including thin section, X Ray Diffraction (XRD), Scanning Electron Microscope (SEM), and X Ray Fluorescence (XRF) (Table 1). Finally the results studied and analyzed to evaluate the ability of using zeolites as soil amendment then to start a series of agricultural experiments by using mixtures of soil and zeolites with different ratios. The used soil was thoroughly characterized using chemical analysis, physical properties and grain size distribution.

2.3. Agricultural Experimental Setup

The Agricultural experimental setup was basically carried out by using RZT and GZT for a primary experiments as indicated in table (2) and Fig. (3). The area of agricultural experiment was divided into five equal area tubs (1m*1m). Tomato and Pepper were chosen as example for important vegetation in Jordan. 17/6/2013 was the starting day were the different tubs planted and 17/10/2103 was the end day. The irrigation program was carried out one time peer week for all tubs.

Table 2: Agricultural experiment setup parameters.

Type	Grain size (mm)	Mixing Ratio TS:ZT	pH for Type	Plant Name
RZT1	1-0.3	75:25	7.8	Tomato+ Pepper
RZT2	1-0.3	50:50	8	Tomato+ Pepper
GZT3	1-0.3	75:25	7.9	Tomato+ Pepper
GZT4	1-0.3	50:50	8	Tomato+ Pepper
TS	Normal	-----	7.7	Tomato+ Pepper

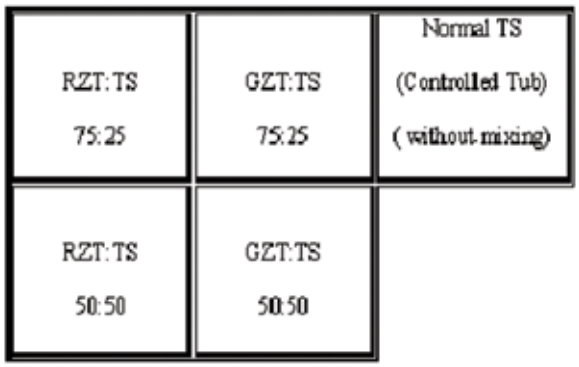

Figure 3: Configuration for the agricultural experiments using tomato and pepper tubs.

3. Results and Discusstion

3.1. Zeolitic Tuff Exploration Results

HV has a height of 1673m above the sea level. field inspection studies indicate that the VT has a thickness of (70m) with a reserve of 16 million tons. A soil bed was recognized on the top of the VT section with about 70 cm in thickness. The northern part of HV is an open mine for the GC for the production of pozzolana for cement industry.

The primary observation of the VT shows that the pyroclastics is highly altered to ZT due to the arid environment and alkaline percolating water. The field investigation and the lithological section shows that the VT is bad sorted, bad cemented, and dominated by large bombs. The VT cross section in the mine is characterized by the absence of bedding with a variety of vertical colors (red, brown, gray, and black) refers for the high alteration and weathering (Fig. 4). The natural zeolite in the area of discovery was formed by the reaction of volcanic glass with percolating alkaline water leading to provide a white gel rim of aluminum silicate (zeolite) filling the cavities of the volcanic tuff (Fig. 5)

Figure 4: Cross section of VT in HV (The GC quarry).

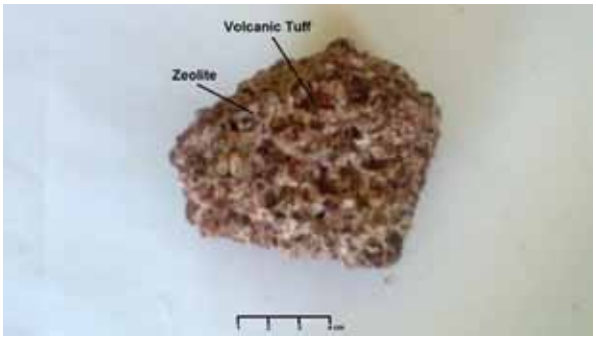

Figure 5: Reddish zeolitic tuff sample from HV.

3.2. Zeolitic Tuff Characterization Results

Thin section results indicate that VT is highly altered to ZT. Fig. (6) shows that the ZT is composed of palagonite matrix, iron oxides, zeolites, clay minerals, and calcite.

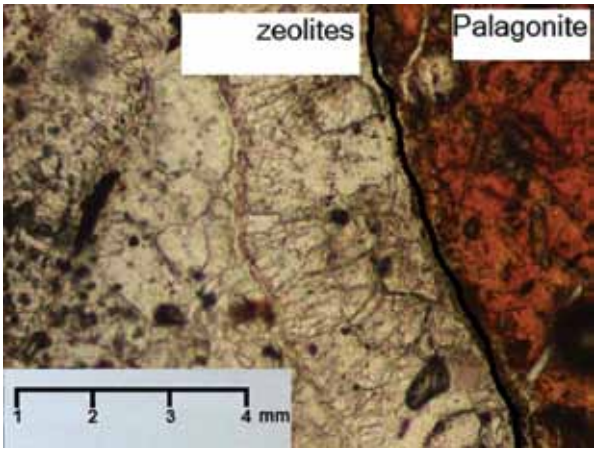

Figure 6: Thin section of VT from HV.

The surface morphology of ZT was examined by SEM and is presented in Fig. 7.The figure shows assemblages of zeolite minerals such as phillipsite and chabazite in addition to clay minerals. The powder X Ray Diffraction (XRD) analysis (using Cu KR as the source for X-rays) of VT was performed for 10 samples from the GC quarry. The XRD patterns of VT are presented in Figure 8. The results show that the VT is composed of zeolitic minerals (phillipsite and chabazite) and other assemblages of minerals such as: (palagonite. smectite, iron oxides and calcite).

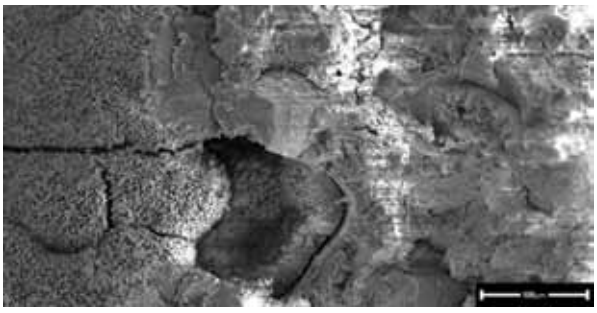

Figure 7: SEM for ZT from HV.

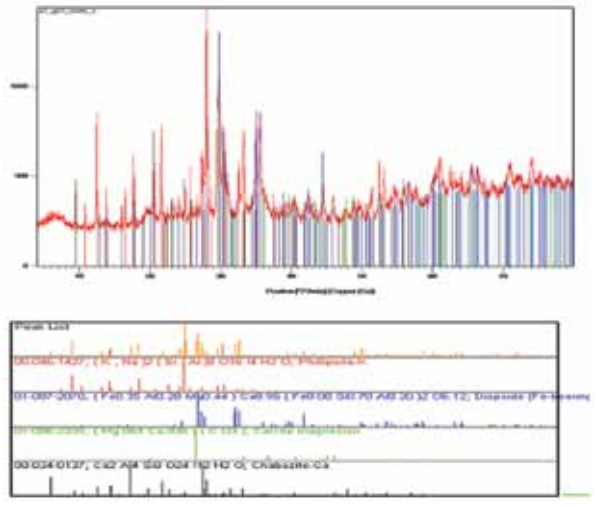

Figure 8: X-Ray Diffraction pattern for ZT from HV.

The chemical composition of black volcanic tuff (BVT), reddish zeolitic tuff (RZT) and grayish zeolitic tuff (GRT) are determined by using X Ray Fluorescence (XRF) apparatus. The results are listed in table 3. The chemical analysis indicates that the ZT from HV contains many elements such as Mg, Mn, Ca, K and Al. Furthermore the silica percentage for the BVT is the highest with an average of (41%) and range between (42.10%) to (40.30%), while the lowest percentage was for the RZT with an average of (40%) and values range between (41.70%) to (39.60%).

The most important oxide in the agriculture issue is Na_2O_3. The results show very low percentage values for ZT ranging between (0.345%) and (0.67) with an average of (0.51), while it's high in the BVT with an average of (3.58%) and values ranging between (4.12%) and (3.03%).

Table 3: Chemical composition (wt %) for volcanic tuff from HV.

Color	Sample #	Sio_2	Na_2O	Fe_2O_3	MgO	Al_2O_3	K_2O	CaO	MnO	TiO_2	P_2O_3	CO_2	Sum
Reddish	RZT1	41.70	0.521	15.50	6.67	15.60	0.94	7.62	0.199	3.28	0.700	6.80	99.53
	RZT2	40.80	0.670	15.80	7.23	16.90	0.80	6.70	0.210	3.17	0.900	6.10	99.28
	RZT3	39.60	0.340	16.01	6.89	16.17	0.82	8.10	0.220	3.50	0.810	6.90	99.36
Grayish	GZT1	38.20	1.44	13.20	6.44	14.60	0.58	11.6	0.178	3.37	0.728	9.00	99.33
	GZT2	39.30	1.20	14.50	6.90	15.70	0.71	8.70	0.240	3.41	0.691	8.00	99.35
	GZT3	40.00	1.60	13.70	6.70	15.10	0.92	9.60	0.191	3.52	0.710	7.61	99.65
Black	BVT1	40.30	3.03	15.60	8.07	12.20	0.50	8.90	2.203	3.84	0.205	4.20	99.05
	BVT2	42.10	4.12	12.39	9.97	11.33	1.02	9.70	1.801	3.17	0.600	3.20	99.40
	BVT3	41.80	3.90	13.45	8.70	11.90	0.80	8.20	2.530	3.67	0.320	4.70	99.97

Ion exchange capacity (CEC) is an important property for zeolites to be used as an agricultural amendment. The three main zeolitic tuff types (RZT, BZT and GZT) from HV were subjected to the CEC measurements. The ZT was sieved into the grain size of (1-0.3) mm which has the highest zeolitic minerals content (Al Dwairi 2007). Table (4) shows the results of the CEC values expressed by meq/100gm. The ZT from HV has a high CEC. The highest CEC value is obtained for RZT (189), while the CEC for BZT is (132). The lowest value or CEC obtained was for GZT (118). pH ranges from 8 to 7.7 for Pozzolana, TS and different mixing types (Table 2).

Table 4: The CEC values for (1-0.3mm) ZT from HV.

Color	Sample #	CEC Meq/100gm	Average
Reddish	RZT1	167	170
	RZT2	175	
	RZT3	189	
Brownish	BZT1	132	129
	BZT2	127	
	BZT3	129	
Grayish	GZT1	118	115
	GZT2	115	
	GZT3	113	

3.3. Tafila Soil Characterization Results

The various physical and chemical properties for Tafila soil are shown in Tables (5) and (6). The results of size distribution indicate that the clay size is the highest with a percentage ranges between (45.1) and (46.2), the silt size range between (45.3) and (42.8), and the sand size range between (9.0) and (11.2); according to sieve analysis the texture of this soil is silty clay. The chemical analysis shows a good percentage of $CaCO_3$ ranges between (27.6) and (26.1).

Table 5: The particle size distribution for TS.

Size fraction	TS1 (%)	TS2 (%)	TS3 (%)
Sand	9.1	10.2	10.3
Silt	45.3	44.3	42.8
Clay	45.1	45.2	46.2
Total	99.5	99.7	99.3

Table 6: Physical and chemical characteristics of the Tafila soil (Al Eis area).

Oxides (%)	**TS at depth 10 cm**	**TS at depth 20 cm**	**TS at depth 30 cm**
SiO_2	52.60	51.89	52.21
Na_2O	0.41	0.37	0.31
Fe_2O_3	4.17	8.81	9.71
MgO	2.77	3.10	3.51
Al_2O_3	8.12	7.98	8.52
K_2O	1.48	1.55	1.68
CaO	18.02	18.83	18.80
MnO	0.07	0.06	0.06
TiO_2	0.71	0.76	0.78
pH	7.7	7.7	7.7
EC	1.30	0.96	0.81
$CaCO_3$%	26.9	27.6	26.1

3.4. Agricultural Experiments Observation

The agricultural results expressed by using comparison between the different parameters (growing, yield and root assemblages) are carried out for different planted tubs (Table 7). All the mixed ZT tubs compared with the controlled TS gave good results for improving different growing parameters. The primary experiments for tubs with the mixing ratio of 50: 50 TS: ZT show best results observed for tomato and pepper vegetables. The results of the majority of the agricultural

experiments are shown in figures (9, 10, 11, 12, and 13).

Table 7: The comparison between planted tubs after 3 months planting.

Vegetables	Tub	Average plant height (cm)	Plant Root assemblages	Yield
Tomato	50:50 TS:RZT	1.32	Long, distributed,	Available and observed
	75:25 TS:RZT	95		
	50:50 TS:GZT	1.12		
	75:25 TS:GZT	80		
	TS (Control)	28	Condense, short,	No yield observed
Pepper	50:50 TS:RZT	80	Long, distributed,	Available and observed
	75:25 TS:RZT	50		
	50:50 TS:GZT	70		
	75:25 TS:GZT	45		
	TS (Control)	20	Condense, Short,	No yield observed

Figure 9: Tomato planted in RZT and TS with a mixing ratio of 50:50 after 3 months.

Figure 10: Tomato planted in GZT and TS with a mixing ratio of 50:50 after 3 months.

Figure 11: pepper planted in RZT and TS with a mixing ratio of 25:75 after 3 months.

Figure 12: Tomato Roots planted in RZT and TS with a mixing ratio of 50:50 after 3 months.

Figure 13: Pepper roots planted in RZT and TS with a mixing ratio of 50:50 after 3 months.

4. Conclusions and Recommendations

The Jordanian natural ZT from HV is suitable for agricultural applications due to its low Na_2O %, high cation exchange, suitable mineral content, and stable pH. ZT is therefore used to promote better plant growth by improving the value of fertilizers. They retain valuable plant growth and improve the quality of the soil and can also be used as a slow release fertilizer or a soil amendment. When applying ZT to agricultural production, one should emphasize that their natural source suitable and is of uniform characteristics and unique properties such as cation exchange capacity, pH, and Na content.

The results of this study strongly suggest the use of ZT from HV as a soil amendment to improve the soil properties. Also, more preparation and processing for ZT are recommended. For wide application in the agricultural sector a production of agricultural commodity is needed.

For the sake of commercial purpose, extensive research that pertains agricultural experiments using mixtures of soil and zeolites is highly needed and recommended.

Acknowledgement

The author expresses special thanks to Mr. Mousa Al Qaisi, the manager of The GC for his assistant and support. Also, the author is deeply grateful for the staff of the GC for their corporation and help. Thanks and appreciations extend to Faculty for Factory program.

References

[1] Al Dwairi, R., 2007, Characterization of the Jordanian zeolitic tuff and its potential use in Khirbet es Samra wastewater treatment plant. Unpublished PhD Thesis, The University of Jordan, Amman, Jordan, 185 P.

[2] Al Dwairi, R., Khoury, H., and Ibrahim, K., 2009, Mineralogy and Authigenesis of Zeolitic Tuff from Tall-Juhira and Tall Amir, South Jordan. Jordan Journal of Earth and Environmental Sciences, 2, 81- 88.

[3] Al Dwairi, R., and Al-Rawajfeh, A., 2012, Recent Patents of Natural Zeolites Applications in Environment, Agriculture and Pharmaceutical Industry. Recent Patents on Chemical Engineering, 5, 20-27.

[4] Al Dwairi, R., Sharadqah, I., 2014. Mineralogy, geochemistry and volcanology of volcanic tuff rocks from Jabal HulaitAl_ Gran, South of Jordan (New Occurrence). Jordan J. Civil Eng 8, 2.

[5] Dwairi, I.,1987, A chemical study of the palagonitic tuffs of the Aritain area of Jordan, with special reference to nature, origin and industrial potential of the associated zeolite deposits. PhD thesis, Hull University, UK, 408 P.

[6] Dwairi, I., 1998, Evaluation of Jordanian zeolite tuff as a controlled slow-release fertilizer for NH4. Environmental Geology, Springer, 34, 293-296.

[7] Ghrir, A., 1998, The distribution, nature, origin, and economic potential of zeolite deposits in Uneiza, Mukawir, and Tell Hassan of Jordan. Unpublished M. Sc. Thesis, university of Jordan, Amman, Jordan.169 p.

[8] Gottardi, G., 1978, Mineralogy and crystal chemistry of zeolites: In sand, L. B., and Mumpton, F. A. Natural Zeolites: Occurrence, Proprites, and Uses. Pergamon press, 331- 44.

[9] Ibrahim, K., 1993, The geological framework for the Harrat Ash-Shaam Basaltic super-group and its volcano tectonic evolution. Natural Resources Authority, Geological Mapping Division, bulletin 25, Amman, 33 P.

[10] Khoury, H. N., Ibrahim, H., Al Dwairi, M., and Torrente, R., 2015, Wide spread zeolitization of the Neogene – Quaternary volcanic tuff in Jordan. Journal of African Earth Sciences ,101, Pp420–429 (In Publication)

[11] Manolov I., Antonov D., Stoilov G., Tsareva I., and Baev M., 2005, Jordanian Zeolitic Tuff as a Raw Material For The Preparation of Substrates Used For Plant Growth. Journal of Central European Agriculture, 6, 485-494.

[12] Mumpton, F., 1978, Natural Zeolitization: A new industrial mineral commodity: In sand, L. B., and Mumpton, F. A. Natural Zeolites: Occurrence, Proprites, and Uses. Pergamon press, 330 P.

[13] Mumpton, F., 1985, Development uses for natural zeolites: a critical commentary. In: D. kallo and H. S. Sherry (eds.) Occurrence, properties and utilization of natural zeolites. Akademiai Kiado, Budapest, 333-366.

[14] Reshidat, R., 1991, Evaluation of natural phillipsite tuff for agricultural application. Unpublished M.Sc. Thesis, Yarmouk University, Irbid, Jordan, 212 P.

[15] Tarawneh, K. 2004. Mineralogy and petrography of new occurrences deposits of the zeolitic tuff in northeast Jordan. University of Mining and Geology “St. Ivan Rilski”. Annual Vol. 47, part 1, Geology and Geophysics, 27-32, Sofia-Bulgaria.

JJEES Guide for Authors

The Jordan Journal of Earth and Environmental Sciences (JJEES)

INSTRUCTIONS TO AUTHORS:

The Jordan Journal of Earth and Environmental Sciences (JJEES) is the national journal of Jordan in earth and environmental sciences. It is an internationally refreed journal dedicated to the advancement of knowledge. It publishes research papers that address both theoritical and applied valuable subjects and matters in both Arabic and English languages in the various fields of geoscience and environmental disciplines. JJEES is published quarterly by the Hashemite University.

Submitted articles are blindly and rigorously reviewed by distinguished specialists in their respected fields.

The articles submitted may be authenitic research papers, scientific reviews, technical/scientific notes.

SUBMISSION OF PAPERS

Online: For online submission upload one copy of the full paper including graphics and all figures at the online submission site, accessed via http://jjees.hu.edu.jo. The manuscript must be written in MS Word Format. All correspondence, including notification of the Editor's decision and requests for revision, takes place by e-mail and via the Author's homepage, removing the need for a hard-copy paper trail.

By Mail: Manuscripts (1 original and 3 copies) accompanied by a covering letter may be sent to the Editor-in-Chief. However, a copy of the original manuscript, including original figures, and the electronic files should be sent to the Editor-in-Chief. Authors should also submit electronic files on disk (one disk for text material and a separate disk for graphics), retaining a backup copy for reference and safety.

Note that contributions may be either submitted online or sent by mail. Please do NOT submit via both routes. This will cause confusion and may lead to delay in article publication. Online submission is preferred.

FORMATE GUIDE:

1. The research papers should be printed on one side of the paper, be duoble-line spaced, have a margin of 30 mm all around, and no more than 30 pages (7,500 words, font size 13). The title page must list the full title and the names and affiliations of all authers (first name, middle name and last name). Also, their addresses, including e-mail, and their ranks/positions must be included. Give the full address, including e-mail, telephone and fax, of the author who is to check the proof.

2. The research must contain the title and abstract, keywords, introduction, methodology, results, discussion, and recommendations if necessary. The system of international units must also be used. Scientific abbreviations may be used provided that they are mentioned when first used in the text. Include the name(s) of any sponsor(s)of the research contained in the paper, along with grant number(s).

3. Authors should submit with their paper two abstracts, one in the language of the paper and it should be typed at the beginning of the paper followed by the keywords before the introduction. As for the other abstract, it should be typed at the end of the paper on a separate sheet. Each abstract should not contain more than 200 words.

4. Captions and tables should be numbered consecutively according to their occurrence in the research with headings. When mentioned in the text, the same consecutive numbers should be used. Captions and tables must be typed on separate sheets of paper and placed at the end of the paper.

5. The author(s) should submit a written consent that he or she will not publish the paper in any other journal at the same time of its publication in JJEES. After the paper is approved for publication by the editorial board, the author does not have the right to translate, quote, cite, summarize or use the publication in the other mass media unless the editor-in-chief submits a written consent according to the policy of JJEES. Submitted material will not be returned to the author unless specifically requisted.

6. DOCUMENTATION:

- References:

a. To cite sources in the text, use the author-date method; list the last name(s) of the author(s), then the year. Examples: (Holmes, 1991); (Smith and Hutton 1997).

b. In the event that an author or reference is quoted or mentioned at the beginning of a paragraph or sentence or an author who has an innovative idea, the author’s name is written followed by the year between two brackets. Example: Hallam(1990).

c. If the author’s name is repeated more than once in the same volume, alphabets can be used. Example: (Wilson, 1994 a; Wilson, 1994 b).

d. Footnotes may be used to solve any ambiguity or explain something as in the case of a term that requires illustration. In this case, the term is given a number and the explanation is written in a footnote at the bottom of the page.

e. If the number of authors exceeds two, the last name of the first author followed by et al. is written in the text. Example: (Moore et al.). Full names are written in the references regardless of their number.

f. Prepare a reference section at the end of the paper listing all references in alphabetical order according to the first author's last name. This list should include only works that been cited.

- Books:

Hunt, J. 1996. Petroleum Geochemistry and Geology. 2nd Ed., H. W. Freeman and Company, New York.

- Chapter in a book:

Shinn E. A., 1983. Tidal Flat Environment, In: Carbonate Depositional Environments, edited by Scholle, P. A., Bebout, D. G., and Moore, C. H., The American Association of Petroleum Geologists, Tulsa, Oklahoma, U.S.A. pp. 171-210.

- Periodicals:

Sexton, P. F., Wilson, P. A.,and Pearson, P. N., 2006. Paleoecology of Late Middle Eocene Planktonic Foraminifera and Evolutionary Implication, Marine Micropaleontology, 60(1): 1-16.

- Conferences and Meetings:

Huber, B. T. 1991. Paleogene and Early Neogene Planktonic Foraninifer Biostratigraphy of Sites 738 and 744, Kerguelen Plateau (southern Indian Ocean). In: Barron, J., Larsen, B., et al. (Eds.), Proceedings of the Ocean Drilling Program. Scientific Results, vol. 119. Ocean Drilling Program, College station, TX, pp. 427-449.

- Dissertations:

Thawabteh, S. M. 2006. Sedimentology, Geochemistry, and Petrographic Study of Travertine Deposits along the Eastern Side of the Jordan Valley and Dead Sea, M. Sc. Thesis, The Hashemite University.

- Unpublished:

Makhlouf, I. M. and El-Haddad, A. 2006. Depositional Environments and Facies of the Late Triassic Abu Ruweis Formation, Jordan, J. Asian Earth Sciences, England, in Press.

- Illustrations:

a. Supply each illustration on a separate sheet, with the lead author's name, the figure number and the top of the figure indicated on the reverse side.

b. Supply original photographs; photocopies and previously printed material are not acceptable.

c. Line artwork must be high-quality laser output (not photocopies).

d. Tints are not acceptable; lettering must be of reasonable size that would still be clearly legible upon reduction, and consistent within each figure and set of figure.

e. Electronic versions of the artwork should be supplied at the intended size of printing; the maximum column width is 143 mm.

f. The cost of printing color illustrations in the Journal may be charged to the author(s).

7. Arranging articles in JJEES is based on the editorial policy.

8. The author should submit the original and two copies of the manuscript, together with a covering letter from the corresponding author to the Editor-in-Chief.

9. The editorial board's decisions regarding suitability for publication are final. The board reserves the right not to justify these decisions.

10. In case the paper was initially accepted, it will be reviewed by two specialized reviewers.

11. The accepted papers for publication shall be published according to the final date of acceptance.

12. If the author chooses to withdraw the article after it has been assessed, he/she shall reimburse JJEES the coast of reviewing the paper.

13. The author(s) will be provided with one copy of the issue in which the work appears in addition to 20 off prints for all authors. The author(s) must pay for any additional off prints of the published work.

14. Statement transferring copyright from the authors to the Hashemite University to enable the publisher to disseminate the author's work to the fullest extent is required before the manuscript can be accepted for publication. A copy of the Copyright Transfer Agreement to be used (which may be photocopied) can be found in the first issue of each volume of JJEES.

15. Articles, communications or editorials published by JJEES represent the sole opinion of the authors. The publisher bears no responsibility or liability whatsoever for the use or misuse of the information published by JJEES.

16. Submission address:

Prof. Dr. Eid A. Al-Tarazi
Editor-in-Chief,
Jordan Journal of Earth and Environmental Sciences,
The Hashemite University,
P.O. Box 150459, Zarqa, 13115, Jordan.
Phone: 00962-5-3903333 / Ext. 4229
Fax: 00962-5-3826823
E-Mail: jjees@hu.edu.jo
http:// jjees.hu.edu.jo/

JJEES
Jordan Journal of Earth and Environmental Sciences

تمهيد

انه من دواعي سروري وغبطتي أن يتم نشر العدد الثالث الخاص للمجلة والذي يتضمن الأبحاث التي لها علاقة بموضوعات المجلة والتي قدمت في المؤتمر الدولي الذي عقد برعاية كريمة من صاحبة السمو الملكي الأميرة سمية بنت الحسن المعظمة خلال الفترة ٣-٥/٤/٢٠١٤ في عمان وبدعم من العديد من المؤسسات الحكومية والأكاديمية والدولية، حيث كان المؤتمر تحت عنوان:

Building International Networks for Enhancement of Research in Jordan

إن الأبحاث التي قبلت للنشر بهذا العدد تعتبر ذات أهمية كبيرة للأردن، حيث أنها تتحدث في مواضيع الجيولوجيا الاقتصادية والخامات المعدنية وتطويرها، مثل الزيولايت واليورانيوم والخامات الطينية وصناعة الإسمنت في الأردن. هذا ولقد تم إرسال الأبحاث التي تم تقديمها للنشر في هذا العدد للتقييم وذلك حسب الأصول المتبعة للمجلة.

أتقدم بخالص الشكر والتقدير للزملاء أعضاء هيئة التحرير للمجلة على جهودهم في دعم هذا العدد الخاص، إضافة إلى الجهود الطيبة من المحرر اللغوي الدكتور قصي الذبيان والسيد عبادة الصمادي المحرر المخرج الفني في الجامعة الهاشمية.

رئيس هيئة التحرير
الأستاذ الدكتور عيد عبد الرحمن الطرزي
مجلة علوم الأرض والبيئة
كلية الموارد الطبيعية والبيئة
الجامعة الهاشمية،
الزرقاء، الأردن

المملكة الأردنية الهاشمية

الجامعة الهاشمية

المجلة الأردنية
لعلوم الأرض والبيئة

JJEES

مجلة علمية عالمية محكمة

العدد الخاص ٣

http:// jjees.hu.edu.jo/

ISSN 1995-6681

المجلة الأردنية لعلوم الأرض والبيئة
مجلة علمية عالمية محكمة

المجلة الأردنية لعلوم الأرض والبيئة: مجلة علمية عالمية محكمة ومفهرسة ومصنفة، تصدر عن الجامعة الهاشمية وبدعم من صندوق البحث العلمي– وزارة التعليم العالي والبحث العلمي، الأردن.

هيئة التحرير

ترسل البحوث إلى العنوان التالي:

رئيس تحرير المجلة الأردنية لعلوم الأرض والبيئة

عمادة البحث العلمي والدراسات العليا

الجامعة الهاشمية

الزرقاء ١٣١٣٣ – الأردن

هاتف ٣٩٠٣٣٣٣–٥–٩٦٢+ فرعي ٤٢٢٩

Email: jjees@hu.edu.jo, Website: www.jjees.hu.edu.jo

المملكة الأردنية الهاشمية

الجامعة الهاشمية

المجلة الأردنية لعلوم الأرض والبيئة

JJEES

مجلة علمية عالمية محكمة

تصدر بدعم من صندوق دعم البحث العلمي

http://jjees.hu.edu.jo/

المجلد (٦) العدد الخاص (٣) ISSN 1995-6681 حزيران ٢٠١٤ / شعبان ١٤٣٥